

ALMA MATER STUDIORUM · UNIVERSITÀ DI
BOLOGNA

SCUOLA DI SCIENZE
Corso di Laurea in Astrofisica e Cosmologia

The Complex Potential Technique In Stellar Dynamics

Relatore:
Chiar.mo Prof.
Luca Ciotti



Presentata da:
Francesco Venezia

Sessione II - 2° seduta
Anno Accademico: 2016/2017

Contents

1	Introduction	6
1.1	The Complex-shift method	10
2	Complexification of the simple harmonic oscillator	13
2.1	Real harmonic oscillator (R.H.O.)	14
2.1.1	Isotropic R.H.O.	15
2.2	Complex harmonic oscillator (C.H.O.)	15
2.2.1	Isotropic C.H.O.	17
3	Complexification of the Coulomb potential	20
3.1	Complex Coulomb potential	21
4	Complexification of General potentials	24
4.1	Complex shifted spherical potential and Epicycles	25
4.2	The Complex shift for the Plummer sphere	30
4.3	Motion in shifted Plummer potential	33
4.3.1	Epicyclic theory for the shifted Plummer sphere	35
4.3.2	Motion in Plummer potential with $a \rightarrow 0$	42
5	Astrophysical consequences	46
5.1	Epicyclic frequencies and energies	47
5.2	Zero-velocity curves and resonances	52
6	Discussion and Conclusions	80
	Appendix A	86
	The Epicyclic Theory	86

Sommario

In questo lavoro di tesi il metodo dello shift complesso, introdotto da Appell in gravità nel caso di massa puntiforme (e applicato tra l'altro in elettrodinamica da Newman, Carter, Lynden-Bell) e le sue estensioni per ottenere coppie potenziale-densità per sistemi significativamente divergenti dalla simmetria sferica (Ciotti, Giampieri, Marinacci et al.) vengono presentati e sviluppati ulteriormente nelle loro implicazioni fisiche. L'obiettivo principale è studiare il metodo di complessificazione sotto due diversi aspetti: prima come teoria dipendente dal tempo; in secondo luogo, considerandolo come una estensione per sistemi integrabili (ad esempio potenziali sferici) per derivare nuove famiglie di potenziali gravitazionali, le cui proprietà dinamiche sono qui studiate per la prima volta. In particolare, viene dato ampio spazio al modello di Plummer complesso, utilizzato sia come modello di test per verificare quanto trovato per potenziali sferici shiftati in generale, sia per introdurre i primi studi sulla dinamica dei sistemi soggetti a questo tipo di campo gravitazionale, tramite l'applicazione dell'approssimazione epiciclica. Infine, verranno mostrate alcune applicazioni pratiche in campo astrofisico dei risultati ottenuti, sempre incentrate sul modello di Plummer; ad esempio per modellare realisticamente il potenziale gravitazionale generato da galassie ellittiche o a spirale, nonché nell'ambito della Teoria delle onde di densità per le strutture a Spirale.

Abstract

In this thesis work the complex-shift method, introduced by Appell in gravity to the case of a point mass (and applied among others in electrodynamics by Newman, Carter, Lynden-Bell), and its extensions to obtain density-potential pairs for self-gravitating systems departing significantly from spherical symmetry (Ciotti, Giampieri, Marinacci et al.) are presented and developed further more in their physical implications. The main focus is to investigate the complexification method under two different frameworks: first as a time-dependent theory; second, to consider it as an extension of integrable systems (e.g. spherical potential) to derive new families of gravitational potentials, whose dynamical properties are studied here for the first time. In particular, considerable space is given to the shifted Plummer potential, used both as a test model to verify what found for generic shifted spherical potential as well as to introduce the first step into the dynamics involving systems subdue to that kind of gravity field, throughout the application of epicyclic approximation to the orbits in this Plummer axi-symmetric potential. Finally, some practical astrophysical potential application, always focusing on the Plummer model, are shown, for instance in order to model realistically enough the gravitational potential generated by elliptic or spiral galaxies, as well as within the contest of Theory of density waves for Spiral Structures.

Chapter 1

Introduction

In a large number of astrophysical applications of Stellar Dynamics, scientists have to deal with stellar systems largely departing from spherical symmetry, with a variety of shapes and patterns. As first statement to keep in mind there is the fact that those structures are in *Macroscopic* equilibrium; this assumption is suffragated by two main results:

- The observed structures have an high level of symmetry and very much regular shape, i.e. disc-like shape for spiral galaxies or spherical/-spheroidal form for elliptical galaxies and so on.
- The characteristic time scale for the macroscopic equilibrium of those systems to be reached, known as the violent relaxation time (τ_{Relax}), is very much smaller compared to the age of the Universe, also known as the Hubble time-scale (τ_H), i.e. $\tau_{Relax} \ll \tau_H$

So, in order to understand the behaviour of these systems, it is important to clarify how the orbits of the stars constituting the astrophysical system are realized, what are their main features, what kind of self-gravitating potential the stellar system generates.

And it is at this point that one of the main problems still not fully understood in theoretical astrophysics comes to light: the study and search for the gravitational field generated by a general density distributions, i.e. the so-called density-potential pairs obeying to the Poisson Equation:

$$\nabla^2\Phi(\mathbf{x}) = 4\pi G\rho(\mathbf{x}) \quad (1.1)$$

Throughout the years, this problem has been attacked from different points of view, from the development of mathematical methods in order to find exact analytical density-potential pairs for very special configuration, in general

using symmetry arguments, to the creation of numerical method to extend, within a certain level of approximation, the analytical results to some more general cases.

In particular, for system with a high degree of symmetry, i.e. spherical systems, which means systems where the potential depends only on the radial component of spherical coordinates, it can be said that it is always possible, in principle, to build analytical density-potential pairs, thanks to the 1° and 2° Newton's Theorems, which allows to define a standard procedure, technically speaking, to generate fully integrable models, that is models whose Hamilton-Jacobi equation are separable.

But, of course stellar systems are not perfectly spherical; so it comes natural to find techniques to generates new, non spherical and possibly fully analytical density-potential pairs and studying the orbits within such kind of potential fields. But to achieve this goal is far from being trivial; in the first place, there is not exist standard techniques to produce pairs diverging from spherical symmetry. In fact even going from considering spherical systems to systems with cylindrical symmetry, like disk galaxies, it is not an easy passage, not just because of mathematical difficulties, involved when moving from 1-dimensional problems to 2D problems (which implies going from ordinary differential equations (ODE) to partial differential equations (PDE)), but more importantly because there are no theorems ensuring the integrability of those systems.

In order to overcome these issues one of the analytical method poorly investigated in an astrophysical contest and here presented, which has been a foundation for the purpose of this work, is the so-called complex-shift method, introduced by Appell (1887) in gravity to the case of a point mass and applied among others in electrodynamics by Newman (1965, 1973), Carter (1968), Lynden-Bell(1962, 2000, 2002, 2004), and Kaiser (2004) to determine remarkable properties of the electromagnetic field of rotating charged configurations. This method has been extended, in order to obtain new and explicit density-potential pairs for self-gravitating systems departing significantly from spherical symmetry, by Ciotti & Giampieri (2007), Ciotti & Marinacci(2008) and few others, finding the astonishing property to generate axisymmetric density-potential pairs from a complexified spherical potential or, furthermore, triaxial pairs from axially symmetric density configuration/potential.

The interest in this method comes from the question whether a system with a lower degree of symmetry created from the complexification of a parent system with a high level of symmetry, i.e. a spherical one, keeps trace of some

properties of the parent distribution, specifically concerning its integrability. Due to these premises, it is important to remark that this thesis comes to be an exploratory work in a field where major results almost certainly are to be discovered without the.

Under the research perspectives presented up to now, in this thesis work I am going to study a generalization of the complex shift method. In particular, in this first chapter, the complex shift method, in his conceptual origin, together with some detailed and more technical aspects are briefly described in the following presented. In Chapters 2 & 3 it will be introduced one first attempt to generalize the complexification as portrayed by Ciotti et al. (2007,2008) considering two full complexified systems, i.e. provided by a time-dipendent complex shift (which is equivalent to work in C^3 instead of the usual R^3 vector space), namely the complex harmonic oscillator and the complex Coulomb-like potential field and some delicate aspects concerning integrability in C^3 will be presented. In Chapter 4, under a different point of view, the attention will be put on slightly more general complexified potential, with a constant complex shift parameter and some properties of the orbits generated by such a potential will pointed out and discussed, in particular epicyclic expansion, Zero-velocity curves, escapes and resonances will be briefly adressed in the contest of complexification. In Chapter 5 some astrophysical applications for the obtained results in previous chapters will be exposed and analyzed. Finally, in Chapter 6 the main results found in previous sections will be highlighted and discussed in more depth.

Notation

For the purposes of the following work, we briefly summarize the notation adopted.

\mathbf{x}, \mathbf{y} : bold variables are used to indicate R^3 -vector, with components labelled as x_j, y_j etc., with $j = 1, 2, 3$.

\mathbf{z} : this variable is used to indicate a generic C^3 -vector, with components $z_j = x_j + iy_j$ with $j = 1, 2, 3$ and $i = \sqrt{-1}$ being the imaginary unit.

$\langle \cdot | \cdot \rangle$: the standard inner product over the reals.

x, y, z : roman letters, in a mathematical context, indicate the modulus of the corresponding bolded vectors.

\wedge : the wedge symbol indicates the standard cross product over R^3 , also extended the complex vector space C^3 .

ϵ_{ijk} : the completely anti-symmetric Levi-Civita symbol, defined as such: it is 1 if (i, j, k) is an even or cyclic permutation of (1, 2, 3), -1 if it is an odd or anticyclic permutation, and 0 if any index is repeated.

$\dot{[\cdot]}, \ddot{[\cdot]}$: One or more dots, either for scalar, vector and so on, indicates the corresponding derivation with respect to time.

1.1 The Complex-shift method

In this section we analyze the concepts at the basis of the development of the complex-shift method (e.g. see Ciotti & Giampieri (2007)). As stated in the very introduction to this work, the complexification of the physical systems that are going to be analyzed is obtained by the introduction of a complex shift to the original (real) case, as it is commonly done for the complex-shift method. The purpose for the generalization is to investigate the integrability of systems significantly different from spherical symmetry, because, as it is known, the majority of the available explicit density-potential pairs refers to spherical symmetry and only few axially symmetric pairs are known. To this goal, in the present introduction we illustrate briefly the original complex-shift method as developed by Apell, while in the first chapter we are going to study the properties of complexified simple harmonic oscillator, moving on with the complexification of the Coulomb potential in the second chapter and finally in the third one extending the eventually obtained results to the case of more general potentials, in order to expand the already known properties found in previous work by Ciotti & Giampieri(2007) and Ciotti & Marinacci(2008) et al.

The real purpose of this first part of the work is to understand if an integrable, spherical, gravitational system, once shifted in a complex vector space by the complex-shift method, generates an integrable system not spherically symmetric, as it is shown in the above mentioned articles, and if this is just a pure "lucky fortuity" or if instead there is a deeper structure in the complexification of physical problems in order to transform them into analytically solvable problems. So the basic idea under this work is to find out if the complex-shift method is a particular case of a deeper theory, if it represents a sort of equilibrium point for a complex theory of gravitation.

The constant Complex-shift method

We start by extending the complexification of a point charge Coulomb field discussed by Lynden-Bell(2004b), to the gravitational potential $\Phi(\mathbf{x})$ generated by a density distribution $\rho(\mathbf{x})$. Using \mathbf{x} to indicate the position vector, while $\langle \mathbf{x} | \mathbf{y} \rangle \equiv x_i y_i$ is the standard inner product (repeated index summation convention implied if not differently indicated).

So first let's assume that $\rho(\mathbf{x})$ and $\Phi(\mathbf{x})$ satisfy the Poisson equation (1.1) and let's now define a complex-shift for the position vector, so we replace \mathbf{x} with $\mathbf{x} - i\mathbf{a}$, where \mathbf{a} is a constant real vector .

In this way, we introduce the complexified gravitational potential Φ^C as:

$$\Phi(\mathbf{x}) \rightarrow \Phi^C(\mathbf{x} - i\mathbf{a}) \quad (1.2)$$

The idea behind the proposed method is based on the recognition that 1) the Poisson equation is a linear PDE, and that 2) the complex shift is a linear coordinate transformation; from these two properties, and from eq.(1.1) and (1.2) it follows that:

$$\nabla^2 \Phi^C(\mathbf{x} - i\mathbf{a}) = 4\pi G \rho^C(\mathbf{x} - i\mathbf{a}) \quad (1.3)$$

where ρ^C is the complexified counterpart of the real density distribution. Thus, by separating the real and imaginary parts of Φ^C and ρ^C obtained from the shift of a known real density-potential pair we obtain two real density-potential pairs.

A distinction is a must here between electrostatic and gravitational problems: in fact, while in the former case, a density (charge) distribution with negative and positive regions can be (at least formally) accepted, in the gravitational case the obtained density components have physical meaning only if they do not change sign, which may impose restriction on the nature of either the real or the imaginary part of the density distribution (and the potential connected to it).

Quite interestingly, some general result about the sign of the real and imaginary parts of the shifted density can be obtained by considering the behavior of the complexified self-gravitational energy and total mass. In fact, from the linearity of the shift, it follows that the volume integral over the whole space

$$W_c \equiv \frac{1}{2} \int \rho^C \Phi^C d\mathbf{x} = \frac{1}{2} \int \Re[\rho^C] \Re[\Phi^C] - \Im[\rho^C] \Im[\Phi^C] d\mathbf{x} \quad (1.4)$$

coincides with the self-gravitational energy W of the real unshifted seed density. Therefore the imaginary part of W_c is zero, which means:

$$-G \iint \frac{\Re[\rho^C(\mathbf{x})] \Im[\rho^C(\mathbf{x}')] }{\|\mathbf{x} - \mathbf{x}'\|} d\mathbf{x} d\mathbf{x}' = 0 \quad (1.5)$$

and W_c is the difference of the gravitational energies of the real and the imaginary parts of the shifted density. The vanishing of the double integral (1.5) shows that the integrand necessarily changes sign, so that the constant complex shift cannot generate two physically acceptable densities.

Additional informations are provided by considering that, by means of the same arguments just illustrated, the total mass of the complexified distribution M_c coincides with the total (real) mass of the seed density distribution $M = \int \rho d\mathbf{x}$ and so, also in this case like in the former:

$$\int \Im[\rho^C] d\mathbf{x} = 0 \quad (1.6)$$

from eq.(1.5) and (1.6) it can be stated that also $\Re[\rho^C]$ is a function not *a priori* positive-defined over the whole space, but it depends on the particular parent density and shift vector used.

Chapter 2

Complexification of the simple harmonic oscillator

As a preliminary work, in this chapter they are going to be investigated the properties and the constants of motion for the harmonic oscillator starting from its equation of motion. it will be considered firstly in R^3 and, in that contest, some well-known results from classical mechanics about indipendent integrals of motion will be recollected for the anisotropic harmonic oscillator as well as for the isotropic one.

Subsequently the same equation of motion will be complexified, considering it in C^3 , where the real and imaginary part of the equation will be analyzed both separately and together in order to define and interpret the complex counterpart of the real integrals of motion previously found, namely the "complex energy" for the ansotropic harmonic oscillator and the "complex energy" together with the "complex angular momentum" for the isotropic case.

2.1 Real harmonic oscillator (R.H.O.)

Let's consider first the equation of motion for the well-known simple anisotropic harmonic oscillator, described by the R^3 -vector \mathbf{x} :

$$\ddot{\mathbf{x}} = -A\mathbf{x}, \quad (2.1)$$

where A is a diagonal, positive defined matrix, represented by:

$$A = \begin{pmatrix} k_1 & 0 & 0 \\ 0 & k_2 & 0 \\ 0 & 0 & k_3 \end{pmatrix},$$

where the k_i are the elastic constants for the three coordinates x_1, x_2 and x_3 . Let's now multiply scalarly eq.(2.1) by the velocity vector, $\dot{\mathbf{x}}$:

$$\langle \ddot{\mathbf{x}} | \dot{\mathbf{x}} \rangle = -\langle A\mathbf{x} | \dot{\mathbf{x}} \rangle, \quad (2.2)$$

where the usual standard inner product over the reals is intended: $\langle \mathbf{x} | \mathbf{y} \rangle = x_i y_i$.

We can recognize in both members the total derivative with respect to time of the kinetic energy(left member) and of the potential energy (right member):

$$\langle \ddot{\mathbf{x}} | \dot{\mathbf{x}} \rangle = \frac{1}{2} \frac{d \|\dot{\mathbf{x}}\|^2}{dt}, \quad \text{and} \quad \langle A\mathbf{x} | \dot{\mathbf{x}} \rangle = \frac{1}{2} \frac{d \langle \mathbf{x} | A\mathbf{x} \rangle}{dt}, \quad (2.3)$$

where $\|\dot{\mathbf{x}}\|^2 = \langle \dot{\mathbf{x}} | \dot{\mathbf{x}} \rangle$ and $\langle \mathbf{x} | A\mathbf{x} \rangle = \langle A\mathbf{x} | \mathbf{x} \rangle$, due to the simmetry of the matrix A . So (2.2) can be rewritten as:

$$\frac{d}{dt} \left[\frac{1}{2} \|\dot{\mathbf{x}}\|^2 + \frac{1}{2} \langle A\mathbf{x} | \mathbf{x} \rangle \right] = 0, \quad (2.4)$$

Where we recall the classic results of energy conservation, E_{TOT} to be indentified with the quantity in square brackets. Repeating the same treatment component by component, it is also evident that not only E_{TOT} , but also the 3 energies E_i are constants of motion, so that we have:

$$E_{TOT} = \sum_{i=1}^3 E_i. \quad (2.5)$$

2.1.1 Isotropic R.H.O.

In order to analyze additional properties of the harmonic oscillator, let's now consider the *isotropic* harmonic oscillator, whose equation of motion is exactly the same as the previous case, but now the coefficient matrix A is proportional to the identity matrix I , so we can identify its entries with a simple numerical constant, i.e. $A = kI$.

As known from classical mechanics, the particular symmetry of this problem, which comes naturally to be discussed in spherical coordinates, gives us another constant of motion besides the total energy as it was before, which is the total angular momentum \mathbf{J} , defined by the standard cross-product over R^3 :

$$\mathbf{J} = \mathbf{x} \wedge \dot{\mathbf{x}}, \quad (2.6)$$

where the cross product between two vectors \mathbf{u} and \mathbf{v} is defined as usual:

$$(\mathbf{u} \wedge \mathbf{v})_i = \epsilon_{ijk} u_j v_k, \quad (2.7)$$

through the Levi-Civita symbol. The proof the \mathbf{J} is an integral of motion, in this case, is elementary; in fact, proceeding with time differentiation of (2.6), we have:

$$\frac{d}{dt}(\mathbf{x} \wedge \dot{\mathbf{x}}) = \dot{\mathbf{x}} \wedge \dot{\mathbf{x}} + \mathbf{x} \wedge \ddot{\mathbf{x}} = -\mathbf{x} \wedge A\mathbf{x}, \quad (2.8)$$

but $A = kI$, so

$$-\mathbf{x} \wedge A\mathbf{x} = -\mathbf{x} \wedge (kI\mathbf{x}) = -k(\mathbf{x} \wedge \mathbf{x}) = 0. \quad (2.9)$$

This completes the proof and concludes our summary of the standard results concerning the dynamical properties of the real harmonic oscillator.

2.2 Complex harmonic oscillator (C.H.O.)

Now we are ready to investigate the properties for the complexified counterpart of the R.H.O.. First we introduce the complex vector of $\mathbf{z} = (z_1, z_2, z_3)$ over C^3 , with:

$$\mathbf{z} = \begin{pmatrix} x_1 + iy_1 \\ x_2 + iy_2 \\ x_3 + iy_3 \end{pmatrix} = \mathbf{x} + i\mathbf{y} \quad (2.10)$$

Let's consider first the case for the anisotropic complex harmonic oscillator, described by the equation of motion:

$$\ddot{\mathbf{z}} = -B\mathbf{z}, \quad (2.11)$$

where B is a constant matrix, diagonal and hermitian:

$$B = \begin{pmatrix} h_1 & 0 & 0 \\ 0 & h_2 & 0 \\ 0 & 0 & h_3 \end{pmatrix}.$$

The question now arises about the number and meaning of the conserved quantities following by eq. (2.11). Following the same approach adopted for the R.H.O., let's now scalarly multiply eq. (2.11) by complex velocity $\dot{\mathbf{z}}$, where the adopted scalar product is the standard inner product defined over the reals, following Ciotti & Giampieri (2007):

$$\langle \ddot{\mathbf{z}} | \dot{\mathbf{z}} \rangle = -\langle B\mathbf{z} | \dot{\mathbf{z}} \rangle. \quad (2.12)$$

Note that in the procedure of complexification, the scalar product is *not* a scalar product in the usual meaning, as the product of a complex vector $\mathbf{w} = \mathbf{u} + i\mathbf{v}$ with itself is *not* a real, positive quantity. So also the "norm" is not a norm in technical sense, in fact we have $\|\mathbf{w}\|^2 = \|\mathbf{u}\|^2 - \|\mathbf{v}\|^2 + 2i\langle \mathbf{u} | \mathbf{v} \rangle$, where the operators at the right hand side are the *true* norm and scalar product over R^3 .

So now, working in the exact same way we did for the real case, we come up with a quantity constant in time, that can be written as:

$$\frac{d}{dt} \left[\frac{1}{2} \|\dot{\mathbf{z}}\|^2 + \frac{1}{2} \langle \mathbf{z} | B\mathbf{z} \rangle \right] = 0, \quad (2.13)$$

where:

$$\|\dot{\mathbf{z}}\|^2 = \langle \dot{\mathbf{z}} | \dot{\mathbf{z}} \rangle = \langle \dot{\mathbf{x}} + i\dot{\mathbf{y}} | \dot{\mathbf{x}} + i\dot{\mathbf{y}} \rangle = \|\dot{\mathbf{x}}\|^2 - \|\dot{\mathbf{y}}\|^2 + 2i\langle \dot{\mathbf{x}} | \dot{\mathbf{y}} \rangle, \quad (2.14)$$

and in the very same way:

$$\langle \mathbf{z} | B\mathbf{z} \rangle = \|\mathbf{x}\|^2 - \|\mathbf{y}\|^2 + 2i\langle B\mathbf{x} | \mathbf{y} \rangle, \quad (2.15)$$

From the above expressions, we can see that the "complex energy" obtained as constant of motion can be expressed as:

$$E^C = \Re[E^C] + i\Im[E^C], \quad (2.16)$$

where:

$$\Re[E^C] = E_x - E_y, \quad \text{and} \quad \Im[E^C] = \langle \dot{\mathbf{x}} | \dot{\mathbf{y}} \rangle + \langle B\mathbf{x} | \mathbf{y} \rangle, \quad (2.17)$$

This implies that both the (real) quantities $\Re[E^C]$ and $\Im[E^C]$ are integrals of motion, of course. For the real part of E^C the expression labelled as E_x and E_y are the (real) energies for the R.H.O. described by the coordinate \mathbf{x} and \mathbf{y} respectively; in fact it is indeed possible to solve the complex equation of motion dividing the real and the imaginary part:

$$\ddot{\mathbf{z}} = -B\mathbf{z} \rightarrow \ddot{\mathbf{x}} + i\ddot{\mathbf{y}} = -B(\mathbf{x} + i\mathbf{y}) . \quad (2.18)$$

So the C.H.O. is formally equivalent to two real harmonic oscillators, completely independent from one another. Even though this, the equalities in eq. (2.17) tell us that the real and imaginary part of the complex coordinates are not independent and that the system described by the "real coordinate" \mathbf{x} has the same energy as the one described by the "imaginary coordinate" \mathbf{y} up to an arbitrary constant. In fact if we study the equation of motion for \mathbf{x} and \mathbf{y} separately, it is easy to see that E_x and E_y are constants of motion by themselves, which implies that $\Re[E^C]$ is indeed an integral of motion by linearity; in the same way the time derivative of $\Im[E^C]$ is identically zero, so it does not add any new constraint for the physics involved in the systems considered.

To complete the parallel between the real and complex harmonic oscillator, it is remarkable to see how, working with complex coordinates, also the complex energy E^C can be seen as the sum of three complex energies, one for each component z_i , and the same can be done with the expressions for $\Re[E^C]$ and $\Im[E^C]$, so that:

$$E^C_{TOT} = \sum_{i=1}^3 E^C_i . \quad (2.19)$$

So far, for the C.H.O., working in C^3 , we found 4 complex integrals of motion, the "complex energie" E^C_i and their sum, E^C_{TOT} (but just three linearly independent), but if we think in terms of vector in R^6 -vector space, isomorphic to C^3 , there are 8 constants of motion, with 6 of them linearly independent.

2.2.1 Isotropic C.H.O.

Moving on with the comparison between the R.H.O. and the C.H.O., we now study the case for the isotropic Complex oscillator, which means, as before,

that the coefficient matrix B can now be considered as proportional to the identity matrix via a numerical constant.

Also in this case, assuming to identify the cross product in C^3 as the standard cross product in R^3 (eq.(2.7)), because the problem comes naturally to have spherical symmetry, it is possible to define a complex vector, that we are going to call "complex angular momentum", as:

$$\mathbf{J}^C = \mathbf{z} \wedge \dot{\mathbf{z}}, \quad (2.20)$$

In the very same way as we did for the real case (eq.(2.8)), it is possible to demonstrate that the above quantity is a constant of motion for the problem studied, i.e.:

$$\frac{d\mathbf{J}^C}{dt} = 0. \quad (2.21)$$

So, if we develop the calculus for eq. (2.20) in terms of the real and imaginary part, we found that:

$$\mathbf{J}^C = (\mathbf{x} + i\mathbf{y}) \wedge (\dot{\mathbf{x}} + i\dot{\mathbf{y}}) = \mathbf{J}_x - \mathbf{J}_y + i[\mathbf{x} \wedge \dot{\mathbf{y}} + \mathbf{y} \wedge \dot{\mathbf{x}}], \quad (2.22)$$

where \mathbf{J}_x and \mathbf{J}_y are the angular momentum for the single \mathbf{x} and \mathbf{y} coordinates respectively, and they can be expressed in the very much way as it is in eq.(2.7). From eq.(2.21) and (2.22) comes that:

$$\frac{d\Re[\mathbf{J}^C]}{dt} = \frac{d}{dt}[\mathbf{J}_x - \mathbf{J}_y] = 0, \quad (2.23)$$

and

$$\frac{d\Im[\mathbf{J}^C]}{dt} = \frac{d}{dt}[\mathbf{x} \wedge \dot{\mathbf{y}} + \mathbf{y} \wedge \dot{\mathbf{x}}] = 0. \quad (2.24)$$

As it was for the anisotropic C.H.O., it is still possible to separate the equation of motion for the isotropic case as well and easily verify that \mathbf{J}_x and \mathbf{J}_y are independently integrals of motion, which means that the equalities in eq.(2.23) and (2.24) are identically verified, as it is easy to show; in particular the second one happens to be just a validation for the antisymmetry of the cross product as we have been using it up to now:

$$\frac{d}{dt}[\mathbf{x} \wedge \dot{\mathbf{y}} + \mathbf{y} \wedge \dot{\mathbf{x}}] = 0, \quad \Longleftrightarrow \quad \mathbf{x} \wedge \mathbf{y} = -\mathbf{y} \wedge \mathbf{x}. \quad (2.25)$$

From there, as it was for the energy in the anisotropic case (which is still true

here), we can affirm that the complexification for the isotropic harmonic oscillator produce two dinamically indipendent, real harmonic oscillators, whose coordinates are linked by eq.(2.23) and have the same total angular momentum up to an arbitrary constant.

Maybe the extremely special nature of the harmonic oscillator, its completely analytical formulation, due to the fact the the force is proportional uniqueky to the position vector, makes that system not so interesting once complexified, reproducing just two almost identical systems, dinamically equivalent to their real progenitor.

Chapter 3

Complexification of the Coulomb potential

In this chapter we are going to study the properties for the complexified Coulomb potential. For Coulomb potential, is intended a tipology of central potential, which means a potential depending only on the radial distances from the source of the potential itself, in particular depending on the inverse of the radial distance; as it is known, the force acting on a test particle due to the presence of the potential field is given by the gradient of the potential itself and, for the Coulomb potential, this operation gives rise to a force proportional to the inverse square of the radial distance from the source of the force, which is nothing but the Newton's universal gravitation law.

In this respect, as the Coulomb potential allows to completely solve the two body problem, the complexification for this type of potential happens to play a fundamental step to understand the role of the complexification method in modelling more complicated potentials significantly departing from spherical symmetry.

3.1 Complex Coulomb potential

First, we recall the procedure of complexification of Coulomb potential, which means considering the following expression:

$$\Phi = -\frac{k}{\|\mathbf{x}\|}, \quad (3.1)$$

here k is a non-negative constant (always positive in the gravitational case with respect to the electrostatic one) and $\|\mathbf{x}\|$ is the norm of the vector position \mathbf{x} , defined as usual as the square root of the standar inner product of the position vector with itself.

Now the complex version of the above potential is obtained by replacing \mathbf{x} with the corresponding complex vector $\mathbf{z} = \mathbf{x} + i\mathbf{y}$, so that

$$\Phi^C = -\frac{k}{\|\mathbf{z}\|}, \quad (3.2)$$

where $\|\mathbf{z}\|$ is the "norm" over C^3 , obtained by means of the standard inner product over the reals, as described in the previous Chapter. Therefore, $\|\mathbf{z}\|$ is given by:

$$\|\mathbf{z}\| \equiv \langle \mathbf{z} | \mathbf{z} \rangle^{\frac{1}{2}} = (\|\mathbf{x}\|^2 - \|\mathbf{y}\|^2 + 2i\langle \mathbf{x} | \mathbf{y} \rangle)^{\frac{1}{2}}. \quad (3.3)$$

In order to separate the real and imaginary of Φ^C , let's multiply and divide (3.2) by the norm of complex conjugate of \mathbf{z} , \mathbf{z}^* , i.e. $\|\mathbf{z}^*\| = \langle \mathbf{z}^* | \mathbf{z}^* \rangle^{\frac{1}{2}} = [\|\mathbf{x}\|^2 - \|\mathbf{y}\|^2 - 2i\langle \mathbf{x} | \mathbf{y} \rangle]^{\frac{1}{2}}$, so that:

$$\Phi^C = -\frac{k}{\|\mathbf{z}\|} = -\frac{k}{\|\mathbf{z}\|\|\mathbf{z}^*\|} \|\mathbf{z}^*\| = -\frac{k}{[(\|\mathbf{x}\|^2 - \|\mathbf{y}\|^2)^2 + 4\langle \mathbf{x} | \mathbf{y} \rangle^2]^{\frac{1}{2}}} [\|\mathbf{x}\|^2 - \|\mathbf{y}\|^2 - 2i\langle \mathbf{x} | \mathbf{y} \rangle]^{\frac{1}{2}} \quad (3.4)$$

In order to explicitly separate the real and imaginary part, due to the presence of the square roots, it is convenient to convert the expression for \mathbf{z} from Cartesian to polar representation, so that we define in full generality:

$$\|\mathbf{z}\|^2 = \rho e^{i\theta}, \quad \|\mathbf{z}^*\|^2 = \rho e^{-i\theta}, \quad (3.5)$$

where:

$$\rho = [(\|\mathbf{x}\|^2 - \|\mathbf{y}\|^2)^2 + 4\langle \mathbf{x} | \mathbf{y} \rangle^2]^{\frac{1}{2}}, \quad \text{and} \quad \theta = \arctan \frac{2\langle \mathbf{x} | \mathbf{y} \rangle}{\|\mathbf{x}\|^2 - \|\mathbf{y}\|^2}. \quad (3.6)$$

Therefore we can write:

$$\|\mathbf{z}\| = \sqrt{\rho} e^{i\frac{\theta}{2}}, \quad \|\mathbf{z}^*\| = \sqrt{\rho} e^{-i\frac{\theta}{2}}. \quad (3.7)$$

In this way it is straight-forward to identify the real and imaginary part of the complex Coulomb potential:

$$\Re[\Phi^C] = -\frac{k}{\sqrt{\rho}} \cos \frac{\theta}{2}, \quad \text{and} \quad \Im[\Phi^C] = \frac{k}{\sqrt{\rho}} \sin \frac{\theta}{2}. \quad (3.8)$$

With this introductory exercise, we recovered the expression give by Lynden-Bell and we presented the basic idea behind the complexification technique. However, before proceeding with our work, a few comments are in order: first, it is quite remarkable the fact that the imaginary part of the complex potential happens to have the opposite sign compared to the real one for a generic value of θ .

Second, in the very same way, it is possible to repeat the algebraic manipulation for the equation of motion associated with Coulomb potential:

$$\ddot{\mathbf{z}} = -\frac{k}{\|\mathbf{z}\|^3} \mathbf{z}. \quad (3.9)$$

From this, by expressing the variables in terms of the real part and the imaginary part, we get:

$$\ddot{\mathbf{x}} + i\ddot{\mathbf{y}} = -\frac{k}{[\|\mathbf{x}\|^2 - \|\mathbf{y}\|^2 + 2i\langle\mathbf{x}|\mathbf{y}\rangle]^{\frac{3}{2}}}(\mathbf{x} + i\mathbf{y}). \quad (3.10)$$

Now, following the same procedure as in eq. (3.4), we come to the following expression:

$$\ddot{\mathbf{x}} + i\ddot{\mathbf{y}} = -\frac{k}{[(\|\mathbf{x}\|^2 - \|\mathbf{y}\|^2)^2 + 4\langle\mathbf{x}|\mathbf{y}\rangle^2]^{\frac{3}{2}}}(\|\mathbf{x}\|^2 - \|\mathbf{y}\|^2 - 2i\langle\mathbf{x}|\mathbf{y}\rangle)(\mathbf{x} + i\mathbf{y}) \quad (3.11)$$

From equation above it is apparent that it is possible to formally separate the equations of motion for the real and imaginary part of \mathbf{z} and to introduce the associated conservation laws (for example a complex energy E^C and a complex angular momentum \mathbf{J}^C , by repeating the geometrical treatment used in the real case). However, it is also clear that the two sets of coordinate \mathbf{x} and \mathbf{y} are mixed, as in the "force" expression they appear mixed. In a sense, this shows that while it is possible to use the complexification technique to

produce density-potential pairs from a shifted potential(as we will discuss in details in the next Chapters), it is not possible to "separate" the dynamical properties of the real and imaginary components of the shifted potentials, as we obtain for the equations of motion of \mathbf{x} and \mathbf{y} :

$$\ddot{\mathbf{x}} = -\frac{k}{\rho^{\frac{3}{2}}}[\cos \frac{3\theta}{2}\mathbf{x} + \sin \frac{3\theta}{2}\mathbf{y}], \quad (3.12)$$

and

$$\ddot{\mathbf{y}} = -\frac{k}{\rho^{\frac{3}{2}}}[-\sin \frac{3\theta}{2}\mathbf{x} + \cos \frac{3\theta}{2}\mathbf{y}], \quad (3.13)$$

where, as it is important to remark, $\rho = \rho(\mathbf{x}, \mathbf{y})$ and $\theta = \theta(\mathbf{x}, \mathbf{y})$.

Chapter 4

Complexification of General potentials

In this Chapter we analyze some previously unexplored dynamical properties of axi-symmetric potentials generated by a constant complex shift of a parent spherical symmetric system. In particular we focus on the epicyclic approximation, with the hope that in such limiting case possible integrability evidences will emerge while maintaining the mathematical treatment at a reasonable level of difficulty.

First, we consider the epicyclic frequencies; we obtain the complex analogous of the Rayleigh's formula for the radial epicyclic frequency, and we showed that this quantity can be purely real. Quite surprisingly, we show that the vertical epicyclic frequency can also be purely real, as for example in the specific case of the Plummer model discussed in detail in the following Sections. Second, we determine the general expression of the complex force in the equatorial plane (where epicyclic expansion is performed). It is shown that for general spherically symmetric parent systems, the radial force in the equatorial plane may be purely real. At the same time the vertical force may be purely imaginary, consistently with the vanishing of the mass associated with the imaginary part of the shifted density.

After that, in order to verify some of the results obtained for generic spherical potentials, we moved to study the axial potential generated by the complex shift of the Plummer model, recalling its main features. The equations of motion for a test particles in the shifted Plummer potential have been then obtained (also within the context of epicyclic theory) and studied, in order to extrapolate some initial information about the allowed orbits and their relation with the shift-vector.

Finally, the analysis conducted up to this moment has been repeated for the case of small shift.

4.1 Complex shifted spherical potential and Epicycles

As a first inspection, in this Section the formulae for the epicyclic frequencies, exposed in detail in Appendix A, will be recasted for a specific family of potentials, i.e. complex shifted spherically symmetric potential. As first step, let's notice that a complexified spherical potential can be written as:

$$\Phi(r) \rightarrow \Phi[\sqrt{R^2 + (z + ia)^2}] \equiv \Phi(r^C), \quad (4.1)$$

where it has been defined a "complex radius" $r^C = \sqrt{R^2 + (z + ia)^2}$. From there, one can recall the derivatives of the above potential with respect to the cylindrical coordinates R and z , obtaining:

$$\frac{\partial \Phi(r^C)}{\partial R} = \frac{\partial r^C}{\partial R} \frac{\partial \Phi(r^C)}{\partial r^C} = \frac{R}{\sqrt{R^2 + (z + ia)^2}} \frac{\partial \Phi(r^C)}{\partial r^C}, \quad (4.2)$$

and

$$\frac{\partial \Phi(r^C)}{\partial z} = \frac{\partial r^C}{\partial z} \frac{\partial \Phi(r^C)}{\partial r^C} = \frac{z + ia}{\sqrt{R^2 + (z + ia)^2}} \frac{\partial \Phi(r^C)}{\partial r^C}. \quad (4.3)$$

Note that the 2 expressions above give the complex force components.

At this point, applying one more time the derivation chain rule together with the very definition for the vertical epicyclic frequency and the Rayleigh's Formula for the radial epicyclic frequency, after some algebraic manipulation it is possible to write in a quite handful way the epicyclic frequencies for any generic shifted spherical potential:

$$k_R^2 = \frac{3R_0^2 - 4a^2}{[R_0^2 - a^2]^{\frac{3}{2}}} \left. \frac{\partial \Phi(r^C)}{\partial r^C} \right|_{r^C=\sqrt{R_0^2-a^2}} + \frac{R_0^2}{R^2 - a^2} \left. \frac{\partial^2 \Phi(r^C)}{\partial r^{C2}} \right|_{r^C=\sqrt{R_0^2-a^2}}, \quad (4.4)$$

and for the vertical one:

$$k_z^2 = \frac{R_0^2}{[R_0^2 - a^2]^{\frac{3}{2}}} \left. \frac{\partial \Phi(r^C)}{\partial r^C} \right|_{r^C=\sqrt{R_0^2-a^2}} - \frac{a^2}{R_0^2 - a^2} \left. \frac{\partial^2 \Phi(r^C)}{\partial r^{C2}} \right|_{r^C=\sqrt{R_0^2-a^2}}. \quad (4.5)$$

From the above expressions it is immediate to recognize that, first, not only the positiveness but also the reality of frequencies is not guaranteed, in particular the vertical one due to the presence of a minus sign and the square roots of the expression $R_0^2 - a^2$ (which are real for $R_0^2 \geq a^2$) in the denominators. Second, that, for $a = 0$, we re-obtain the usual expressions for the frequencies

in an ordinary spherical potential. However, as we will see, for the case the Plummer model, that singularity for the square roots is exactly cancelled out from the derivatives of the potential.

Nevertheless, it is quite remarkable that the epicyclic frequencies can actually be solely real, purely real numbers, even starting from a full complexified potential, without previously selecting either its real or imaginary part, as the normal procedure for the complexification of real physical quantities usually requires.

The complexification procedure will be extensively presented in next Section for the peculiar case of the Plummer model, from where it will be demonstrated in particular that the epicyclic frequencies calculated with the above method are the same obtained from the real part of the shifted Plummer potential. This interesting fact may indicate, at least in the case of shifted Plummer potential, that the epicyclic theory for nearly circular orbits subdue to a complexified spherical potential is affected only by the real part of the complex potential field, so its imaginary part does not have any dynamical role in the evolution of the stellar system, it does not "oscillate" at least in the equatorial plane; this seems to be a logical conclusion if we recall eq.(1.6), which states that the imaginary part of the density of any complex shifted stellar system, integrated over the whole space is identically zero, so that the imaginary part of the potential comes from an object of null mass. This appears to be consistent also with another dynamical consideration: in fact, for a shifted spherical potential $\Phi(r^C)$, the components of the force, i.e. the gradient of the potential with respect to the cylindrical coordinates (R, z) do exist and they are not trivially real, i.e.:

$$\begin{cases} F_R(R, z) \equiv -\frac{\partial\Phi(r^C)}{\partial R} = -\frac{R}{\sqrt{R^2+(z+ia)^2}} \frac{\partial\Phi(r^C)}{\partial r^C}, \\ F_z(R, z) \equiv -\frac{\partial\Phi(r^C)}{\partial z} = -\frac{z+ia}{\sqrt{R^2+(z+ia)^2}} \frac{\partial\Phi(r^C)}{\partial r^C}. \end{cases} \quad (4.6)$$

From there, dividing the two above equations for each other, it comes evident that the two components of the force field are proportional to one another and, in particular:

$$F_z(R, z) = \frac{z+ia}{R} F_R(R, z), \quad (4.7)$$

this last expression, where evaluated in the equatorial plane, for nearly circular orbit (epicyclic orbits), i.e. for $(R, z) = (R_0, 0)$, gives another

important information, in fact:

$$\begin{cases} F_R(R_0, 0) = -\frac{R_0}{\sqrt{R_0^2 - a^2}} \frac{\partial \Phi(r^C)}{\partial r^C} \Big|_{r^C = \sqrt{R_0^2 - a^2}}, \\ F_z(R_0, 0) = -\frac{ia}{\sqrt{R_0^2 - a^2}} \frac{\partial \Phi(r^C)}{\partial r^C} \Big|_{r^C = \sqrt{R_0^2 - a^2}}; \end{cases} \quad (4.8)$$

so that:

$$F_z(R_0, 0) = \frac{ia}{R_0} F_R(R_0, 0), \quad (4.9)$$

From eq. (4.8) and (4.9) it can be deduced that, for epicyclic trajectories, the radial component of the force is real for any kind of potential of the examined family (whose orbital families satisfy the request that $R_0^2 \geq a^2$ for the reality of the square roots), while the vertical component is purely imaginary and not identically zero, even though it comes from the imaginary part of the complex potential, being without mass as already said. So, even in the equatorial plane, there is an imaginary vertical force emerging from the complexification procedure, but eventually not affecting the epicyclic frequencies, so a force with no dynamical meaning apparently.

From what just said, it is evident that the starting point of all this work (so the attempt to generalize the complex shift method for time dependent shift vector, i.e. the complexification for Newton's second law of dynamics) seems to be incompatible with the complexification of the Poisson's equation, which is the starting point for the study we are going to exposed in the followings of this Chapter; in fact, if we start by considering a generic shifted potential:

$$\Phi(\mathbf{x}) \rightarrow \Phi(\mathbf{x} + i\mathbf{y}) \equiv \Phi^C(\mathbf{z}), \quad (4.10)$$

where \mathbf{y} is a generic time-dependent shift vector $\mathbf{y}(t)$, it can be recast as a complex potential, with a real and imaginary part $\Phi^C = \Re[\Phi^C] + i\Im[\Phi^C]$, which are generally function of both the real and imaginary of the complex variable \mathbf{z} , (\mathbf{x}, \mathbf{y}) . From there, the equations of motion for the real and imaginary part of the complexified variables are, as expected:

$$\begin{cases} \ddot{\mathbf{x}} = -\nabla_{\mathbf{x}} \Re[\Phi^C](x, y), \\ \ddot{\mathbf{y}} = -\nabla_{\mathbf{y}} \Im[\Phi^C](x, y). \end{cases} \quad (4.11)$$

At this point, if we take the particular case of a time-independent complex shift, which means a constant vector \mathbf{a} , as done for the standard complexification of Poisson's equation, some inconsistencies appears, in fact if we change

the definition of the complex variable as $\mathbf{z} = \mathbf{x} + i\mathbf{a}$, it come immediately that, for the equations of motion, we have:

$$\ddot{\mathbf{z}} = \ddot{\mathbf{x}}, \quad (4.12)$$

which implies that:

$$\nabla_{\mathbf{a}} \Im[\Phi^C](\mathbf{x}, \mathbf{y}) = 0, \quad (4.13)$$

so there should not be any "imaginary force" acting on the system, but what has been proved just above is exactly the opposite, except if the value $\mathbf{y} = \mathbf{a}$ is a critical point for the complex potential, which means:

$$\nabla_{\mathbf{y}} \Im[\Phi^C](\mathbf{x}, \mathbf{y})|_{\mathbf{y}=\mathbf{a}} = 0. \quad (4.14)$$

Thus, to emphasize once more this last point, it seems that the imaginary part of a complexified gravitational system cannot be defined as trivially null, but without playing any dynamical role in the evolution of the system itself.

Furthermore, if we now consider the expression for the angular velocity for circular epicyclic orbits in a general shifted potential,

$$\Omega_0^2 = \frac{J_z^2}{R_0^4},$$

we found that:

$$\Omega_0^2 = \frac{1}{\sqrt{R_0^2 - a^2}} \left. \frac{\partial \Phi(r^C)}{\partial r^C} \right|_{r^C = \sqrt{R_0^2 - a^2}}, \quad (4.15)$$

Comparing this last expression with that for the vertical frequency in eq. (4.5) it is evident that, in general,

$$k_z^2 \neq \Omega_0^2, \quad (4.16)$$

which means that the system resulting from the complexification of a generic spherically symmetric potential does not keep, generally speaking, the information from the parent system to have epicyclic closed orbits moving in a plane, as stated in the part of Appendix A dedicated to spherical systems.

Although what just explained, thinking in the opposite way, the condition to have planar orbits, i.e. $k_z^2 = \Omega_0^2$, in order to be satisfied, can be used as a constraint equation to identify those potentials with spherical symmetry that, once complexified, keep trace of that specific property; so, a complex shifted potential, in this context, must satisfy the following condition:

$$\left. \frac{\partial^2 \Phi}{\partial r^{C^2}} \right|_{r^C = \sqrt{R_0^2 - a^2}} - \frac{1}{\sqrt{R_0^2 - a^2}} \left. \frac{\partial \Phi}{\partial r^C} \right|_{r^C = \sqrt{R_0^2 - a^2}} = 0, \quad (4.17)$$

which, considering eq. (4.15), can be rewritten as:

$$k_z^2 = \frac{1}{R_0^2 - a^2} \left[R_0^2 \Omega_0^2 - a^2 \frac{\partial^2 \Phi}{\partial r^{C^2}} \right]_{r^C = \sqrt{R_0^2 - a^2}}. \quad (4.18)$$

The above equation can be, in principle, solved for $\Omega_0^2 = \Omega_0^2(R_0^2, a^2, \partial^2 \Phi)$ as function of the shift parameter, the circular radius R_0 and the second derivatives of the potential calculated for the value of the complex radius in the equatorial plane. In particular, it can be pointed out that, for small value of the shift parameter, the k_z and Ω_0 are indeed proportional, which is logic thinking that for $a \rightarrow 0$, the spherical case should be got back.

Recalling eq. (4.18) in the form exposed in eq. (4.17), it can be seen as a complete equation evaluated for $r^C = \sqrt{R_0^2 - a^2}$:

$$\left[\frac{\partial^2 \Phi}{\partial r^{C^2}} - \frac{1}{r^C} \frac{\partial \Phi}{\partial r^C} \right]_{r^C = \sqrt{R_0^2 - a^2}} = 0. \quad (4.19)$$

It is interesting to solve the above equation in general, for any value of r^C , re-writing it in the following form:

$$\frac{\Phi''(x)}{\Phi'(x)} = \frac{1}{x}, \quad (4.20)$$

where $x = r^C$ and the single and double apexes indicating first and second derivation with respect to x respectively. Integrating eq. (4.19) once we obtain:

$$\frac{d(\ln \Phi')}{d(\ln x)} = 1 \quad \Rightarrow \quad \ln \Phi'(x) = \ln x + C, \quad (4.21)$$

with C being an integrating constant; performing another integration, the final results for this treatment is obtained:

$$\Phi(x) = Ax^2, \quad (4.22)$$

where the second integration constant has been dropped because every potential is always defined up to a constant. What just achieved is important because it tells us that, for any value of r^C , the only family of potentials guaranteeing the resonance condition between the vertical epicyclic frequency and the deferent's angular velocity, is the harmonic potential. This is trivial because the epicyclic approximation is implemented as a series expansion of

the equations of motion for nearly circular orbits in the equatorial plane, leading to the equations of two independent harmonic oscillator in the meridional plane for the radial and vertical coordinates; but, of course, this does not confirm anything about the existence of other tipologies of potential satisfying the condition for the particular value of $r^C = \sqrt{R_0^2 - a^2}$.

Lastly, we remember that the resonance condition to have closed orbits, as presented up to now (see Appendix A) can be expressed more generally, because it is sufficient that the ratio between k_z^2 and Ω_0^2 is a positive rational number, i.e.:

$$k_z^2 = \frac{m^2}{n^2} \Omega_0^2 \quad (4.23)$$

So that, every m circular revolutions there are n vertical oscillations.

4.2 The Complex shift for the Plummer sphere

As first exercise, here some properties for the axisymmetric potential generated from the shifted Plummer sphere will be briefly recalled; keeping in mind that the complex shift here presented is implemented by a constant vector \mathbf{a} , the starting point is the relative potential $\Psi = -\Phi$, where:

$$\Psi(r) = \frac{GM}{b} \frac{1}{\sqrt{1+r^2}}, \quad (4.24)$$

where r is the norm of the position vector, normalized to the model scale-length b . By means of Poisson's equation, it is easy to see that the density distribution associated to the Plummer potential is:

$$\rho = \frac{3M}{4\pi b^3} \frac{1}{[1+r^2]^{\frac{5}{2}}}. \quad (4.25)$$

Following the notation adopted by Ciotti & Giampieri (2007), for sake of simplicity, potentials and densities will be rescaled by the normalized density (M/b^3) and potential (GM/b) so that, after the complexification of the radial variable, we have:

$$\rho^C = \frac{3}{4\pi} (\Re[\Psi^C] + i\Im[\Psi^C])^5, \quad (4.26)$$

where also the shift a , norm of the shift vector \mathbf{a} , is expressed in b units. As it is clearly to see, the shifted potential Ψ^C depends on the inverse square root of the expression $1 - a^2 + r^2 - 2iaz$ where $z = r \cos \theta$, being θ the

colatitude of the considered point defined by the position vector. Defining now the polar form of the above mentioned complex expression, in order to write in a suitable way its square root, we have:

$$w^2 \equiv 1 - a^2 + r^2 - 2iaz \equiv de^{i\phi}, \quad (4.27)$$

with

$$d = \sqrt{(1 - a^2 + r^2)^2 + 4a^2z^2} \quad \text{and} \quad \tan \phi = \frac{-2az}{1 - a^2 + r^2}, \quad (4.28)$$

and the interest is for values of $a < 1$, so that $\cos \phi$ is positive everywhere. The square root now is:

$$w = \sqrt{d}e^{i(\pi k + \phi/2)}, \quad (k = 0, 1), \quad (4.29)$$

and it is transformed into a single-valued function of (r, z) by cutting the complex plane along the negative real axis and assuming $k = 0$, so that the model's equatorial plane is mapped into the line $\phi = 0$. These choices are made to fulfill the requirement that the complex potential Ψ^C reduces to Ψ when $a = 0$, so that, by simple algebra, the real and imaginary part of Ψ^C are then given by:

$$\Re[\Psi^C] = \sqrt{\frac{d + 1 + r^2 - a^2}{2d^2}}, \quad \text{and} \quad \Im[\Psi^C] = \frac{az}{d^2\Re[\Psi^C]}, \quad (4.30)$$

and, from eq. (4.26), the expressions of the (normalized) axisymmetric densities are computed:

$$\Re[\rho^C] = \frac{3\Re[\Psi^C]}{4\pi} \left[\Re[\Psi^C]^4 - \frac{10a^2z^2}{d^4} + \frac{5a^4z^4}{d^8\Re[\Psi^C]^4} \right], \quad (4.31)$$

and

$$\Im[\rho^C] = \frac{3\Im[\Psi^C]}{4\pi} \left[5\Re[\Psi^C]^4 - \frac{10a^2z^2}{d^4} + \frac{5a^4z^4}{d^8\Re[\Psi^C]^4} \right]. \quad (4.32)$$

It is straight-forward to notice that, as $\Im[\Psi^C]$ changes sign crossing the equatorial plane, so it does the $\Im[\rho^C]$, which means that the density-potential pair cannot be used to model a gravitational system.

Focusing now on the real axisymmetric density-potential pair generated by the shifted Plummer sphere, we investigate now the asymptotic expansion for these objects near the origin, for $r \rightarrow 0$, and in the far field region, for

$r \rightarrow \infty$.

Near the origin, it is possible to write $d \approx 1 - a^2 + r^2[1 + 2a^2 \cos^2 \theta / (1 - a^2)]$, so that the leading terms for the real part of the complexified potential and density give:

$$\Re[\Psi^C] \approx \frac{1}{\sqrt{1 - a^2}} - \frac{r^2[1 - a^2(3 \cos^2 \theta - 1)]}{2(1 - a^2)^{\frac{5}{2}}}, \quad (4.33)$$

and

$$\Re[\rho^C] \approx \frac{3}{4\pi(1 - a^2)^{\frac{5}{2}}} - \frac{15r^2[1 - a^2(7 \cos^2 \theta - 1)]}{8\pi(1 - a^2)^{\frac{9}{2}}}, \quad (4.34)$$

where the omitted terms are all $O(r^4)$. It is important to remark that the isodensity curves are oblate ellipsoids with minor-to-major squared axis ratio $(1 - a^2)/(1 + 6a^2)$.

In the far field region $d \approx r^2 + 1 + a^2(2 \cos^2 \theta - 1)$ and so:

$$\Re[\Psi^C] \approx \frac{1}{r} - \frac{1 - a^2(3 \cos^2 \theta - 1)}{2r^3} + O(r^{-5}), \quad (4.35)$$

and

$$\Re[\rho^C] \approx \frac{15}{4\pi r^5} \left(\frac{1}{5} - \frac{1 - a^2(7 \cos^2 \theta - 1)}{2r^2} \right) + O(r^{-9}), \quad (4.36)$$

So that $\Re[\rho^C]$ coincides with the unshifted seed density and it is spherically symmetric and positive, for $0 < a < 1$.

Moreover, on the model equatorial plane $z = 0$ (where $d = 1 - a^2 + R^2$, and R is the cylindrical radius), the real part of the shifted Plummer potential coincides with the potential of a Plummer sphere of scale-length $\sqrt{1 - a^2}$. However, for $z \neq 0$, a negative term may arise in equation (4.31), and the positivity of $\Re[\rho^C]$ is not guaranteed for a generic value of the shift parameter in the range considered. Indeed, by numerical simulation, it has been revealed that $\Re[\rho^C]$ becomes negative on the symmetry axis $R = 0$ at $z \approx 0.81$ for $a = a_m \approx 0.588$; the negative density region then expands around this critical point for $a > a_m$.

Finally, the most relevant characteristic, as it is evident in Fig. 4.1, is the resulting toroidal shape of the model with the large shift, which reminds similar structures known in literature, as the Lynden-Bell flattened Plummer sphere.

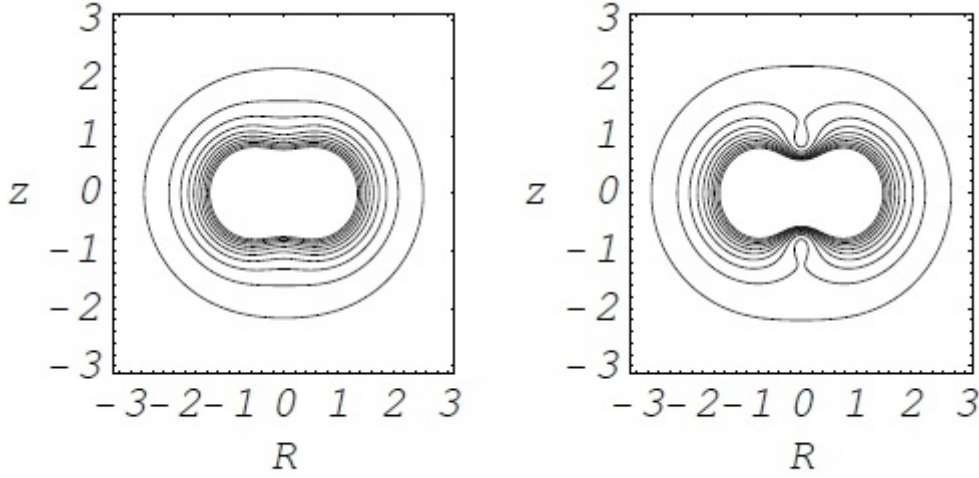


Figure 4.1: Isodensity contours in the (R, z) plane of $Re[\rho^C]$ of the shifted Plummer sphere for $a = 1/2$ (top left) and $a = 23/40$ (top right). The coordinates are normalized to the scale-length b of the corresponding seed spherical model.

4.3 Motion in shifted Plummer potential

In this Section the equations of motion for a test particle, i.e. a star, subject to the potential generated by the real part of the complex-shifted Plummer density distribution eq.(4.30), will be obtained in the most general way, in order to start outlining some properties of the orbits. From now on the focus will be just on $\Re[\Phi^C]$ because, as it is important to remark, the imaginary part of the density distribution, related to the imaginary part of the shifted potential, it is not everywhere positive, thus cannot describe a real gravitational system.

Due to the axial symmetry of the potential form, it comes natural to choose cylindrical coordinates (R, z, α) , where α is the azimuthal angle, to describe the position of the test particle, whose position vector can be written as:

$$\mathbf{x} = R\hat{\mathbf{e}}_R + z\hat{\mathbf{e}}_z, \quad (4.37)$$

where $\hat{\mathbf{e}}_R$, $\hat{\mathbf{e}}_z$ and, as it will be used later on, $\hat{\mathbf{e}}_\alpha$ are the unit vectors referring to the cylindrical frame of reference; differentiating now the position vector with respect to time t , we get the velocity vector:

$$\dot{\mathbf{x}} = \dot{R}\hat{\mathbf{e}}_R + R\dot{\alpha}\hat{\mathbf{e}}_\alpha + \dot{z}\hat{\mathbf{e}}_z, \quad (4.38)$$

and, differentiating once more, the acceleration:

$$\ddot{\mathbf{x}} = [\ddot{R} - R\dot{\alpha}^2]\hat{\mathbf{e}}_R + [2\dot{R}\dot{\alpha} + R\ddot{\alpha}]\hat{\mathbf{e}}_\alpha + \ddot{z}\hat{\mathbf{e}}_z, \quad (4.39)$$

Now, applying Newton's second Law $\mathbf{F} = m\mathbf{a}$, where m is the mass of the test particle (which will be taken unitary from now on), and:

$$\mathbf{F} = -m\nabla\Re[\Phi^C] = -\frac{\partial\Re[\Phi^C]}{\partial R}\hat{\mathbf{e}}_R - \frac{\partial\Re[\Phi^C]}{\partial z}\hat{\mathbf{e}}_z - \frac{\partial\Re[\Phi^C]}{R\partial\alpha}\hat{\mathbf{e}}_\alpha, \quad (4.40)$$

where the Gradient has been derived in cylindrical coordinates of course. The equations of motion, in each coordinate direction, after some simple algebraic passages become:

$$\begin{cases} \ddot{R} - R\dot{\alpha}^2 = \frac{R}{2d^4\Re[\Phi^C]}[d^2 - d(1 - a^2 + R^2 + z^2) - 2(1 - a^2 + R^2 + z^2)^2], \\ \ddot{z} = \frac{z}{2d^4\Re[\Phi^C]}[d^2 - d(1 + a^2 + R^2 + z^2) - 2(1 - (a^2 + R^2 + z^2)^2)], \\ 2\dot{R}\dot{\alpha} + R\ddot{\alpha} = 0. \end{cases} \quad (4.41)$$

Note that, following the indications from previous section, all the quantities are scaled by characteristic length or potential, in order to work with dimensionless expressions. Moreover, in order to simplify the comprehension of the parallel with previous notation, the cylindrical coordinate R and z are related to the spherical radius r and the colatitude θ by:

$$r = \sqrt{R^2 + z^2} \quad \text{and} \quad \theta = \arctan \frac{z}{R}. \quad (4.42)$$

Now, considering the third equation in (4.41) and multiplying it by R , it becomes:

$$\frac{d}{dt}[R^2\dot{\alpha}] = 0, \quad (4.43)$$

which is nothing but the conservation of the z -component of the specific angular momentum (angular momentum per unit mass):

$$J_z \equiv R^2\dot{\alpha} = \text{const.} \quad (4.44)$$

So it has been recalled the general property of an axisymmetric potential, $\Phi(R, z)$ that the angular coordinate α happens to be cyclic for a test particle, which means that the system is invariant under spatial rotation around the axis of symmetry $R = 0$, and this property corresponds indeed to the conservation of the vertical component of the angular momentum.

At this point, eliminating the angular coordinate α from equations of motion for \ddot{z} and \ddot{R} , thanks to the angular momentum conservation, and defining the following quantities for sake of simplicity:

$$\mathcal{F}(R, z, a) = d^2 - d(1 - a^2 + R^2 + z^2) - 2(1 - a^2 + R^2 + z^2)^2, \quad (4.45)$$

and

$$\mathcal{G}(R, z, a) = d^2 - d(1 + a^2 + R^2 + z^2) - 2(1 - (a^2 + R^2 + z^2)^2), \quad (4.46)$$

the system (4.41) can be rewritten in a more handfull way as:

$$\begin{cases} \ddot{R} - \frac{J_z^2}{R^3} = \frac{R}{2d^4 \Re[\Phi^C]} \mathcal{F}(R, z, a), \\ \ddot{z} = \frac{z}{2d^4 \Re[\Phi^C]} \mathcal{G}(R, z, a). \end{cases} \quad (4.47)$$

4.3.1 Epicyclic theory for the shifted Plummer sphere

After the equations of motion for a particle in the axially symmetric potential generated by the real part of the constant complex-shifted Plummer model have been set, to start analyzing some characteristics of the orbits, the Epicyclic approximation will be applied to eq.(4.41); in order to do so, first of all, following the directives presented in Appendix A (where the main features of the epicyclic theory are extensively explained), the effective potential Φ_e will be defined as:

$$\Phi_e = \Re[\Phi^C] + \frac{J_z^2}{2R^2}. \quad (4.48)$$

So that, considering the meridional plane $\mathbb{R}_m^2 = (R, z)$, rotating with the angular velocity of the test mass $\dot{\alpha}(t)$, the equations of motion for the radial and vertical coordinates can be rewritten in the conservative form expressed in eq. (6.12) of Appendix A. At this point, let us focus on near circular orbits in equatorial plane $z = 0$ at a fixed radius $R = R_0$; now expanding in series the equations of motion in the meridional plane, for a little radial displacement $\epsilon = R - R_0$, and truncating the expansion up second order terms, the following set of equations is obtained:

$$\begin{cases} \ddot{\epsilon} = -k_R^2 \epsilon, \\ \ddot{z} = -k_z^2 z. \end{cases} \quad (4.49)$$

where the radial and vertical epicyclic frequencies are the second derivative

of the effective potential, with respect to R and z respectively, calculated for $(R, z) = (R_0, 0)$. So it becomes evident that to study the stability of this orbits, the epicyclic frequencies have to be positive defined. Before explicitly expressing those frequencies for the above system of equations, let us write down the frequencies of the epicyclic approximation for a particle moving in the unshifted Plummer potential $\Phi(r) = 1/\sqrt{1+r^2}$ where, as usual, the spherical radius r is related to the cylindrical coordinates by the relation $r = \sqrt{R^2 + z^2}$; so, by applying the very definition for the epicyclic frequencies, we get for the Plummer sphere:

$$\begin{cases} k_R^{2(unshift)} = \frac{4+R_0^2}{[1+R_0^2]^{\frac{5}{2}}}, \\ k_z^{2(unshift)} = \frac{1}{[1+R_0^2]^{\frac{3}{2}}}, \end{cases} \quad (4.50)$$

which means that stable quasi circular orbits always exists in such a potential, because the epicyclic frequencies are always positive, for any value of R_0 .

Now, re-applying the definition for the epicyclic frequencies (or in an equivalent manner Rayleigh's formula for the radial frequency) for the case of complex shifted Plummer sphere, after some tedious but not difficult algebraic simplifications, it can be written:

$$\begin{cases} k_R^{2(shift)} = \frac{4+R_0^2-4a^2}{[1+R_0^2-a^2]^{\frac{5}{2}}}, \\ k_z^{2(shift)} = \frac{1+R_0^2+2a^2}{[1+R_0^2-a^2]^{\frac{5}{2}}}. \end{cases} \quad (4.51)$$

First it can be noticed that, for $a \rightarrow 0$, the expressions for the unshifted Plummer model are obtained, as first hint to verify the goodness of the adopted approximation. Second and most importantly, for $a < 1$ (which is the case we are interested in from now on, as pointed out in previous Section) both frequencies are real and positive.

Third, for completeness, the general formulas for the frequencies (although they are quite cumbersome), meant as functions of the cylindrical coordinates as well as the shift parameter (R, z, a) , are now reported:

$$\begin{aligned} k_R^2(R, z, a) = & \frac{\mathcal{F}}{2d^4\Re[\Phi^C]} \left[1 - \frac{2R^2}{d^2}(1 - a^2 + r^2) - \frac{R^2\mathcal{F}}{d^4\Re^2[\Phi^C]} - \right. \\ & \left. + \frac{4R^2}{\mathcal{F}}(1 - a^2 + r^2) - \frac{(1 - a^2 + r^2)^2}{d} \right] + \frac{3J_z^2}{R^4}, \end{aligned} \quad (4.52)$$

and

$$k_z^2(R, z, a) = \frac{\mathcal{G}}{2d^4\Re[\Phi^C]} \left[1 - \frac{8z^2}{d^2}(1 - a^2 + r^2) - \frac{z^2\mathcal{G}}{2d^4\Re^2[\Phi^C]} + \right. \\ \left. + \frac{2z^2}{d^4\mathcal{G}\Re[\Phi^C]}(d + (1 - a^2 + r^2)^2 + 2(1 - a^2 + r^2)) \right] \quad (4.53)$$

with the functions $\mathcal{F}(R, z, a)$ and $\mathcal{G}(R, z, a)$ defined in eq. (4.45) and (4.46). In particular in eq.(4.52), the value of J_z^2 is been derived, like for the unshifted potential and as always in the following, from the centrifugal balance, i.e. eq. (6.21):

$$J_z^2 = J_c^2(R_0, 0) = R^3 \frac{\partial Re[\Phi^C]}{\partial R} \Big|_{(R_0, 0)} = - R^3 F_R(R, z) \Big|_{(R_0, 0)}, \quad (4.54)$$

with F_R being the force in the R -direction, i.e. the right-hand side of first equation in system (4.41). In order to be clearer, let us point out that, for the unshifted Plummer potential, the angular momentum squared reads:

$$J_z^2 = \frac{R_0^4}{[1 + R_0^2]^{\frac{3}{2}}}, \quad (4.55)$$

while, for the real part of shifted Plummer model, we have:

$$J_z^2 = \frac{R_0^4}{[1 + R_0^2 - a^2]^{\frac{3}{2}}}. \quad (4.56)$$

Recalling now the system (4.51), in order to have $k_R^2, k_z^2 \geq 0$, and for the existence of the expressions for frequencies themselves, due to the positiveness of the square roots, it is quickly evident that k_z^2 is always positive, while k_R^2 must satisfy the following conditions:

$$\begin{cases} k_R^2 \geq 0 & \iff a < \sqrt{\frac{4+R_0^2}{4}}, \\ k_z^2 \geq 0 & \forall R_0, \end{cases} \quad (4.57)$$

where the above conditions guarantee also the existence of the square root; it is important to remember that all the quantities are scaled to the characteristic length b of the Plummer model.

Finally, in order to extrapolate some more useful information about the stability of the orbits of the epicycles for test mass in Plummer potential,

due to the fact that in the expressions for the epicyclic frequencies the shift is always of order squared (so it is not possible, in principle, to connect analitically k_R and k_z eliminating the constant complex parameter a), it is indeed possible to study the ratio between the above mentioned frequencies, that is:

$$\mathbb{R} \equiv \frac{k_R^2}{k_z^2},$$

which becomes, for the unshifted values:

$$\mathbb{R}^{(unshift)} = \frac{4 + R_0^2}{1 + R_0^2}. \quad (4.58)$$

Writing the above equation as:

$$\mathbb{R}^{(unshift)} = 1 + \frac{3}{1 + R_0^2},$$

it becomes evident that, for no values of the circular radius R_0 , the radial and vertical epicyclic frequencies can have the same value and they can be in a rational proportional ratio, i.e. $\mathbb{R}^{(unshift)} = n$ with $n \in \mathbb{Z}$ iff:

$$R_0^2 = \frac{4 - n}{n - 1}, \quad (4.59)$$

and, due to the positiveness of R_0^2 and, the range of values for n is $1 < n \leq 4$.

Lastly, by definition of the angular velocity for deferent orbit, $\Omega_0 \equiv J_z/R_0^2$, it is immediate to verify that:

$$\frac{\Omega_0}{k_R} = \sqrt{\frac{1 + R_0^2}{4 + R_0^2}}. \quad (4.60)$$

It is remarkable that the above ratio is equal to the opposite of the square rooted frequencies ratio, so that it does happen to have $\Omega_0^2 = k_z^2$ for every R_0 . By means of the previous equation, it is possible to conclude that the ratio between the semi-major and semi-minor axis of the elliptic epicycles is equal to 2 times the ratio between the circular angular velocity and the radial epicyclic frequency, which means that the the axis ratio is not constant everywhere like for the Coulomb-like potential presented in Appendix A (while it can be easily shown that $\Omega_0^2 = k_z^2$, as proved in the just mentioned Appedix), and in order for the ratio to be equal to a rational number n , it has to be:

$$R_0^2 = \frac{1 - 4n^2}{n^2 - 1} \quad \text{with} \quad \frac{1}{2} < n < 1. \quad (4.61)$$

Going back now to the epicyclic frequencies for the shifted Plummer sphere, the "frequencies ratio" can be expressed as follows:

$$\mathbb{R}^{(shift)} = \frac{4 + R_0^2 - 4a^2}{1 + R_0^2 + 2a^2}, \quad (4.62)$$

and it can be rewritten in terms of the unshifted ratio as:

$$\mathbb{R}^{(shift)} = \mathbb{R}^{(unshift)} \left[\frac{1 - \frac{4a^2}{4+R_0^2}}{1 + \frac{2a^2}{1+R_0^2}} \right], \quad (4.63)$$

which exist and it is positive for any value of a and R_0 .

Now, in order for the above proportion to be equal to a rational number n , the norm of the shift vector \mathbf{a} has to be:

$$a^2 = \frac{(4 - n) + (1 - n)R_0^2}{2(n + 2)}, \quad (4.64)$$

and for the positiveness of frequencies ratio, the condition $a^2 < (4 + R_0^2)/4$ (it is important to remark that it comes from the positiveness condition for the radial epicyclic frequency only because the vertical one is always positive) becomes, in terms of n :

$$\frac{-3n(2 + R_0^2)}{2(n + 2)} \leq 0. \quad (4.65)$$

So, with respect to the different values of R_0^2 , for any value of n , the frequency ratio happens to be positive.

Moving on, as the previous case, with the goal to study the axis ratio of the elliptic epicycle, the expression of the angular velocity of the circular orbit in shifted Plummer model can be obtained as:

$$\Omega_0^2 = \frac{1}{(1 + R_0^2 - a^2)^{\frac{3}{2}}}, \quad (4.66)$$

which, this time, happens *not* to be equal to the vertical epicyclic frequency k_z . Writing now the axis ratio as before (eq.(6.34)), we obtain:

$$\frac{b}{a} = 2 \frac{\Omega_0}{k_R} = 2 \sqrt{\frac{1 + R_0^2 - a^2}{4 + R_0^2 - 4a^2}}, \quad (4.67)$$

it depends on the specific value of R_0 and it can be indeed reconducted to the unshifted case simply imposing $a = 0$, but it can also set some constraints on the allowed values of a or R_0 in order to have a rational proportion n ; but it is immediate to see that the axis ratio is very similar to the inverse of the frequencies ratio, so that the conditions of existence and resonance valid for the frequencies ratio will be slightly revised also for the latter one. In particular this time, due to square root, the positiveness of the ratio is requested for the existence of the ratio itself, so that:

$$a^2 < \frac{4 + R_0^2}{4} \vee a^2 > 1 + R_0^2 \quad \forall R_0, \quad (4.68)$$

with the positiveness of all the reported quantities guaranteed by evidence. Having defined the existence conditions for the axis ratio, the request for the deferent's angular velocity and the radial frequency to be in resonance, i.e. $\Omega_0^2/k_r^2 = n^2$ leads to:

$$a^2 = \frac{(1 + R_0^2) - (4 + R_0^2)n^2}{1 - 4n^2}. \quad (4.69)$$

At this point it is to notice that the positiveness of a^2 as function of n^2 is guaranteed for:

$$a^2 \geq 0 \iff n^2 < \frac{1}{4} \vee n^2 \geq \frac{1 + R_0^2}{4 + R_0^2}, \quad (4.70)$$

and by quick and simple algebraic manipulation, it can be checked that the existence, as well as the positiveness, of the axis ratio is assured for any value of n^2 different from $\frac{1}{4}$.

Moving forward with the considerations about the obtained results, it is particularly useful for comparison with next Section to take back the expression for the shifted frequencies ratio in eq.(4.63) and expanding it in series for small value shift parameter a ; retaining the leading terms, this yields:

$$\mathbb{R}^{(shift)} \approx \mathbb{R}^{(unshift)} \left[1 - \frac{2(2 - R_0^2)}{(1 + R_0^2)(4 + R_0^2)} a^2 \right]. \quad (4.71)$$

As final remarkable issue to point out, to test the approach exposed in previous Section about generic shifted spherical potential, it comes natural to apply the above mentioned formulae (eq. (4.4) and (4.5)) for the epicyclic frequencies to the complexified Plummer model, written this time in a simpler way as:

$$\Phi^{PL}(r^C) = -\frac{1}{\sqrt{1 + r^C{}^2}}. \quad (4.72)$$

At this stage, applying eq. (4.4) and (4.5) to the above expression, it is easy to check that the very same expression in eq. (4.51) are obtained.

Beyond the first glance to the legitimacy of the approach just exposed given by this first test onto the shifted Plummer sphere, a couple of remarkable properties should be outlined here:

- 1 The epicyclic frequencies happen to be purely real (within the considered range for the shift parameter $a < 1$), as already proved and so here further verified, even though the starting point was the full complexified Plummer potential, without selecting its real or imaginary part.
- 2 For the specific case of the Plummer model, it is noticeable that all eventual degeneracy for $R_0 = a$ in the expressions for the epicyclic frequencies are exactly cancelled out, therefore excluding critical behavior at $R_0 = a$ for a circular orbit in meridional plane.

Lastly, the condition on the potential to have planar, closed orbits presented in eq. (4.17) coming from the equality between vertical epicyclic frequency $k_z^{2(PL)}$ and deferent angular velocity $\Omega_0^{2(PL)}$, can be turned, for the shifted Plummer model, into an algebraic quadratic equation of 6th degree for the shift parameter a to be satisfied as function of the circular radius R_0 , i.e.:

$$a^6 + (2 - 3R_0^2)a^4 + (3R_0^4 + 8R_0^2 + 5)a^2 - (R_0^6 + R_0^4 - R_0^2 - 1) = 0, \quad (4.73)$$

or, in the very same way, into a 6th-graded algebraic equation for R_0 as function of the shift vector length a , kept as parameter:

$$R_0^6 + (1 - 3a^2)R_0^4 + (3a^4 - 8a^2 - 1)R_0^2 - (a^6 + 2a^4 + 5a^2 + 1) = 0, \quad (4.74)$$

whose solutions can be found, in principle, analitically with easy but tedious arithmetic manipulations. The explicit solutions will not be presented here, but it can be said that among the six roots of each of the above equations, just 2 are real, thus acceptable, because all the others are pure imaginary, so they are not acceptable because this would mean that the shift vector is imaginary, thus the whole shift would become a normal real shift. And finally, as it is for the Plummer model, both a and R_0 enter the formulas squared, these means that there is a unique correspondence between the two quantities in order to preserve the resonance between Ω_0^2 and k_z^2 .

4.3.2 Motion in Plummer potential with $a \rightarrow 0$

In this Section, the same methodology applied for general shifted Plummer potential, will be now applied in the very same way for $\Re[\Phi^C]$ expanded in series of a , truncated to the second order, i.e up to $O(a^2)$. Because the path to the wanted results will be exactly the same as before, just the main expressions for the important quantities will be presented, together with all the considerations about them. Basically, all the approximations we are going to carry out come from the expansions in series to the first leading order of the square root of $(1+x)$, with the x being function of the normalized shift parameter a , considering a little shift, i.e. $a \ll 1$, such that:

$$\sqrt{1+x} \sim 1 + \frac{1}{2}x + O(x^2). \quad (4.75)$$

So, first of all, taking back the expression for the real part of the shifted Plummer model:

$$\Re[\Phi^C] = -\sqrt{\frac{1 - a^2 + r^2 + d}{2d^2}}, \quad (4.76)$$

with the usual definition for the spherical radius r in terms of cylindrical coordinates (R, z) , and with the definition for the norm of the complex variable obtained by adding the constant shift vector, that will be here recalled:

$$d = \sqrt{(1 - a^2 + r^2)^2 + 4a^2z^2}. \quad (4.77)$$

Keeping those in mind, the first step is to approximate d for little values of the shift parameter and, truncating the series expansion to the first leading order, we get:

$$d \sim (1 + r^2) \left[1 + \frac{2z^2 - (1 + r^2)}{(1 + r^2)^2} a^2 \right] + O(a^4). \quad (4.78)$$

Inserting eq. (4.78) in the formula for the potential yields:

$$\Re[\Phi^C] \sim -\frac{1}{\sqrt{1+r^2}} \left[1 - \frac{3z^2 - (1 + r^2)}{2(1 + r^2)^2} a^2 \right] + O(a^4). \quad (4.79)$$

It is remarkable that the shift parameter acts like a repulsive correction to the original spherical model in the elliptical region defined by the relation

$$R^2 \leq 2z^2 - 1$$

, beyond the fact that it carries all the information about the axial simmetry of the generated potential.

At this point, it is possible to derive the equations of motion for a test mass in this potential, which are very much the same as in eq. (4.41), leading to the same conservation of the vertical component of the angular momentum J_z and so the possibility to reduce the degrees of freedom to the (R, z) -plane, useful for the application of the epicyclic approximation; as first step, for sake of completeness, the expression for the radial and vertical components (the only non zero ones) of the force field generated by the approximate potential will be here reported:

$$\begin{cases} F_R = -\frac{R}{(1+r^2)^{\frac{3}{2}}} \left[1 + \frac{3(1+R^2+2z^2)}{2(1+r^2)^2} a^2 \right], \\ F_z = -\frac{z}{(1+r^2)^{\frac{3}{2}}} \left[1 - \frac{9(1+R^2)}{2(1+r^2)^2} a^2 \right]. \end{cases} \quad (4.80)$$

Considering now the epicyclic theory applied to a test mass subject to force field generated by the approximated shifted Plummer potential, described in eq. (4.79), in a completely analogous way as done before for the full shifted Plummer sphere, the radial and vertical epicyclic frequencies are derived by evaluating the expression for the frequencies at $(R, z) = (R_0, 0)$, obtaining the following:

$$\begin{cases} k_R^{2(approx.)} = \frac{4+R_0^2}{[1+R_0^2]^{\frac{5}{2}}} \left[1 + \frac{3}{2(1+R_0^2)} a^2 \right], \\ k_z^{2(approx.)} = \frac{1}{[1+R_0^2]^{\frac{3}{2}}} \left[1 - \frac{9}{2(1+R_0^2)} a^2 \right]. \end{cases} \quad (4.81)$$

These may be re-written in a more explicit way as:

$$\begin{cases} k_R^{2(approx.)} = k_R^{2(unshift)} \left[1 + \frac{3}{2(1+R_0^2)} a^2 \right], \\ k_z^{2(approx.)} = k_z^{2(unshift)} \left[1 - \frac{9}{2(1+R_0^2)} a^2 \right]. \end{cases} \quad (4.82)$$

From there it becomes immediately evident that the radial frequency is proportional to the unshifted Plummer spherical potential, with the proportionality constant being everywhere positive, so all the considerationd presented for the radial epicyclic frequency are valid also in this case, in particular the fact that the radial frequency being everywhere positive guarantees the existence of radial quasi circular stable orbits; at the contrary, for the vertical frequency's positiveness, in terms of the shift parameter a , it has to be:

$$a^2 \leq \frac{2(1+R_0^2)}{9} \quad \Rightarrow \quad a \leq \sqrt{\frac{2(1+R_0^2)}{9}}, \quad (4.83)$$

which is positive for every value of R_0 .

Moreover, considering the ratio between the epicyclic frequencies for this system, it is possible to write:

$$\frac{k_R^2(\text{approx.})}{k_z^2(\text{approx.})} \equiv \mathbb{R}(\text{approx.}) = \frac{4 + R_0^2}{1 + R_0^2} \left[\frac{1 + \frac{3}{2(1+R_0^2)}a^2}{1 - \frac{9}{2(1+R_0^2)}a^2} \right], \quad (4.84)$$

which can be written in a more useful form as:

$$\mathbb{R}(\text{approx.}) = \mathbb{R}(\text{unshift}) \left[\frac{1 + \frac{3}{2(1+R_0^2)}a^2}{1 - \frac{9}{2(1+R_0^2)}a^2} \right], \quad (4.85)$$

where $\mathbb{R}(\text{unshift})$ is the frequency ratio for the unshifted Plummer sphere, i.e. eq.(4.58). Applying another series expansion to the above presented equation, retaining just the leading term, brought to:

$$\mathbb{R}(\text{approx.}) = \mathbb{R}(\text{unshift}) \left[1 + \frac{6}{1 + R_0^2}a^2 \right], \quad (4.86)$$

where it is noticeable the similarity with eq. (4.73), although the different coefficient for the a^2 term, probably due to the deeper level of approximation of latter expression.

At the end, considering the issue concerning the axis ratio and eventual resonances between the deferent's angular velocity and the radial epicyclic frequency, it has been already noticed that the $k_R^2(\text{approx.}) = C k_R^2(\text{unshift})$, with C being positive constant; it is also quite simple to verify that

$$\Omega_0^2(\text{approx.}) = \frac{1}{[1 + R_0^2]^{\frac{3}{2}}} \left[1 - \frac{3}{2(1 + R_0^2)}a^2 \right]. \quad (4.87)$$

So the axis ratio for the approximated shifted Plummer model happens to be smaller than the axis ratio for the unshifted Plummer potential and, in particular, as the ratio between the semi-major and semi-minor axis of the elliptic epicycles is equal to 2 times the ratio between the circular angular velocity and the radial epicyclic frequency, this means that the axis ratio is not constant everywhere and in order for that ratio to be equal to a rational number n , it has to be:

$$R_0^2 = \frac{n^2 - 1 + \sqrt{n^4 + 14n^2 + 1}}{2} \quad \forall n. \quad (4.88)$$

In the end, one more result can be outlined; comparing the expression for the vertical epicyclic frequency, in the approximated potential, in eq. (4.82), with that for the square of the circular angular velocity in eq.(4.87), and considering the ratio between those quantities, we have:

$$\frac{k_z^{2(\text{approx.})}}{\Omega_0^{2(\text{approx.})}} = \frac{1 - \frac{9a^2}{2(1+R_0^2)}}{1 - \frac{3a^2}{2(1+R_0^2)}}, \quad (4.89)$$

where use has been made of the fact that the resonance condition is valid in the unshifted (spherical) case. From eq. (4.89) we deduce that there is no possibility, at least in the case of the approximated shifted Plummer potential for small shift, to have $k_z^2 = \Omega_0^2$ (as the above ratio, in order to be equal to 1, requires that $3 = 1$, obviously false). Nevertheless, nothing precludes the possibility to maintain the resonance condition (so the information about some integrability property) for other values of the shift parameter a and for other families of axially symmetric systems generated from a spherical seed density-potential pairs.

This concludes our dissertation about the properties of shifted spherically symmetric potential and the about the first dynamical characteristics for the orbits in a shifted Plummer potential.

Chapter 5

Astrophysical consequences

In this last Chapter we attempt to list and preliminarily discuss some possible applications of the presented framework.

As a premise, we stress that the following discussion is based on the shifted Plummer model, but this is not a conceptual restriction because the discussion could be extended not much difficulty to shifted model obtained from general spherically symmetric density-potential pairs.

5.1 Epicyclic frequencies and energies

Following the discussion in the previous Chapter, concerning the possible existence of special resonant orbits with $k_z^2 = \Omega_0^2$, in fig. 5.1 and 5.2 we show the trend, as a function of R_0 of the vertical epicyclic frequency and of the deferent's angular velocity, respectively. The curves are relative to different values of the shift parameter a , ranging from $a = 0$ (the spherical plummer model), where $k_z^2 = \Omega_0^2$ at all radii (see discussion in appendix A) to $a_M \sim 0.588$, the maximum value corresponding to a nowhere negative real density distribution.

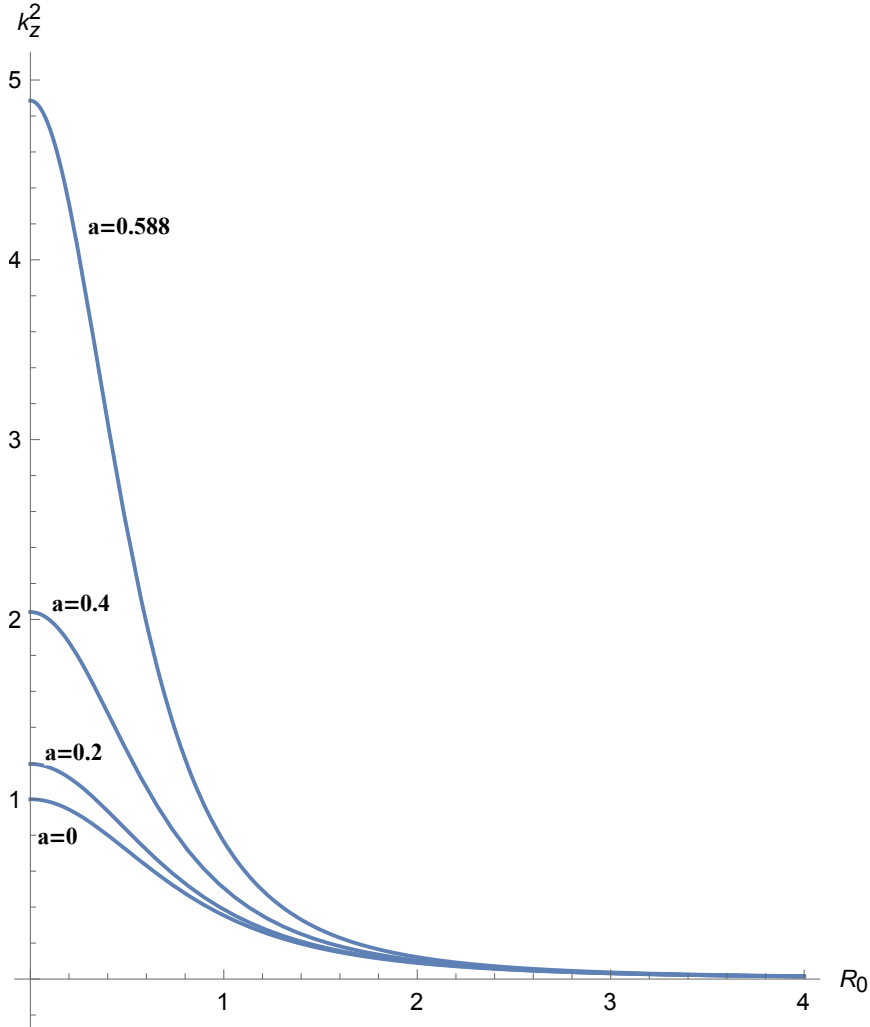


Figure 5.1: k_z^2 , as function of R_0 , for the shift parameter $a = 0, 0.2, 0.4, 0.588$

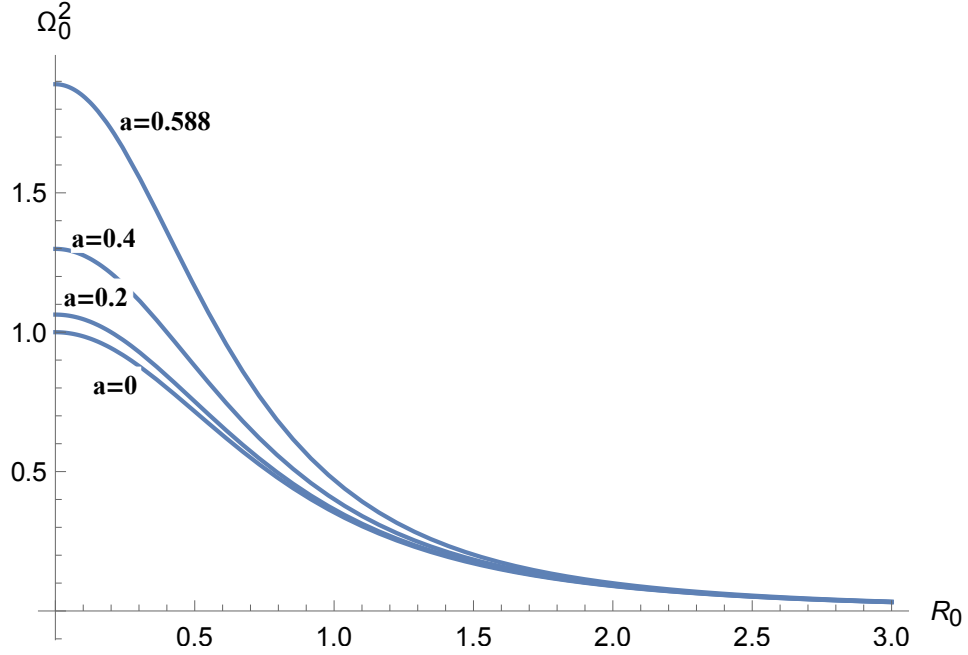


Figure 5.2: Ω_0^2 , as function of R_0 , for the shift parameter $a = 0, 0.2, 0.4, 0.588$

In general, at fixed R_0 , the curves are higher for higher values of shift parametr a . About the existence for the maximum value of a , the value $a_M = 0.588$ has been chosen accordingly to what was found by Ciotti & Giampieri (2007) where it has been stated that, by numerical exploration, it appears that the real part of the shifted Plummer sphere describes a real gravitating system not for all possible value of the parameter a , but instead for values of a such that $a \leq a_M$.

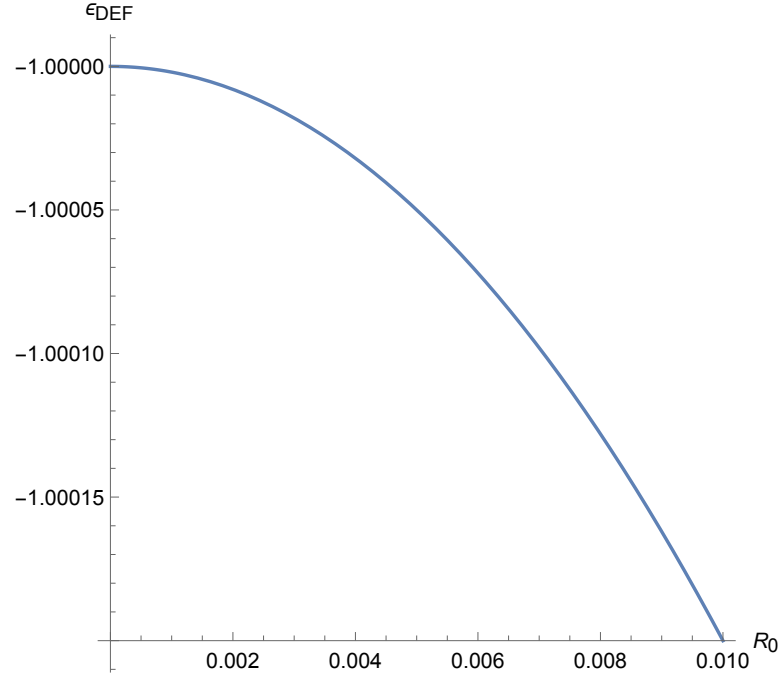
It can be argued, at a first glance, that the trend for both vertical frequency and circular angular velocity are much the same, also because the curves reach their peaks at $R_0 = 0$ for increasing values of a (in particular, as expected, the curves of k_z^2 and Ω_0^2 for the value of the shift parameter $a = 0$ are exactly the same, confirming the validity of the resonance condition in the spherical case), so that it could be that the complexified potential keeps memory, in some way, of the symmetric properties from the parent distribution, and it could be indeed, but the scales are totally different and also the slope of the curves for the k_z^2 are steeper than those for Ω_0^2 ; so, generally speaking, it cannot be stated for sure that the resonance properties of the orbits are conserved for the allowed values of a (in fact, at least for small values of a the resonance condition is not satisfied as verified at the end of previous Chapter); nevertheless, it can be possible that some orbits, associ-

ated to specific values of the complex parameter, may have memory of that resonance.

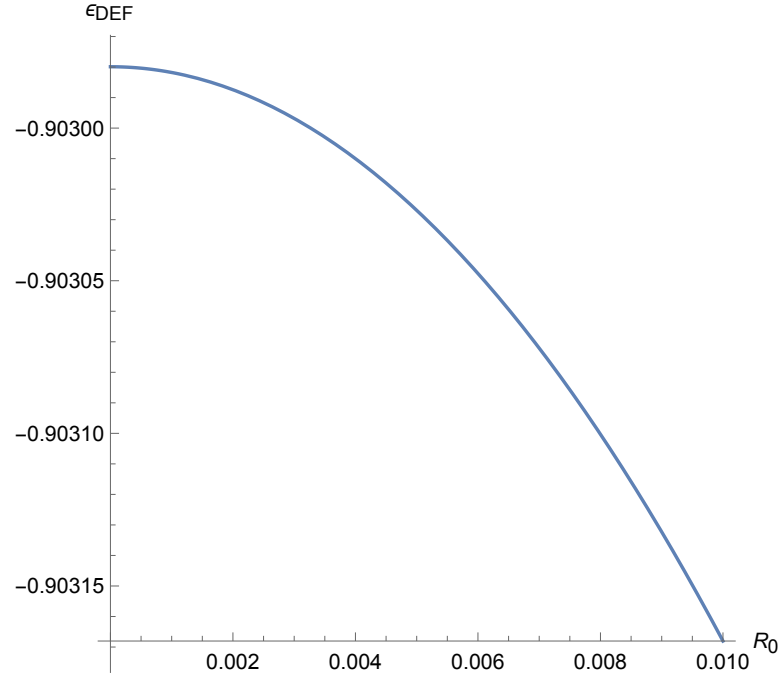
This results is quite interesting because it represents a nice and clean example of a possibly non integrable dynamical system with some integrability property dependent on specific orbits, a situation that was already encountered and duscussed by Hunter (D. Lynden-Bell, private communication).

In order to prepare for the discussion to be carried out in the next Section, we conclude by obtaining the energy associated with circular orbits in the equational plane, as function of the orbital radius R_0 . This quantity is important because it represents the minumum value of the energy for each orbital family. Simple calculations show that, for the Plummer model, we have:

$$E_{DEF}(R_0) = -\frac{2 + R_0^2 - 2a^2}{2(1 + R_0^2 - a^2)^{\frac{3}{2}}} . \quad (5.1)$$

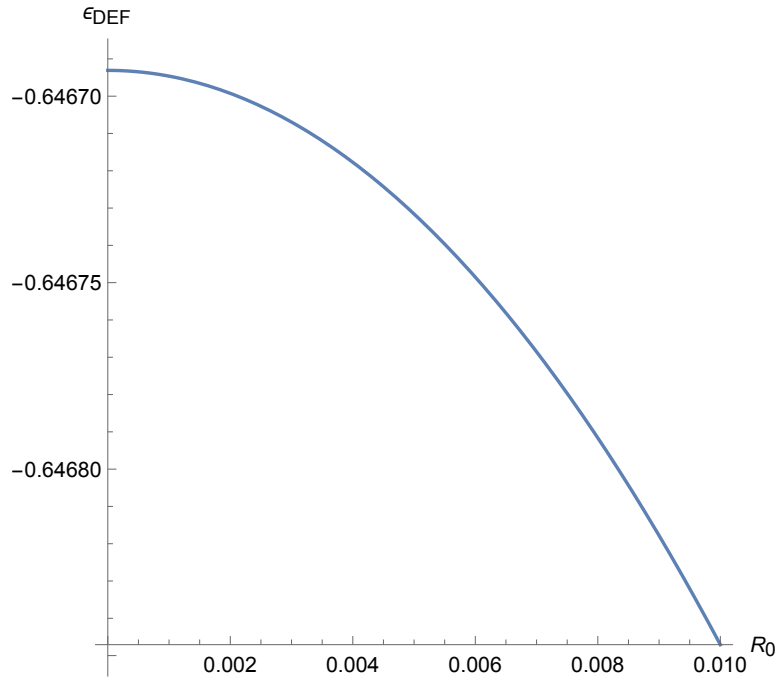


(a) nuovoE_0.pdf

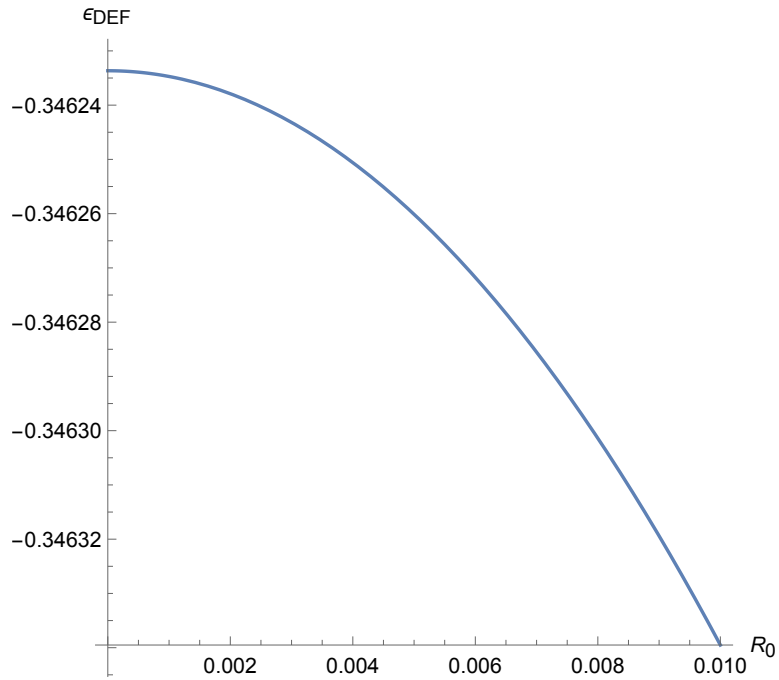
Figure 5.3: Deferent's energy, as function of R_0 , for the shift parameter $a = 0$ 

(a) nuovoE_02.pdf

Figure 5.4: Deferent's energy, as function of R_0 , for the shift parameter $a = 0.2$



(a) nuovoE_04.pdf

Figure 5.5: Deferent's energy, as function of R_0 , for the shift parameter $a = 0.4$ 

(a) nuovoE_0588.pdf

Figure 5.6: Deferent's energy, as function of R_0 , for the shift parameter $a = 0.588$

From the above plots it can be noticed that, first, the energies examined are really small (let us remember that, as usual throughout all this work, all quantities with units of length are scaled to the characteristic length of the Plummer model b , as well as all the energies are defined in units of the characteristic "Plummer energy" GM/b) and, despite a shift in the peak reached at $R_0 = 0$, all trends are very similar, due to the fact that the allowed values for the parameter a are anyway small ones.

5.2 Zero-velocity curves and resonances

Now, it may be important to see how the zero-velocity curves, as they have been introduced in Appendix A, for the Plummer model presented up to now, are done, for the different values of the shift vector's length a . First of all, the focus will be on the spherical Plummer model ($a = 0$); for that, let us consider the radius R_0 corresponding to the minimum amount of energy E_0 an orbit can have, i.e. the circular orbits in the equatorial plane:

$$E_0 = \Phi^{PL}(R_0, 0) + \frac{v_0^2}{2}, \quad (5.2)$$

where the velocity v_0 can be obtained from centripetal balance equation of the potential, so that:

$$v_0^2 = R_0 \frac{d\Phi^{PL}(R_0, 0)}{dR_0}. \quad (5.3)$$

Now, following what presented in appendix A, the zero-velocity curves are defined by:

$$\delta E = \Phi_e f f^{PL}(R_0 + \epsilon, z) - E_0, \quad (5.4)$$

where δE is a little increment in the energy given to the circular orbits and

$$\Phi_e f f^{PL}(R_0 + \epsilon, z) = \Phi^{PL}(R_0 + \epsilon, z) + \frac{J_0^2}{2(R_0 + \epsilon)^2}, \quad (5.5)$$

it is the effective potential for the incremental variables $\epsilon \leq R_0$ and $z \leq 1$, with $J_0 = R_0 v_0$ being the (fixed) vertical angular momentum for the orbital family where the orbit being considered belongs; in fact, also J_0 can be expressed, as already stated previously, in terms of the potential, recalling eq. (5.3):

$$J_0 = \sqrt{R_0^3 \frac{d\Phi^{PL}(R_0, 0)}{dR_0}}, \quad (5.6)$$

and finally, gathering everything together, the function to plot for the zero-velocity curves becomes:

$$\delta E = \Phi^{PL}(R_0 + \epsilon, z) - \Phi^{PL}(R_0, 0) + \frac{R_0}{2} \frac{d\Phi^{PL}(R_0, 0)}{dR_0} \left[\frac{R_0^2}{(R_0 + \epsilon)^2} - 1 \right]. \quad (5.7)$$

At this stage, for the well-known Plummer Sphere with no shift, it can be written:

$$E_0 = -\frac{2 + R_0^2}{2[1 + R_0^2]^{\frac{3}{2}}}, \quad (5.8)$$

and

$$\Phi^{PL}(R_0, 0) = -\frac{1}{\sqrt{1 + R_0^2}} \quad ; \quad \frac{d\Phi^{PL}(R_0, 0)}{dR_0} = \frac{R_0}{[1 + R_0^2]^{\frac{3}{2}}}, \quad (5.9)$$

so that:

$$\delta E[a = 0] = -\frac{1}{\sqrt{1 + (R_0 + \epsilon)^2 + z^2}} + \frac{1}{\sqrt{1 + R_0^2}} + \frac{R_0^2}{2[1 + R_0^2]^{\frac{3}{2}}} \left[\frac{R_0^2}{(R_0 + \epsilon)^2} - 1 \right]. \quad (5.10)$$

The curves for the above expression have been obtained for 4 different values of dimensionless $R_0 = 0.5, 1, 1.5, 2$ with progressively increasing energy δE up to the opening of the curves, which may indicated that the orbits are not bounded anymore in the configuration space(which is not given for sure generally speaking but for 1-dimensional problems, like the Plummer spherical model indeed). In order to plot the effective zero-velocity curves in a more efficient way, instead of plotting eq.(5.10) directly, we shall give a particular definition to δE , as proportional to the absolute value of E_0 , garanting its positiveness indeed, via a constant β :

$$\delta E = \beta |E_0|. \quad (5.11)$$

In this way, the equation for the zero-velocity curves, thanks to the fact that E_0 is everywhere negative, can be written as:

$$E_0(1 - \beta) = \Phi_{eff}(R_0 + \epsilon, z), \quad (5.12)$$

so that, for $\beta = 0$, we get back the Deferent's energy $E = E_0$, and for $\beta = 1$ we have $E = 0$, which is the minimum amount of energy for the escape from potential well, so $\beta = 1$ happens to be, as wanted, the minimum value to have

open curves for every value of E_0 ; this constraction will be particularly useful in studying how the zero-velocity curves react to the same percentage increase (that we are going to fix) from the circular orbit's energy with increasing values of R_0 (and also for increasing value of a , as it will be shown later); this is because, as δE depends on E_0 itself, the curves, obtained from eq. (5.10) exactly, may be not objectively scaled to the same percentage amount of increase in δE passing from a certain value of R_0 to another one.

In fact, as it can be derived for the zero-velocity curves in terms of just δE , a features arising is the fact that, with the increasing values of R_0 , the upper limit, which will be defined as δE_{op} , for the δE in order for the curves to open, becomes lower (always in units of GM/b), but so does E_0 as well; in fact, within our numerical precision, $\delta E_{op} \approx E_0$, which explains the special meaning for $\beta = 1$; in particular:

- $\delta E_{op} = 0.81$ for $R_0 = 0.5$
- $\delta E_{op} = 0.55$ for $R_0 = 1$
- $\delta E_{op} = 0.37$ for $R_0 = 1.5$
- $\delta E_{op} = 0.28$ for $R_0 = 2$

So, for orbital families more distant from the center, it is easier to "escape" from the region bounded by the zero-velocity curves.

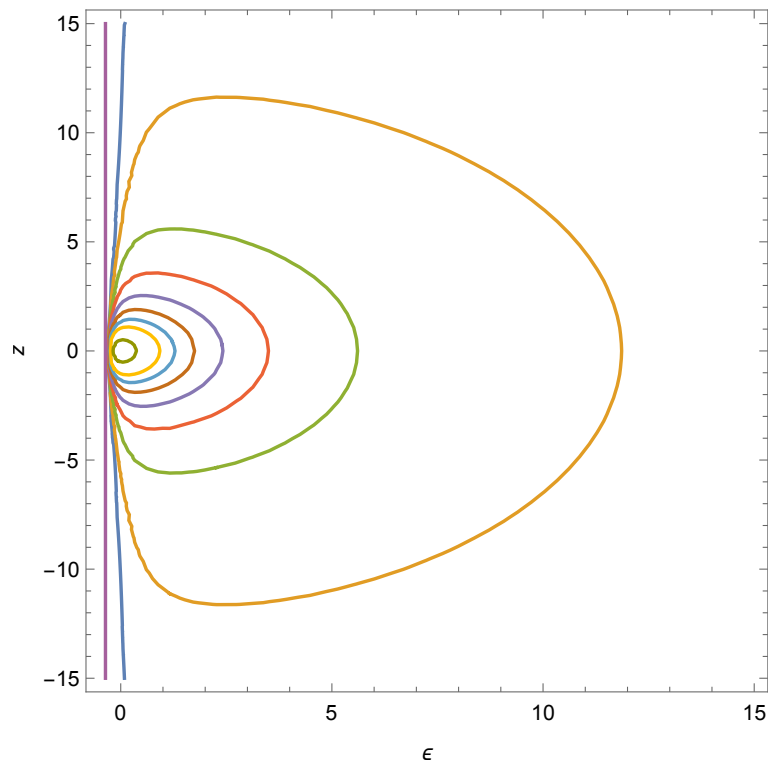


Figure 5.7: Zero-velocity curves for $R_0 = 0.5$

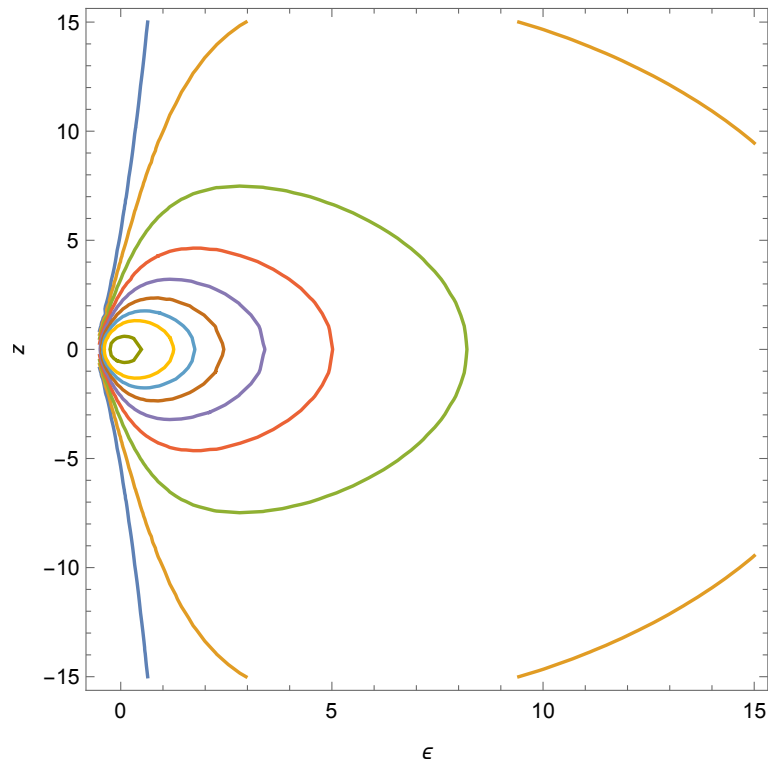


Figure 5.8: Zero-velocity curves for $R_0 = 1$

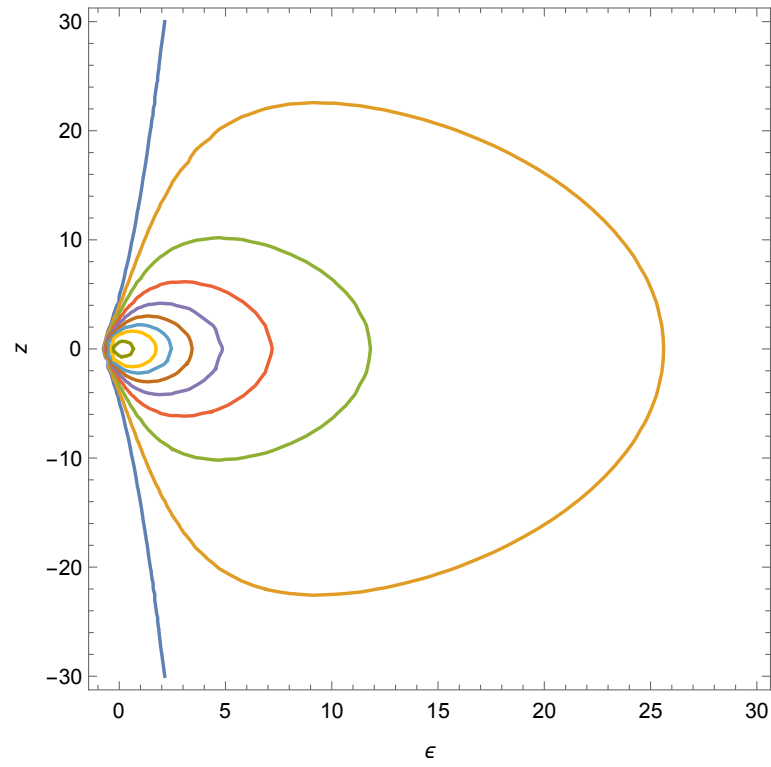


Figure 5.9: Zero-velocity curves for $R_0 = 1.5$

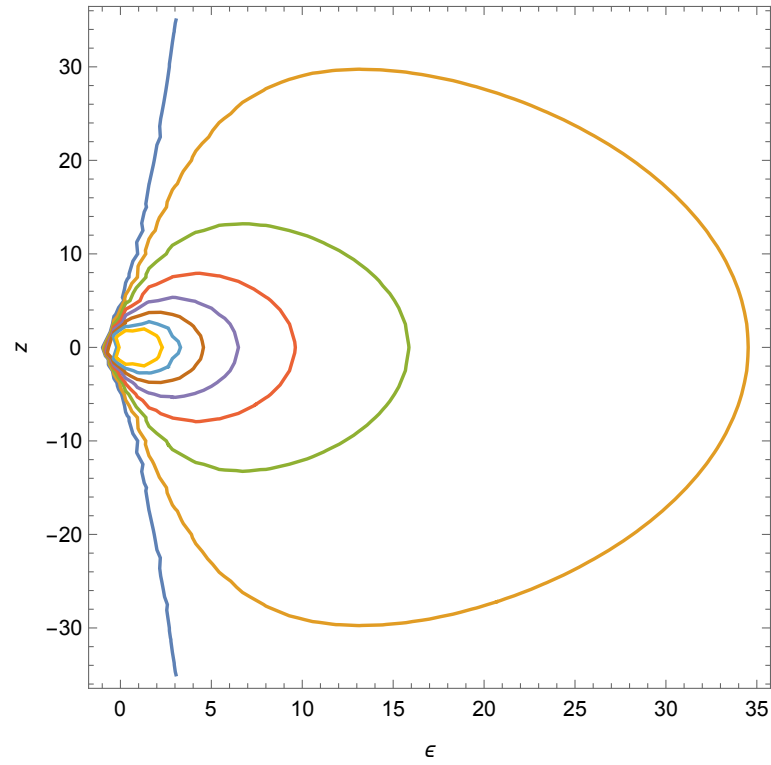


Figure 5.10: Zero-velocity curves for $R_0 = 2$

Now, it would be also interesting to compare the previous curves with the zero-velocity curves obtained in epicyclic approximation, that can be written, from Taylor's expansion of the effective potential around deferent's energy, as:

$$\delta E_{epic} = \frac{k_R^2}{2}[R_0 - \epsilon]^2 + \frac{k_z^2}{2}z^2, \quad (5.13)$$

where the epicyclic frequencies, for the non shifted Plummer model are given in eq.(4.50). So we get, repeating the treatment done for the effective curves in terms of the parameter β :

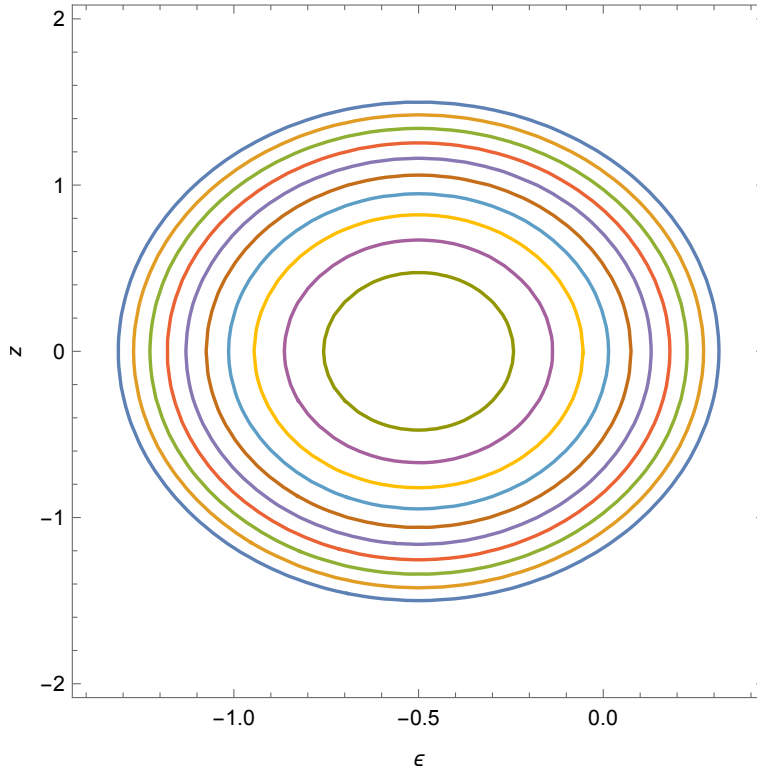


Figure 5.11: Epicyclic Zero-velocity curves for $R_0 = 0.5$

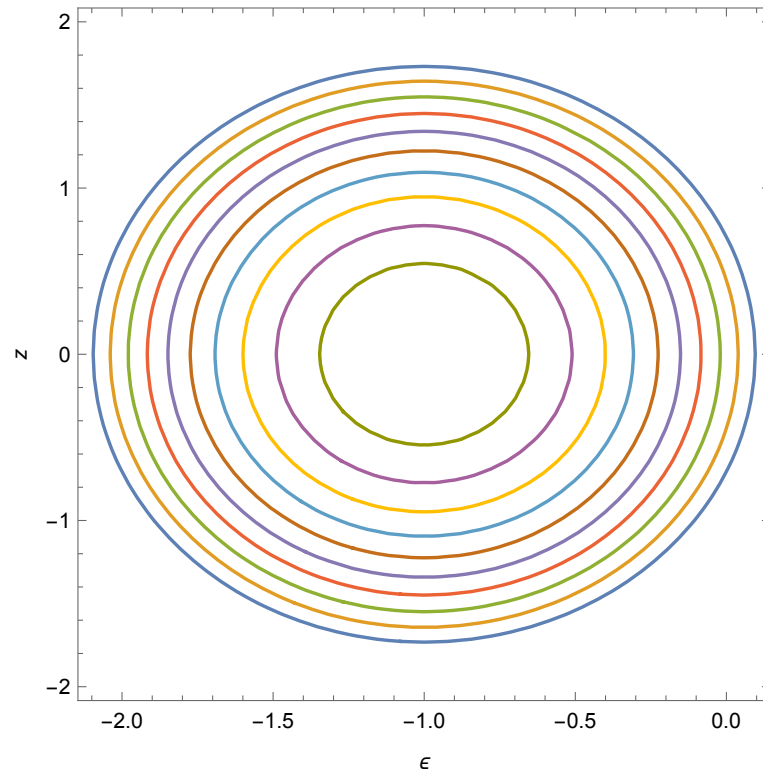


Figure 5.12: Epicyclic Zero-velocity curves for $R_0 = 1$

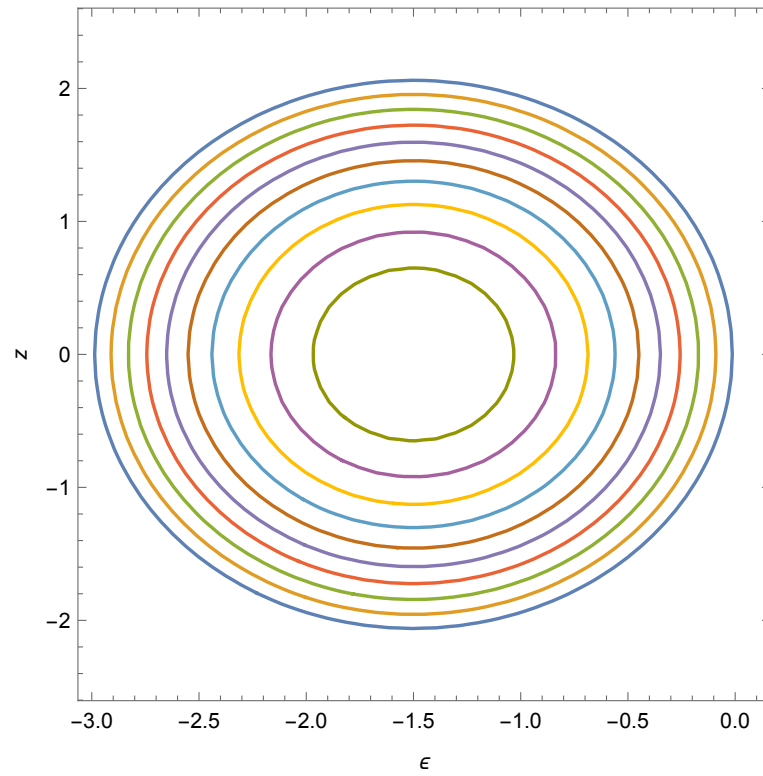


Figure 5.13: Epicyclic Zero-Velocity Curves for $R_0 = 1.5$

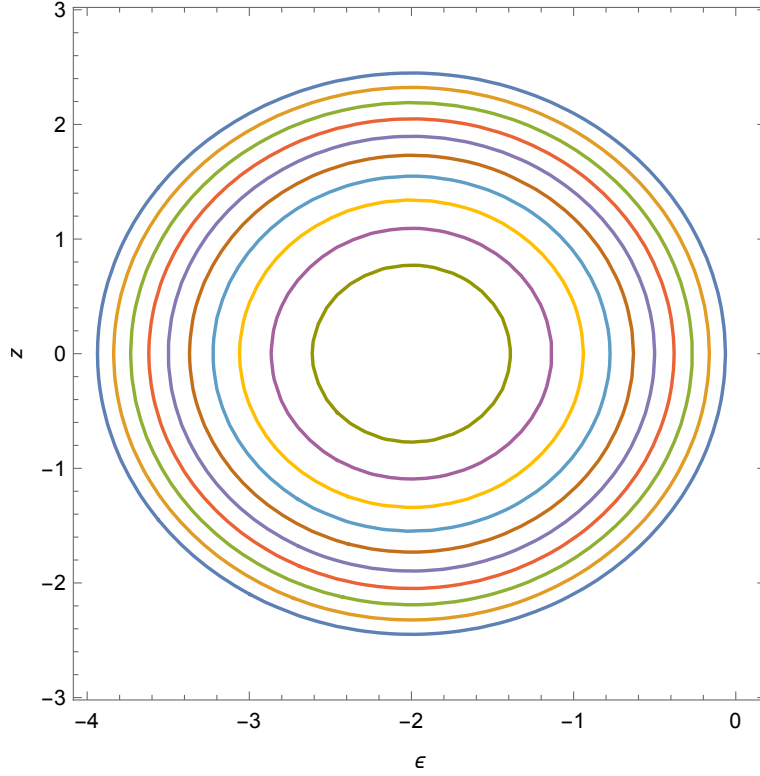


Figure 5.14: Epicyclic Zero-velocity curves for $R_0 = 2$

As expected, the epicyclic zero-velocity curves are ellipses, all closed for any value of the energy increment δE_{epic} , whose major axis are exactly the inverse of the epicyclic frequencies, divided by 2. The difference between the δE for 2 contiguous curves, both for the "real" and epicyclic ones, are approximately of 10%, i.e. $\Delta(\delta E) \approx 0.1$ in units of "Plummer characteristic energy".

In order to investigate the behaviour of the shifted Plummer model for different values of the parameter a , what just done for the spherical case will be repeated in the very same way for the axially symmetric Plummer potential, presenting the zero-velocity curves as well as the epicyclic zero-velocity curves for the three different values of a already used to study the trends for the epicyclic frequencies and the energy of circular orbit, so $a = 0.2, 0.4$ & $a = a_M = 0.588$, and, for each value of a , the 4 values of R_0 already used in the spherical case will be analyzed. Finally, let us recall that, for the epicyclic curves, the frequencies used are those in eq. (4.51).

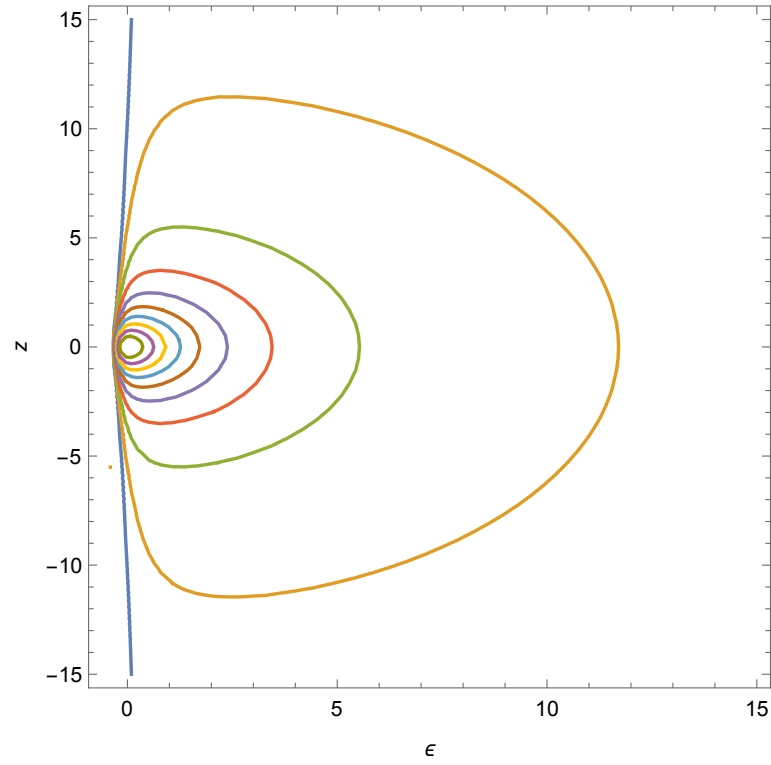


Figure 5.15: Zero-velocity curves for the shift parameter $a = 0.2$ and $R_0 = 0.5$

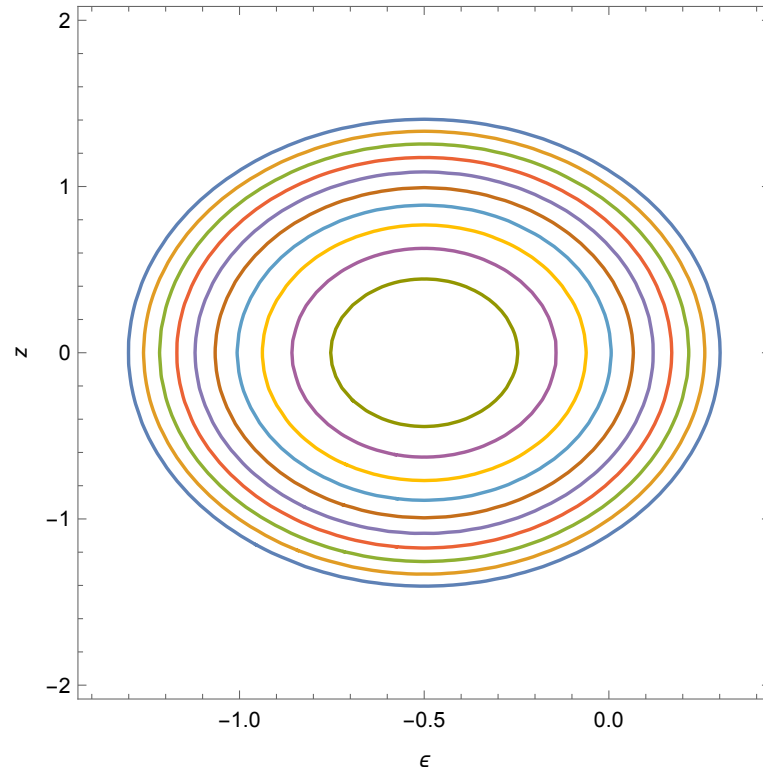


Figure 5.16: Epicyclic Zero-velocity curves for the shift parameter $a = 0.2$ and $R_0 = 0.5$

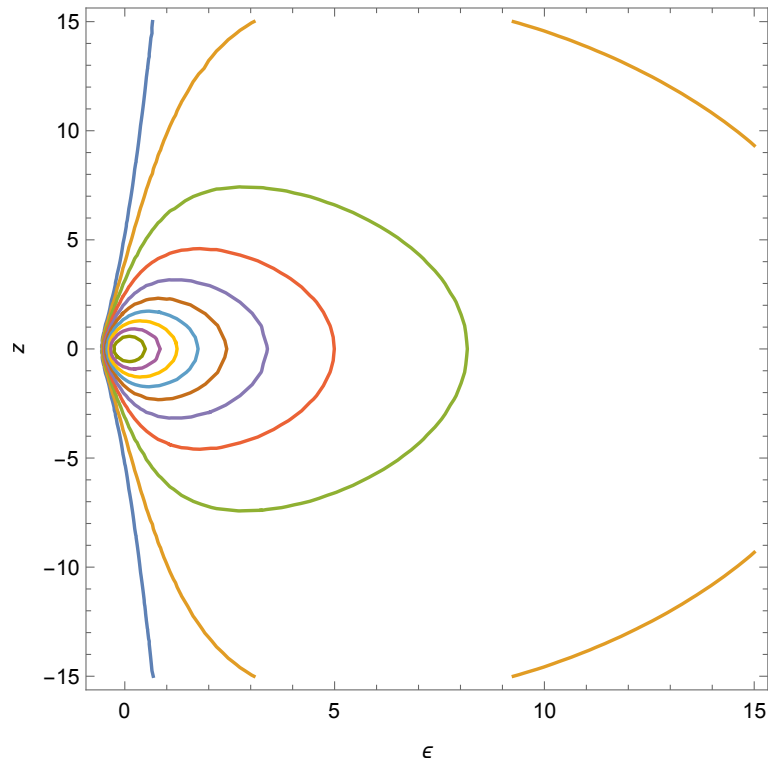


Figure 5.17: Zero-velocity curves for the shift parameter $a = 0.2$ and $R_0 = 1$

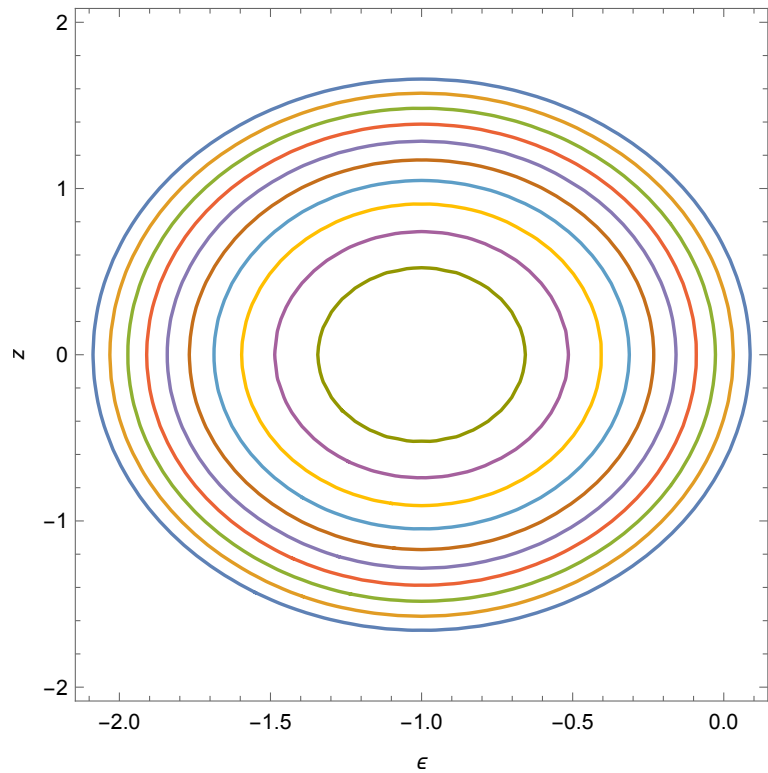


Figure 5.18: Epicyclic Zero-velocity curves for the shift parameter $a = 0.2$ and $R_0 = 1$

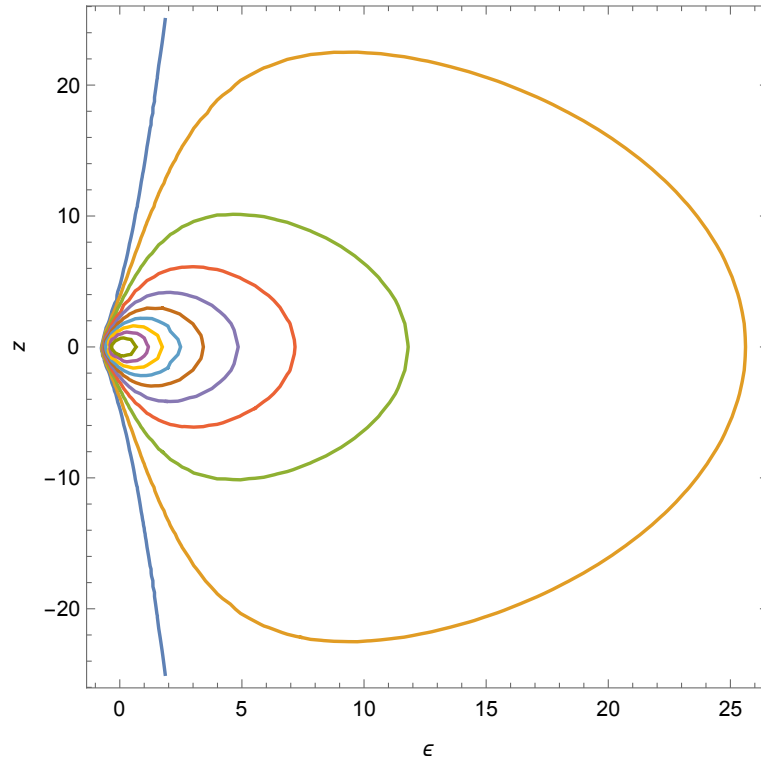


Figure 5.19: Zero-velocity curves for the shift parameter $a = 0.2$ and $R_0 = 1.5$

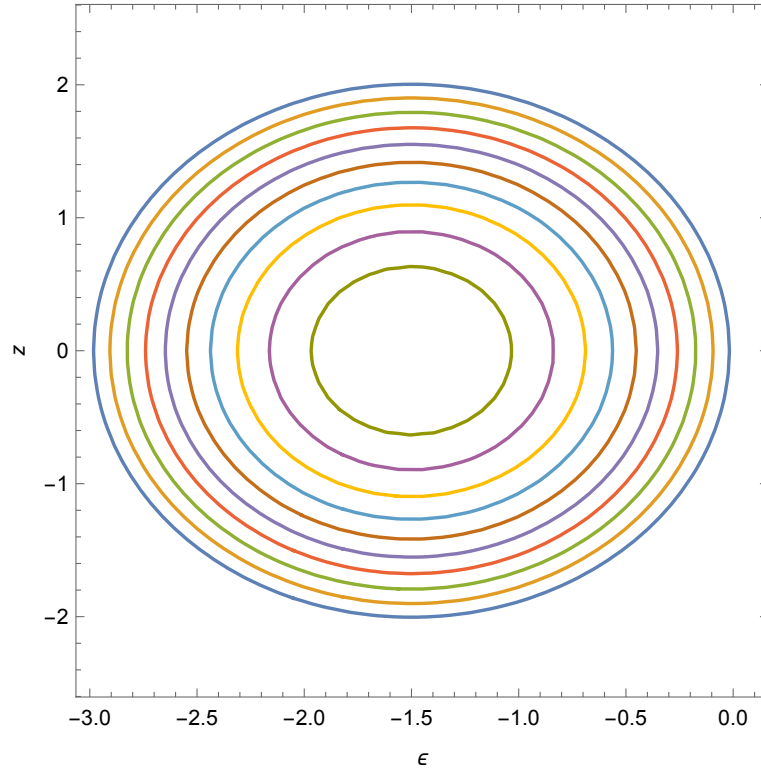


Figure 5.20: Epicyclic Zero-velocity curves for the shift parameter $a = 0.2$ and $R_0 = 1.5$

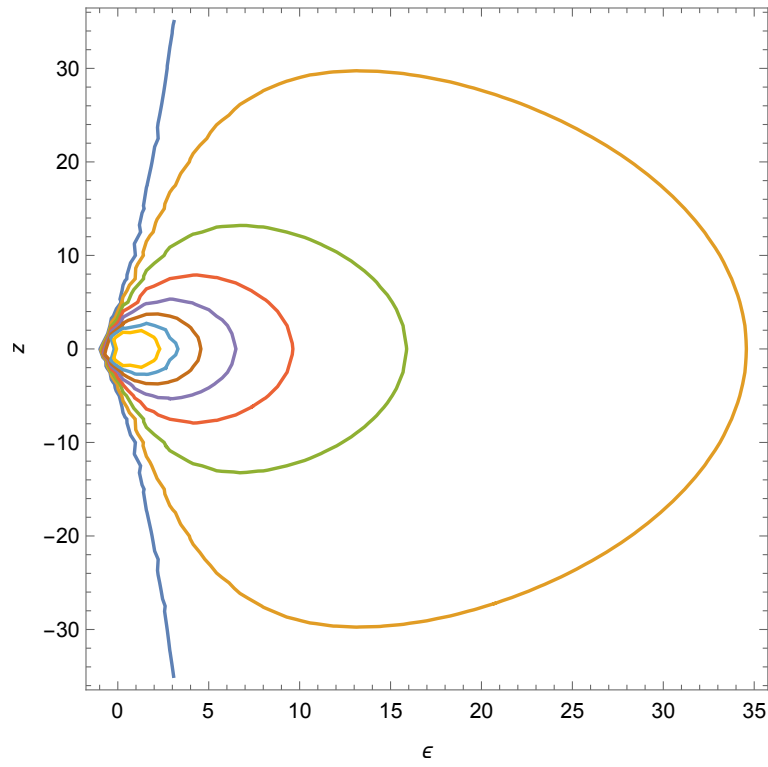


Figure 5.21: Zero-velocity curves for the shift parameter $a = 0.2$ and $R_0 = 2$

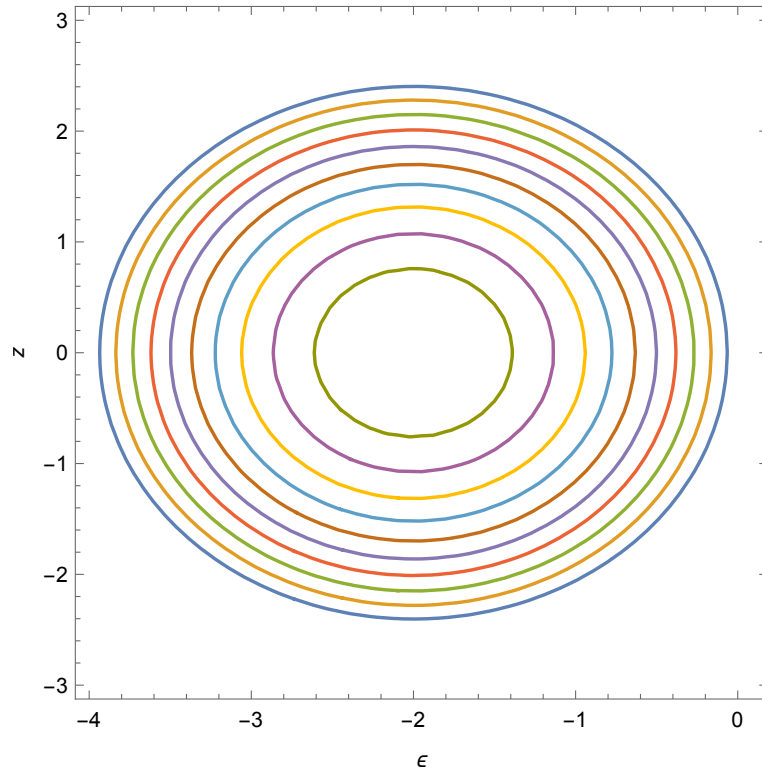


Figure 5.22: Epicyclic Zero-velocity curves for the shift parameter $a = 0.2$ and $R_0 = 2$

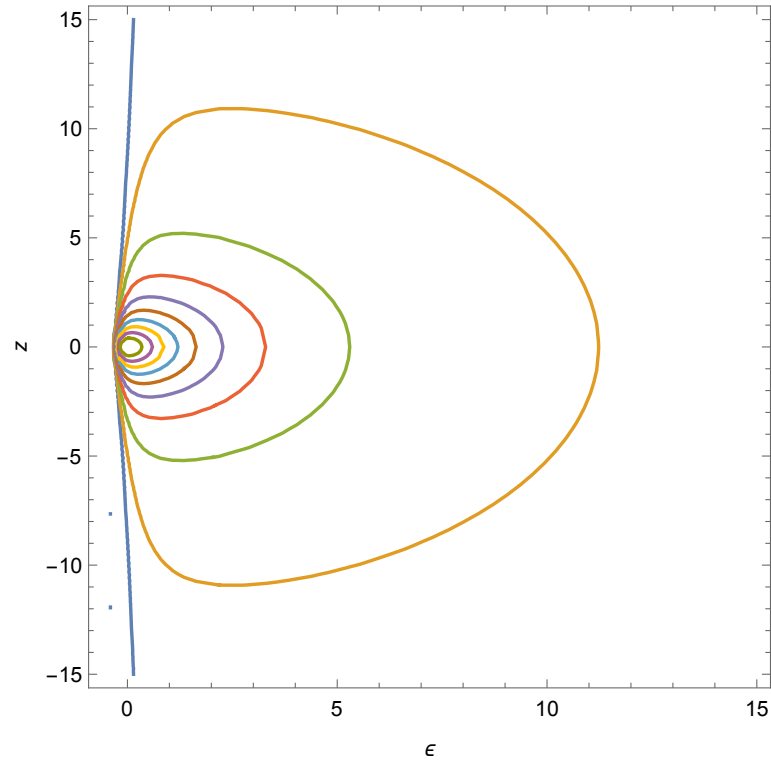


Figure 5.23: Zero-velocity curves for the shift parameter $a = 0.4$ and $R_0 = 0.5$

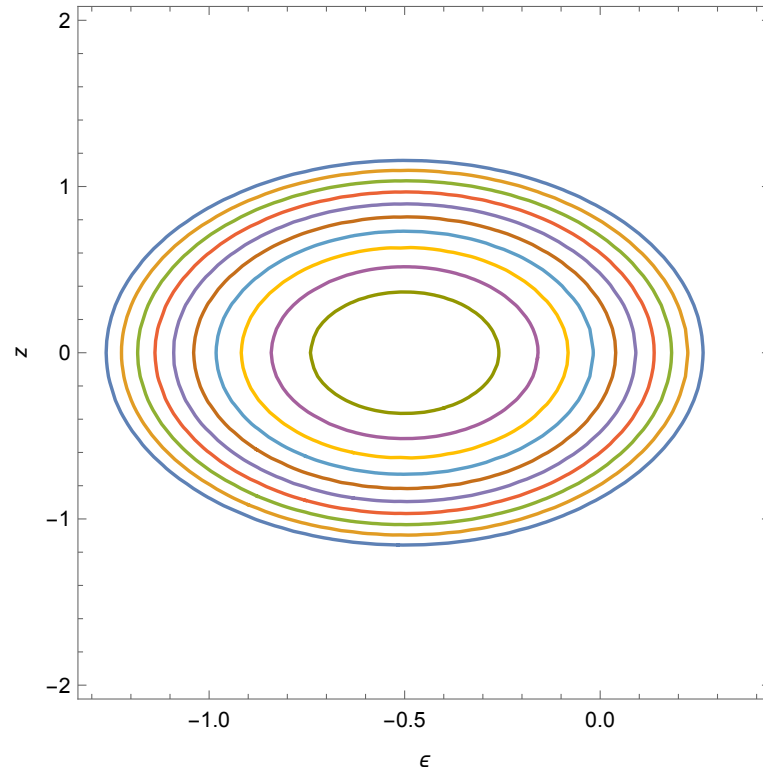


Figure 5.24: Epicyclic Zero-velocity curves for the shift parameter $a = 0.4$ and $R_0 = 0.5$

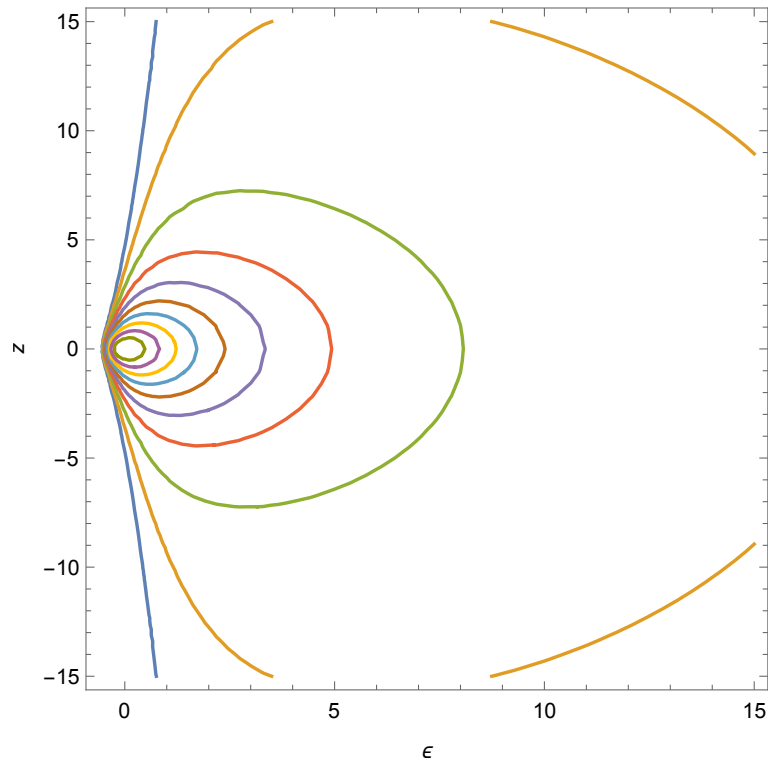


Figure 5.25: Zero-velocity curves for the shift parameter $a = 0.4$ and $R_0 = 1$

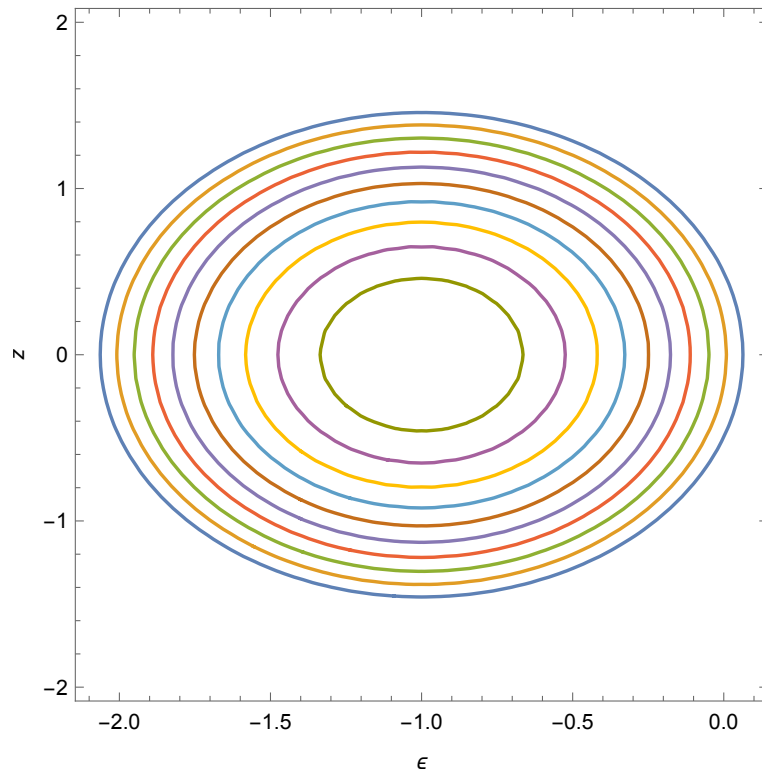


Figure 5.26: Epicyclic Zero-velocity curves for the shift parameter $a = 0.4$ and $R_0 = 1$

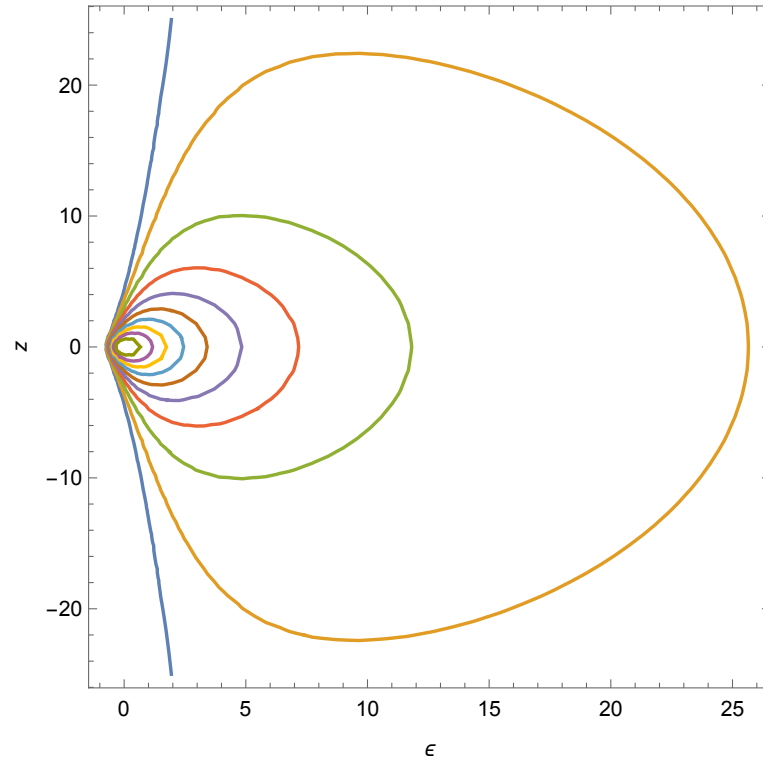


Figure 5.27: Zero-velocity curves for the shift parameter $a = 0.4$ and $R_0 = 1.5$

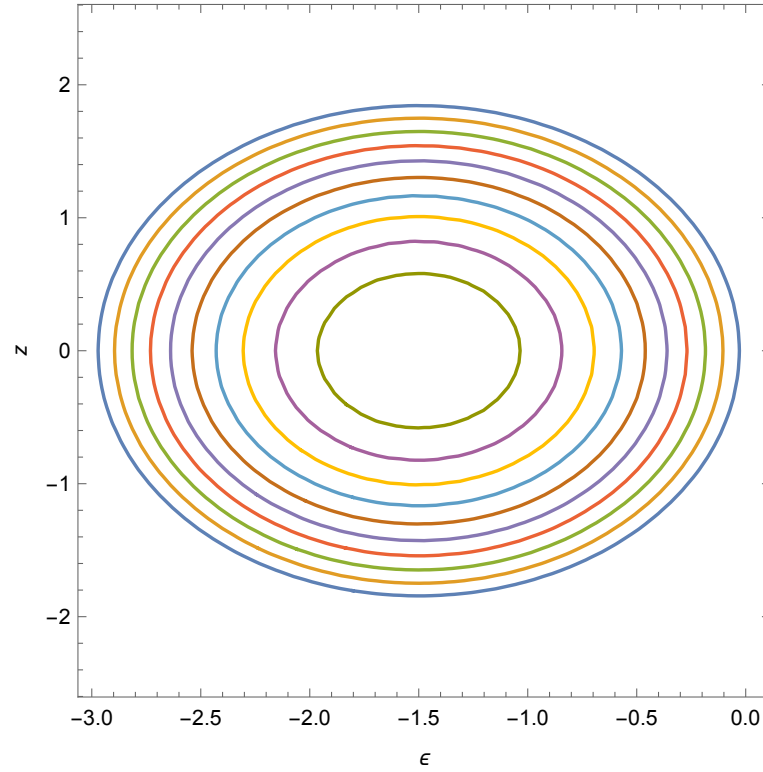


Figure 5.28: Epicyclic Zero-velocity curves for the shift parameter $a = 0.4$ and $R_0 = 1.5$

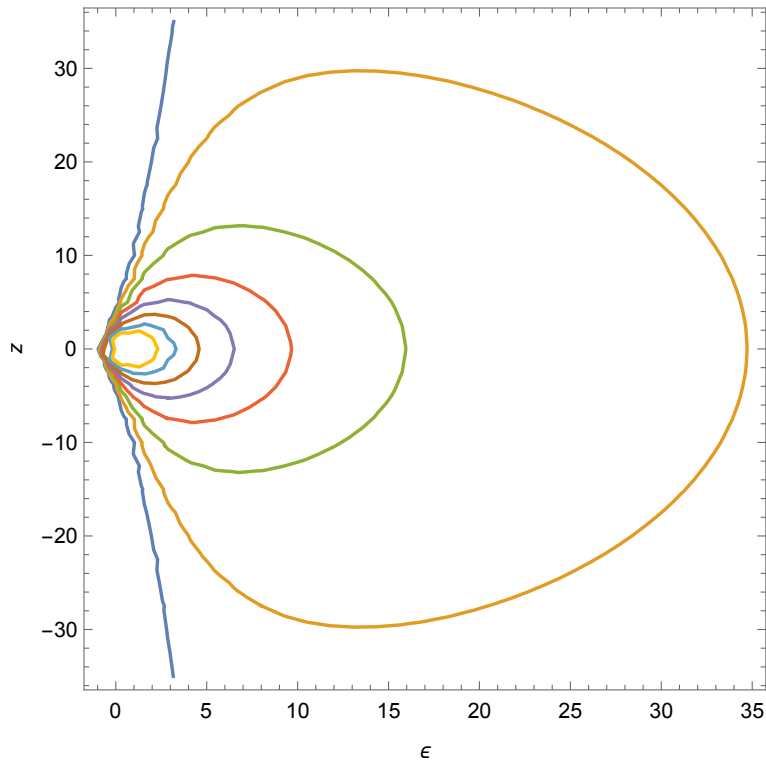


Figure 5.29: Zero-velocity curves for the shift parameter $a = 0.4$ and $R_0 = 2$

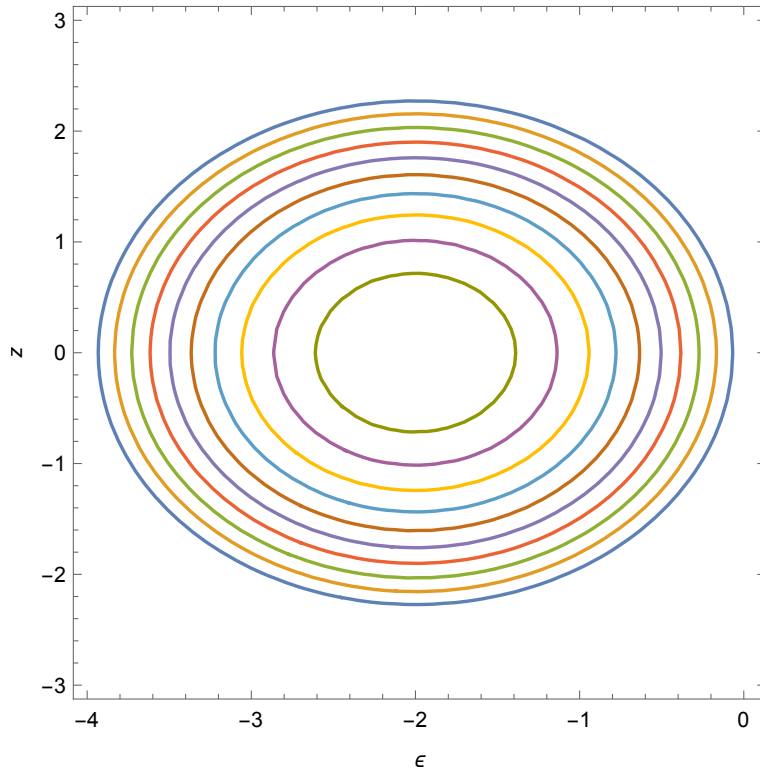


Figure 5.30: Epicyclic Zero-velocity curves for the shift parameter $a = 0.4$ and $R_0 = 2$

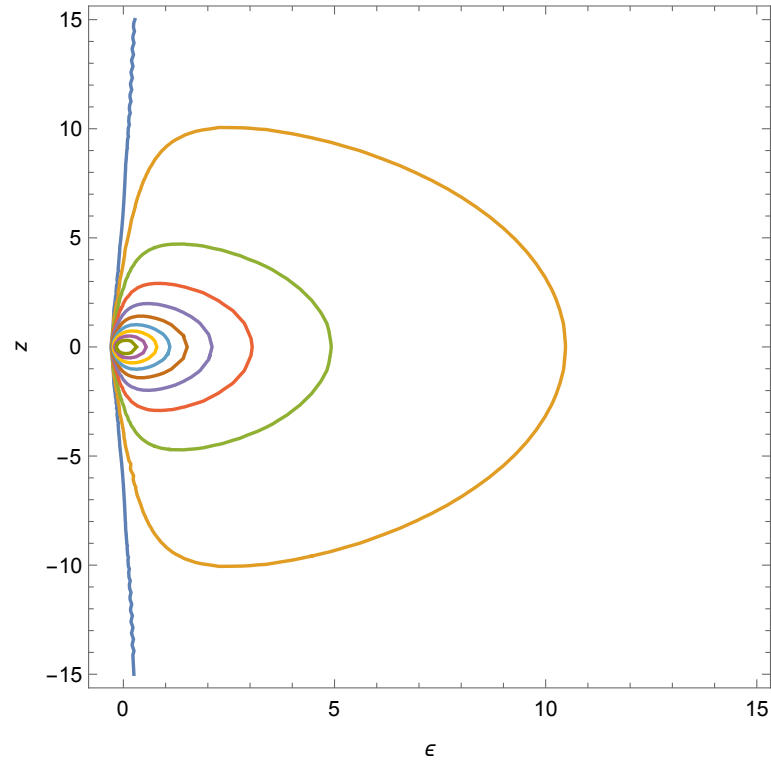


Figure 5.31: Zero-velocity curves for the shift parameter $a = 0.588$ and $R_0 = 0.5$

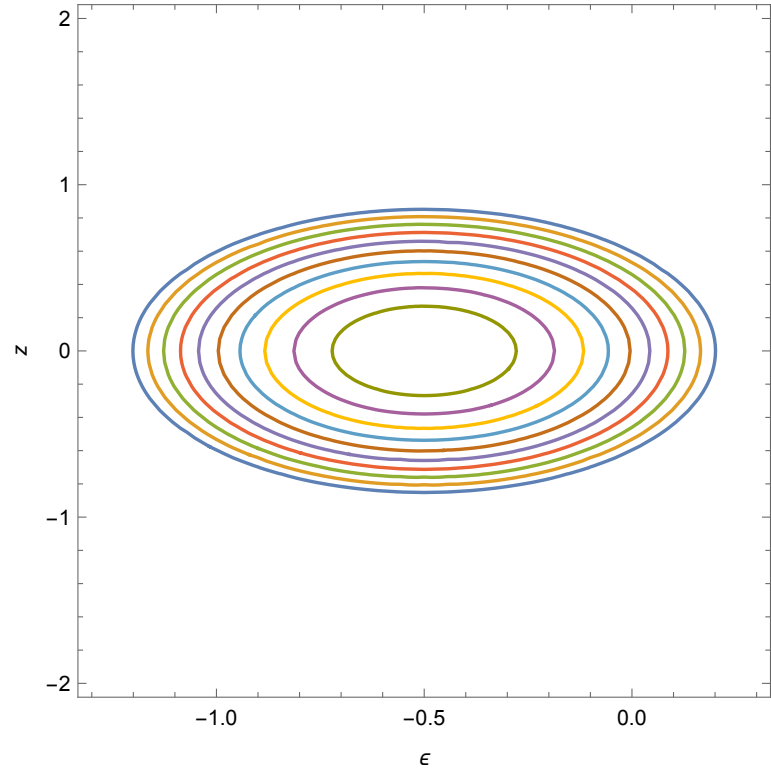


Figure 5.32: Epicyclic Zero-velocity curves for the shift parameter $a = 0.588$ and $R_0 = 0.5$

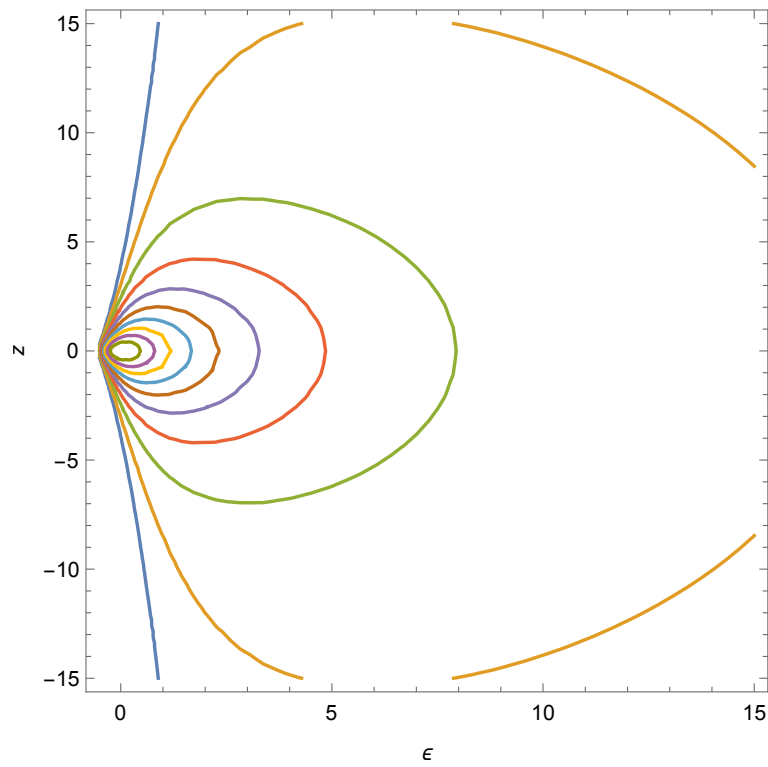


Figure 5.33: Zero-velocity curves for the shift parameter $a = 0.588$ and $R_0 = 1$

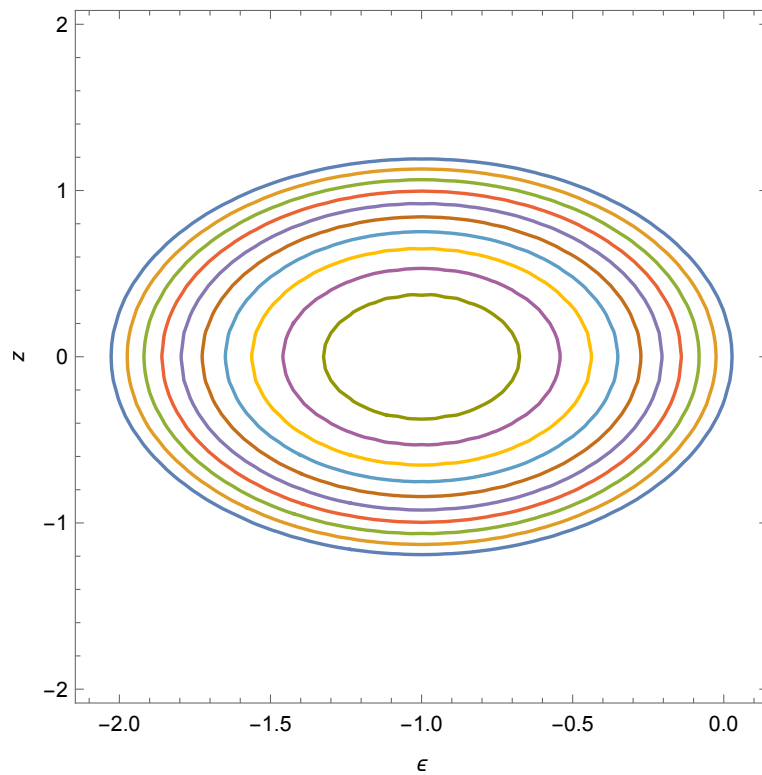


Figure 5.34: Epicyclic Zero-velocity curves for the shift parameter $a = 0.588$ and $R_0 = 1$

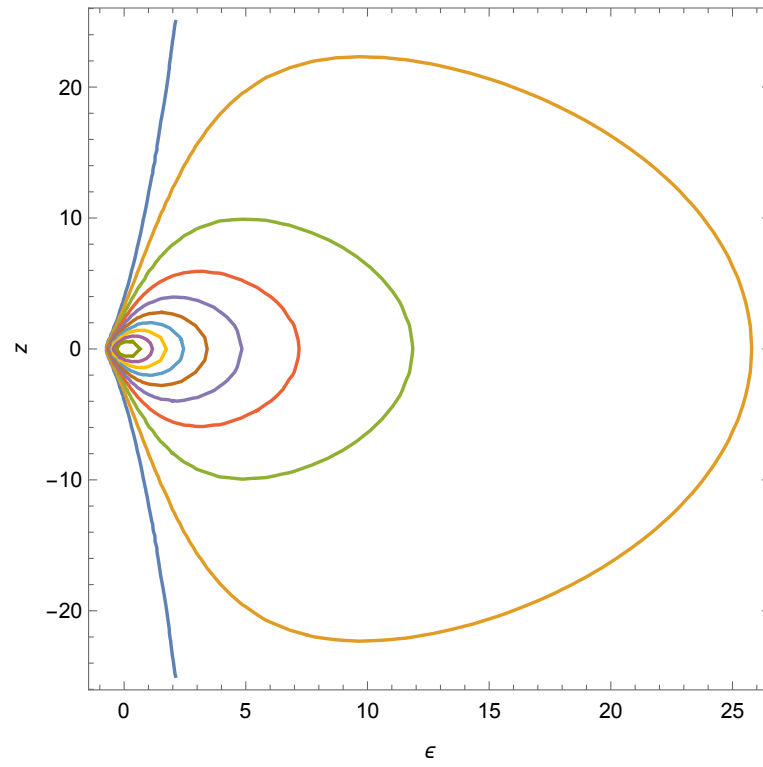


Figure 5.35: Zero-velocity Curves for the shift parameter $a = 0.588$ and $R_0 = 1.5$

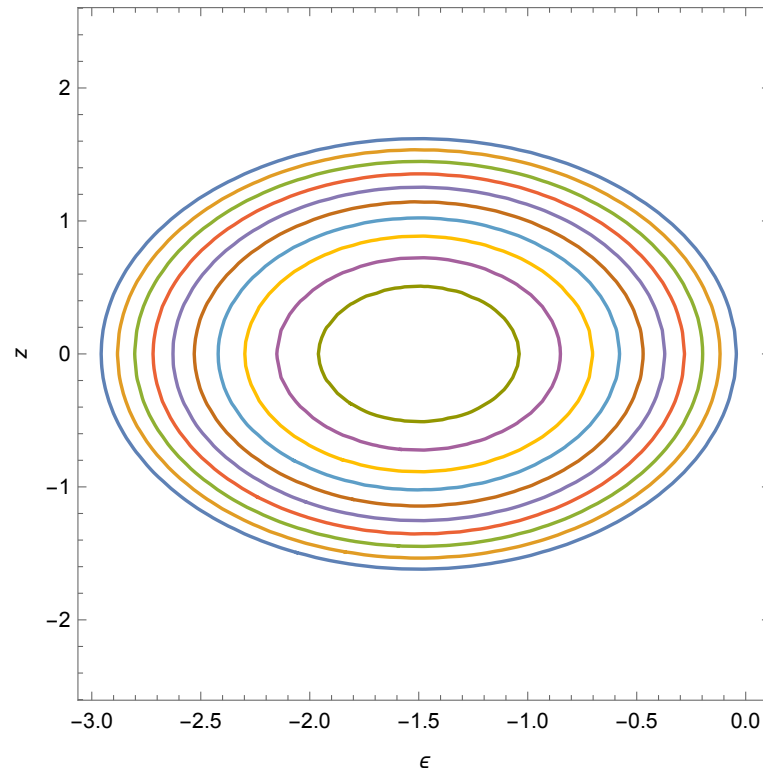


Figure 5.36: Epicyclic Zero-velocity curves for the shift parameter $a = 0.588$ and $R_0 = 1.5$

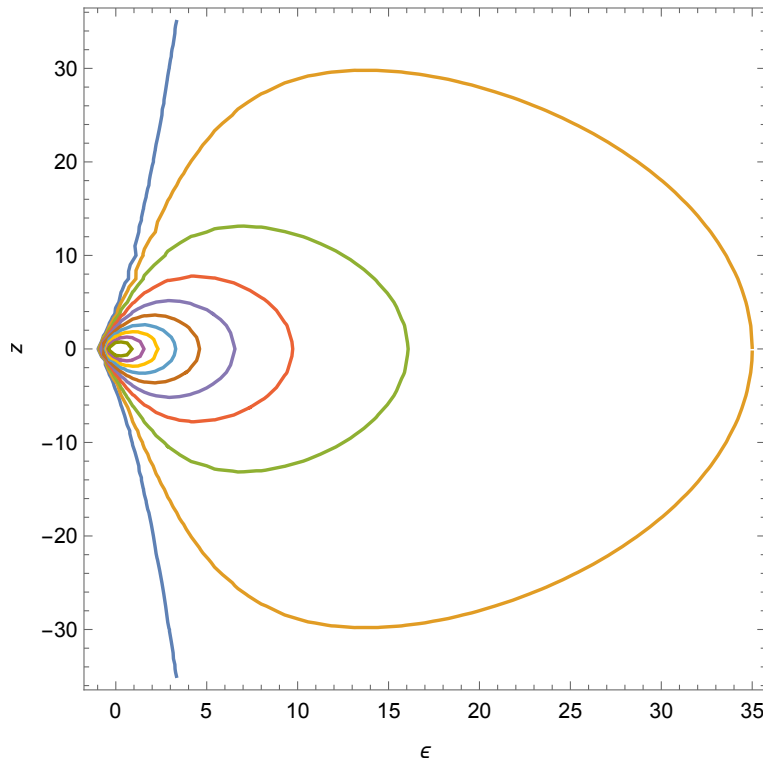


Figure 5.37: Zero-velocity curves for the shift parameter $a = 0.588$ and $R_0 = 2$

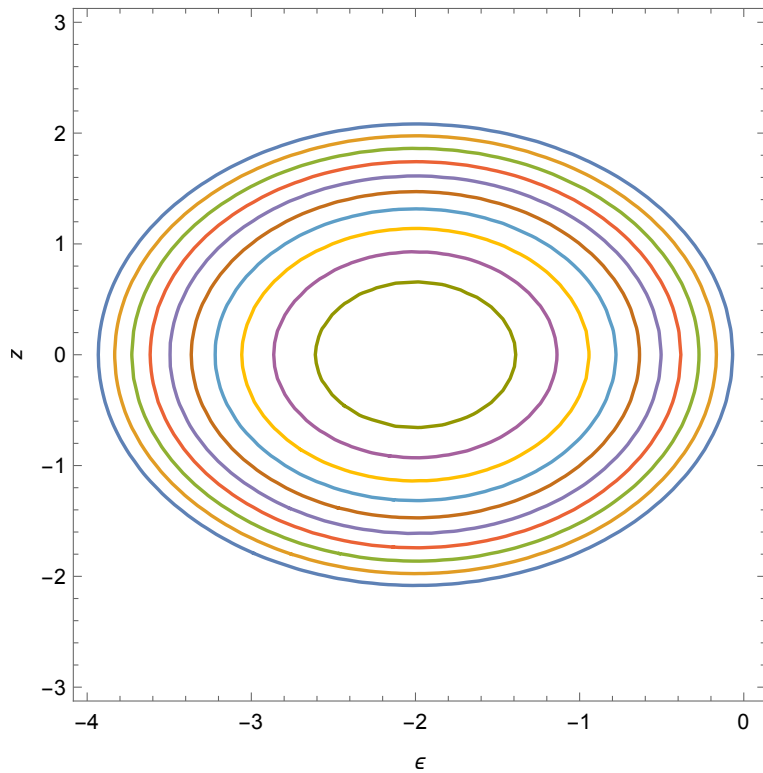


Figure 5.38: Epicyclic Zero-velocity curves for the shift parameter $a = 0.588$ and $R_0 = 2$

So, as done for the spherical Plummer potential, also for the cases above presented, it is possible to highlight the trend for the upper limit of the energy increment to have open curves (for the solely real zero-velocity curves of course) δE_{op} for the different values R_0 :

- $a = 0.2$
 - $\delta E_{op} = 0.82$ for $R_0 = 0.5$
 - $\delta E_{op} = 0.54$ for $R_0 = 1$
 - $\delta E_{op} = 0.37$ for $R_0 = 1.5$
 - $\delta E_{op} = 0.27$ for $R_0 = 2$
- $a = 0.4$
 - $\delta E_{op} = 0.85$ for $R_0 = 0.5$
 - $\delta E_{op} = 0.54$ for $R_0 = 1$
 - $\delta E_{op} = 0.363$ for $R_0 = 1.5$
 - $\delta E_{op} = 0.267$ for $R_0 = 2$
- $a = 0.588$
 - $\delta E_{op} = 0.91$ for $R_0 = 0.5$
 - $\delta E_{op} = 0.55$ for $R_0 = 1$
 - $\delta E_{op} = 0.361$ for $R_0 = 1.5$
 - $\delta E_{op} = 0.265$ for $R_0 = 2$

It is important to remark, first, that the ripples in same plots, especially for those with $R_0 = 1.5$ and $R_0 = 2$ are not real, but due to the numerical precision of the plotting processes, for the scale exposed, which are those just below the energy scales of open curves and, second, the difference of β between 2 contiguous curves is constant, i.e. $\Delta\beta = 10\%$.

The main features we can deduce from the plots as well as from the above list is that, at first instance, the δE_{op} all tend to decreasing with increasing R_0 , at fixed a , but for fixed R_0 , with increasing of the shift parameter, the energy increment for the opening does not have a regular trend, sometimes increasing, for $R_0 = 0.5$ for example, and sometimes decreasing with a , like for $R_0 = 2$, but all the variations are very little, of order of ≈ 0.1 (naturally, this behaviour may be a numerical effect from the plotting procedure). Another important characteristic of the systems presented is the completely different spatial scale between the epicyclic curves and the effective ones; in

fact, as the value for the δE used for the real zero-velocity curves and for the epicyclic ones are the same, it is evident that the latter's scale is roughly 10 times smaller than the formers', so that the motion appears to be much more spatially constrained in epicyclic approximation. Furthermore this gap between the two scales seems to increase, even though not with order of magnitude, with increasing R_0 , which implies also that all the spatial scales grow with it, conversely it seems that there is no such a behaviour with increasing a at fixed R_0 .

Moreover, an important feature arising from the plotted curves is that, with increasing of R_0 and, much less but still present, with the increase of a , the spatial scale of the real curves becomes more sensible to the increment of the *beta* (thus to finer increment in δE). This means that, with the increase of the circular radius, to the same difference in the percentage increment of energy $\Delta\beta$ correspond a greater spatial difference between the curves, or, in terms of δE , to greater change in the scale of two contiguous zero-velocity curves corresponds smaller change in their δE ; in particular, if for $a = 0.2$ and $R_0 = 0.5$ we have that, for two contiguous curves, $\Delta(\delta E) \approx 0.1$, we come for $a = 0.588$ and $R_0 = 2$ with $\Delta(\delta E) \approx 0.001$. This enhanced sensitivity to difference in the energy increment seems anyway to affect very poorly the epicyclic velocity curves which, as already said, have the same β of the real zero-velocity curves, so becoming finer the separation between the δE leads to a finer separation between the elliptic epicyclic velocity curves; this means that, if we would have used the δE for the plots, the epicyclic curves would appear denser, forming a ring-like confined region, essentially because the epicyclic approximation is not good in describing motion with high values of the energy; in fact, at some point, the epicyclic zero-velocity curves would eventually cross the Radial axis to negative values, which would be absurd. Finally, for the epicyclic curves, it can be stated that the main difference, with fixed R_0 and increasing of the shift parameter, is that they become more squeezed along the vertical axis, while there is no significant change for fixed a and varying R_0 .

Now, in order to have a quicker visual impact for the usefulness of the models here presented, it may be interesting to compare the zero-velocity curves from our models with the zero-velocity curves, for instance, of the Binney logarithmic potential:

$$\Phi(R, z) = \frac{v_0^2}{2} \ln \left(R^2 + \frac{z^2}{q^2} \right). \quad (5.14)$$

This potential resembles the potential experienced by a star in an oblate spheroidal galaxy rotating with constant circular velocity v_0 ; it is an an-

alytical potential very much used to model the gravity field for elliptical galaxies as well as the spiral ones and it is quite realistic, compared to the observations. Its zero-velocity curves are those in fig.5.39 (fig.3-2, Binney& Tremaine, Galactic Dynamics, 1987, pag.116). From there, it is quite evident how those curves are very similar to the ones we have obtained for the shifted Plummer potential, for all the used values for the shift parameter a .

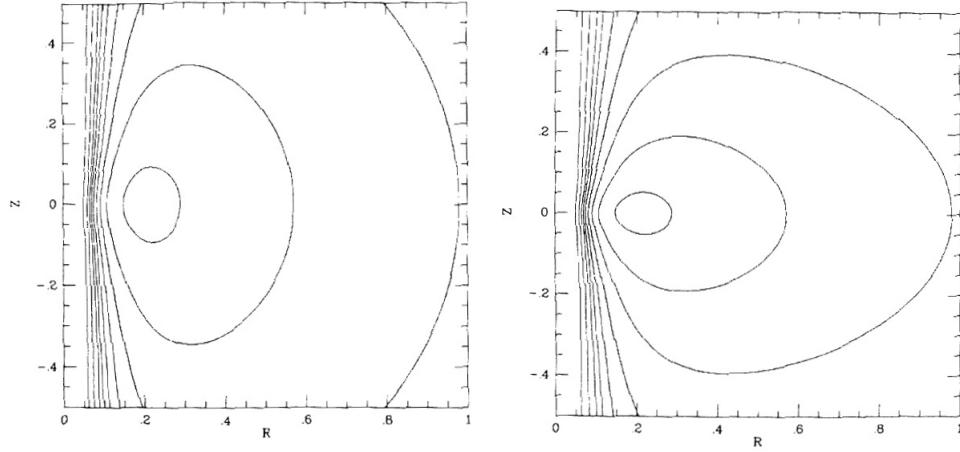


Figure 5.39: Zero-velocity curves for the logarithmic potential for $q = 0.9$ (top); $q = 0.5$ (bottom). Contours are shown for $\Phi_{eff} = -1, -0.5, 0, 0.5, 1, 1.5, 2, 3, 5$ in dimensionless units, assuming $v_0 = 1$

Lastly, to investigate some other potentially interesting applications of models developed in the present work, following what has been done by Binney and Tremaine (Galactic Dynamics, 1987) in the context of Theory of density waves for the explanation of the spiral arms of disk galaxies, it is interesting to analyze, within our models, the trend, as function of the deferent's radius R_0 , of the following quantity:

$$R_{ris}(R_0) \equiv \Omega_0(R_0) - \frac{n}{m} k_r(R_0), \quad (5.15)$$

where Ω_0 and k_r are the circular angular velocity and the radial epicyclic frequency respectively, and n and m are positive integers. The above quantity plays an important role in the definition of resonance regions for density waves, which may be connected to the origin of galactic spiral arms, whose issues will not be treated in details in this work.

For the shifted ($a \neq 0$) and unshifted Plummer ($a = 0$) models studied up to now, the explicit expressions for R_{ris} are the following:

$$R_{ris}(R_0) = \frac{1}{[1 + R_0^2]^{\frac{3}{4}}} - \frac{n}{m} \frac{\sqrt{4 + R_0^2}}{[1 + R_0^2]^{\frac{5}{4}}}, \quad (5.16)$$

for $a = 0$, and

$$R_{ris}(R_0) = \frac{1}{[1 + R_0^2 - a^2]^{\frac{3}{4}}} - \frac{n}{m} \frac{\sqrt{4 + R_0^2 - 4a^2}}{[1 + R_0^2 - a^2]^{\frac{5}{4}}}, \quad (5.17)$$

for $a \neq 0$

So the following plot of $R_{ris}(R_0)$ will be presented for the four values of the shift parameter used until now, i.e. $a = 0$ (unshifted case) and $a = 0.2, 0.4, 0.588$ and, each plot will contain four curves for R_{ris} , for the 4 chosen values of the ratio n/m which, for sake of simplicity, will be called from now on α , so that $\alpha = 1, 1/2, 0, -1/2$. So the trends are presented in fig.5.40,5.41,5.42,5.43 and they appear to be very similar to one another, except for the fact that the peak of the curves with $\alpha = 0.5$ seems to rise slightly and move towards left with the increase of the shift parameter.

But the most interesting thing is to compare what we have obtained from our models with the same plots done by Binney and Tremaine (Galactic Dynamics, 1987, fig. 6-30, pag.411), as presented in fig. 5.44.

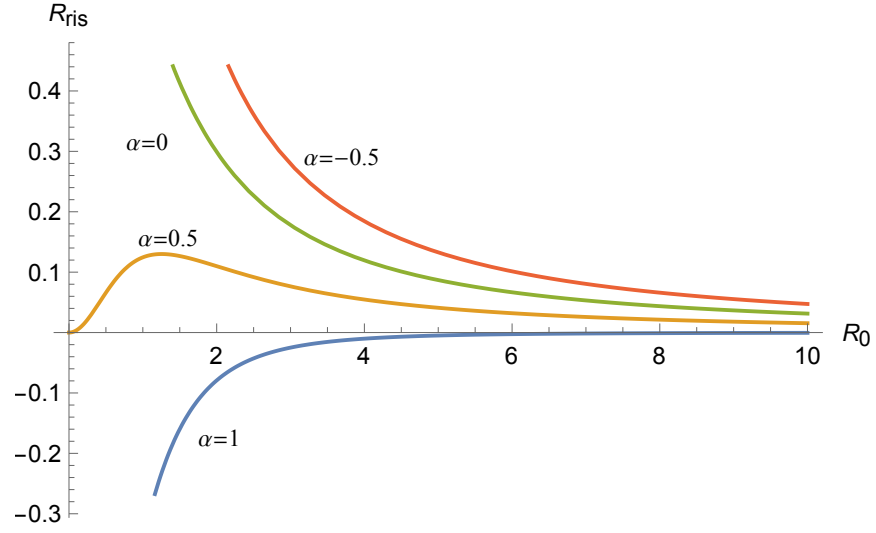


Figure 5.40: R_{ris} , as function of R_0 , for the shift parameter $a = 0$

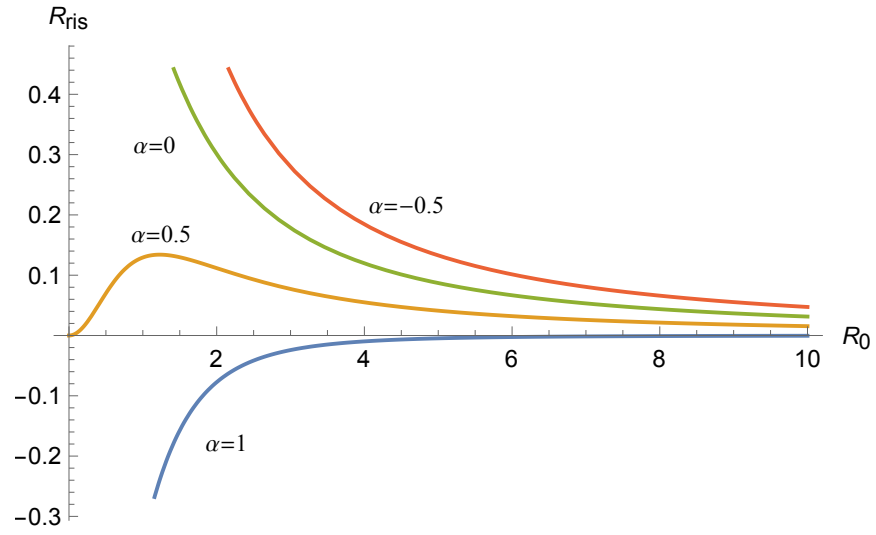


Figure 5.41: R_{ris} , as function of R_0 , for the shift parameter $a = 0.2$

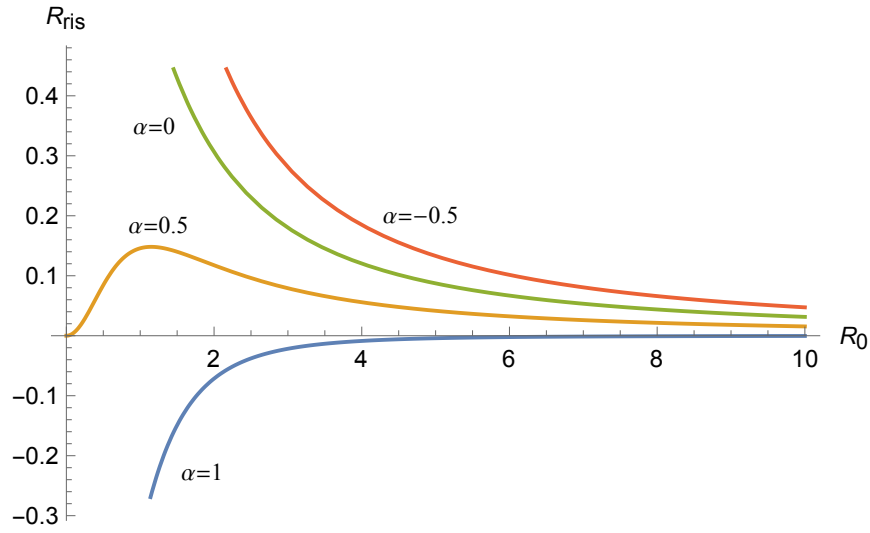


Figure 5.42: R_{ris} , as function of R_0 , for the shift parameter $a = 0.4$

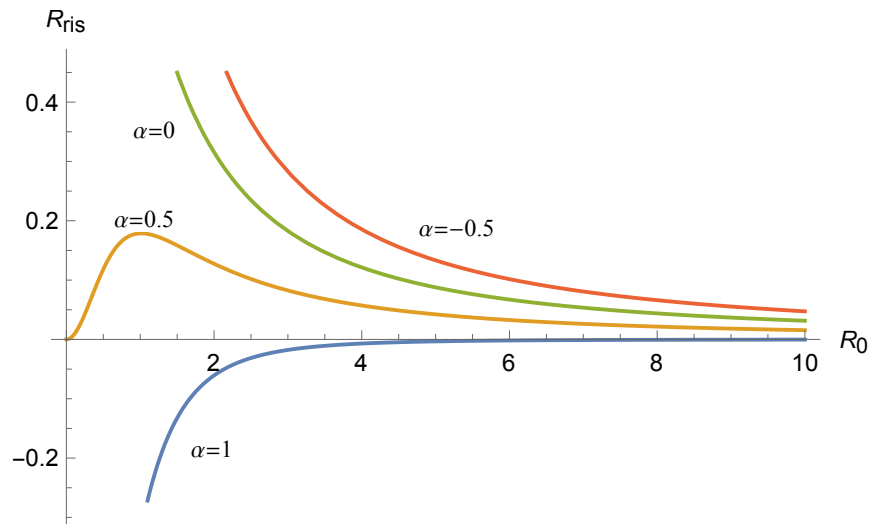


Figure 5.43: R_{ris} , as function of R_0 , for the shift parameter $a = 0.588$

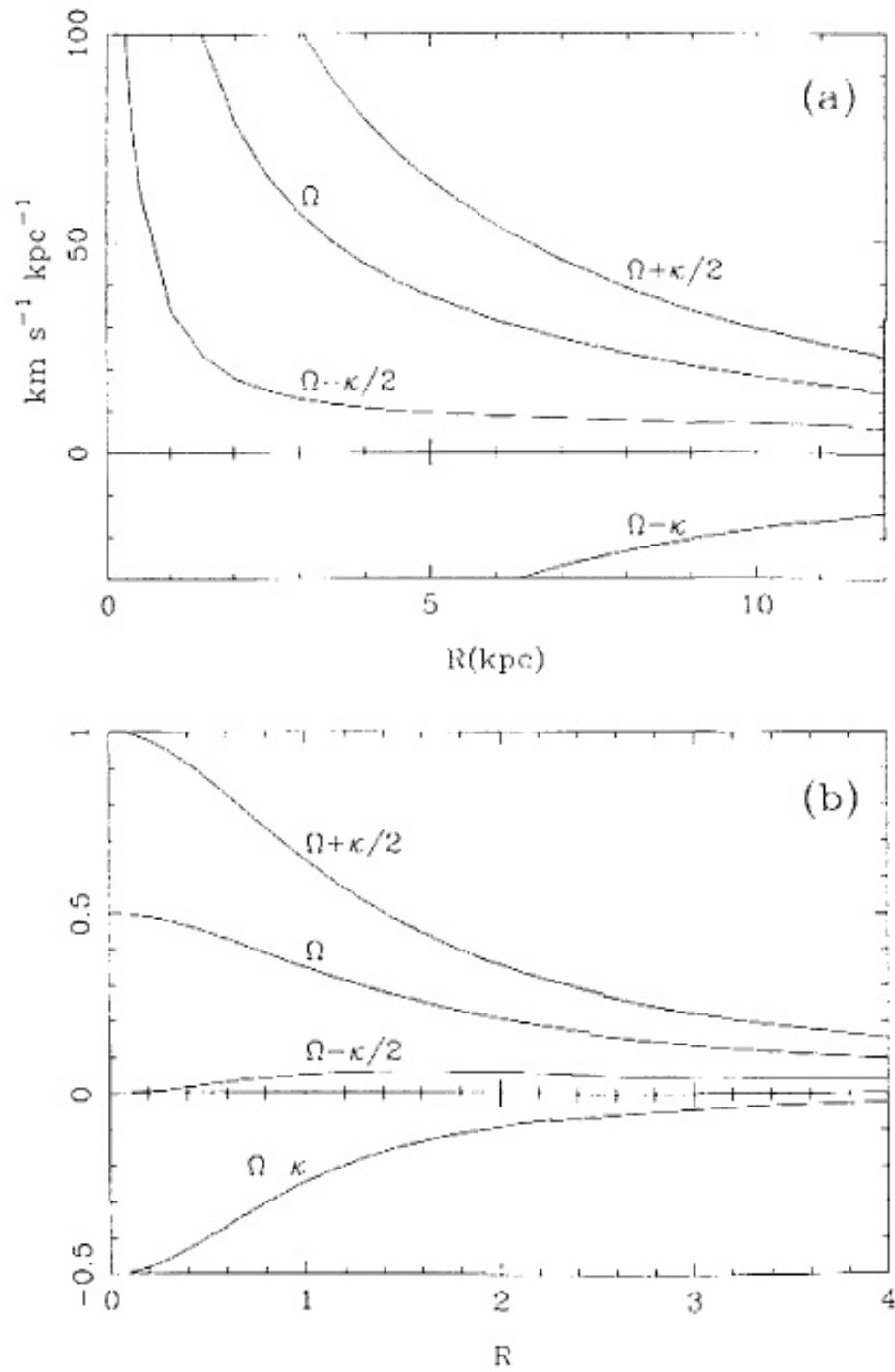


Figure 5.44: Behaviour of R_{ris} in:(a)the Bahcall-Soneira model for the Milky Way; (b) the isochrone Potential

From the comparison between Binney's plots and those from our models, in particular about the important feature that the curve for $\alpha = 0.5$ happens to be near to zero for almost the whole range of values for R_0 (which implies that in that range the circular angular velocity equals the radial epicyclic frequency), it comes evident that the trends are very similar, so our models can have applications in the study of density waves as source for galactic spiral arms.

Chapter 6

Discussion and Conclusions

In the present thesis work some open problems concerning the dynamical properties of orbits in potentials obtained from the complexification of spherical real systems have been preliminarily investigated. The idea behind this work is to understand if the special orbital structure of spherically symmetric real systems is "transferred" at some level in the axially symmetric pairs obtained by the shift. The hope is that some integrability feature is still present in the shifted systems. Of course this would be of the greatest astrophysical interest, as the number of currently known integrable models in Stellar Dynamics is extremely small in absence of spherical symmetry. We recall that integrability is necessary in order to apply the Jeans's Theorem for Phase space distribution functions. According to this framework, we essentially dedicated this work to the investigation of the behaviour of conservation laws in complex shifted systems and we also studied simple orbital properties by extending the epicyclic theory to complex potentials. We were not able to find fully integrable systems; however, we elucidated several important aspects of the phenomenon and we also found indications, by using the complex epicyclic theory, that, for some shifted systems, "local integrability" it is possible, i.e. that a set of measured zero of orbits could be characterized by 3 Integrals of motion. Of course, these orbits cannot be used to build Phase space distribution functions, however they show that, in fact, some integrability may be present in the shifted system, even though, in this preliminary analysis, we do not found any explicit example.

In more details, what just exposed has been investigated, first, by analyzing the model of the harmonic oscillator, deriving the integrals of motion for its complexified version, discussing the properties of both real and imaginary part of what happens to the "complex energy" E^C of the oscillator. After that, we focused on the isotropic complex version of the harmonic oscillator, explicating, as in the previous case, the equations of motion for the system together with its constants of motion and finding out, as expected, that the system, even though complexified, keeps an higher level of symmetry compared to the previous anisotropic case, which is reflected in the presence of another constant of motion next to the complex energy, i.e. a "complex angular momentum" \mathbf{J}^C , and some characteristics of the real and imaginary part of this quantity has been discussed. What has been found, at the end of this first incursion in the field of complexified systems, is that a fully complex, time-dependent, harmonic oscillator's theory reproduces two almost identical, real harmonic oscillators, whose sets of coordinates, i.e. \mathbf{x} and \mathbf{y} respectively, are mixed due to the conservation of $\Im[\mathbf{J}^C]$.

Subsequently, the focus has been driven on considering the complexification of Coulomb potential, so potential proportional to the inverse of the radial distance from the origin of the energy field, and also in this case the real and imaginary part of the complex potential has been pointed out, as well as the real and imaginary part of the force field; the constants of motion obtained also in this case are the complex energy and angular momentum of the system and finally the equations of motion for a test mass in the complex force field generated by the complexified Coulomb potential have been explicitly expressed.

Up to this point the complexification technique applied to the analyzed systems, under a conceptual point of view, has been a coordinate, time-dependent complexification, carried on in order to try to generalize the work presented in the articles by Ciotti & Giampieri (2007) and Ciotti & Marinacci (2008) et al. and eventually discover if it was just a coincidence the fact that some well-known highly symmetric potentials (when suitably complexified) were able to describe well enough systems with a lower degree of symmetry or, hopefully, it was a hint to find a deeper meaning for the complexification procedure developed by Appell, Lynden-Bell et al. (2000, 2004), with the aim to solve the problem of deriving some analytical, exact density-potential pairs for generic matter distribution.

At this stage, we moved to explore another aspect of the complexification procedure, which is the one outlined by Ciotti et al. (2007, 2008) involving a time-independent complex shift. So, starting from the analysis of generic

spherical potentials subject to a constant complex parametric shift, and working out the epicyclic approximation for this system, it has been discovered that the epicyclic frequencies could be purely *real* numbers, i.e.:

$$k_R^2, k_z^2 \in \mathbb{R}, \quad (6.1)$$

independently from taking the fully complexified potential or just its real part. In this way, it appears that the imaginary part of the potential do not have any role in describing the dynamical properties of quasi-circular equatorial orbits. Moreover, in order to verify if a complexified spherical potential keeps memory of the parent system's property to have closed, inclined orbits (implemented by the equality between the vertical epicyclic frequency and the deferent's angular velocity), it has been found that, in general, the just mentioned property is not kept but for potential satisfying eq. (4.19), which, furthermore, happens to be exactly satisfied for any value of the complex radius r^C just for harmonic-like potential; but (4.19) can be converted, for a particular choice of the potential function, into an algebraic equation for the shift parameter a (or for the circular radius R_0 as well) with the aim to find those values satisfying the resonance condition, as function of the epicyclic radius R_0 (or viceversa).

This fact is of great interest because it could be closely related to the integrability of the system that could be modelled on the potential built with these techniques; in particular a stellar system can be modelled as an Hamiltonian system with its own Phase and Configuration space; but, generally speaking, an Hamiltonian n -dimensional system (so possessing a $2n$ -dimensional Phase space) is not integrable, even though the symplectic mathematical structure of the variables describing the system (so possessing vanishing Poisson's brackets) allows it to be completely solved by knowing not $2n - 1$ Integrals of motion as it would be for generic system from classical dynamics, but just $n - 1$ of them; e.g. cylindrically symmetric systems like disk galaxies have quasi non-integrable orbits due to the fact that they have just 2 integrals of motion for the 3D space, giving rise to almost chaotic motions, whose non total chaotic behaviour is described by the fact that orbits do not span the whole configuration space but they are confined between "mathematical structures" generated from constants of motion themselves, i.e. the so called *invariant tori*. At the contrary, for instance, tri-axial systems, in equilibrium, having just the total energy as constant of motion, exhibit fully chaotic behaviour, due to a process, which will not be discussed furthermore in this context, known as "Arnold diffusion". This problem led to the well-known Poincaré classification for the orbits of statistical systems, based upon the notion of integrability and ergodicity, which reads:

- Ergodic system: a physical system with a number of Integrals of motion less than the number of its degrees of freedom, satisfying the Ergodic theorem of Thermodynamic, stating that a system is ergodic if its time average motion is the same as its average over the probability space, so in the measuring time the system can pass through all the possible states in the Phase space.
- Ergodic-Integrable system: a physical system with a number of Integrals of motion equal to the number of its degrees of freedom, whose orbits envelop densely around the *invariant tori*.
- Integrable system: a physical system with a number of Integrals of motion equal to the number of its the degrees of freedom, but with orbits whose equations of motion can be reduced to quadratures, which means exactly, analitically, solvable in a deterministic way.
- Super-Integrable system: a physical system with a number of Integrals of motion greater than the number of its degrees of freedom, whose orbits are not dense on the *invariant tori*, but more like one dimensional patterns and they are *not* ergodic, like it is for the harmonic oscillator or the Coulomb force field, possessing one more constant of motion besides the energy end angular momentum, which is known, for instance within the Kepler's problem, as the Lenz vector.

But, later on, thanks to the work done by Hunter, it as been discovered another class of systems, that we have called in the beginning of this Conclusions:

- "Locally" Integrable System: for sake of example, a system provided with cylindrical simmetry, so with 2 costants of motion, readly (E_{TOT}, J_z) , but admitting, for same specific value of the energy, another integral of motion, so that it can be considered an integrable subfamily of ergodic systems.

In this view, the fact that it is possible to define an analytical solution for the shift parameter a , for a specific value of the deferent radius R_0 (or viceversa), in order to guarantee that the resonance condition coming from the parent spherical potential is still satisfied, it implies that for those orbits another constant of motion could exist such that the orbits belonging to orbital family defined by that value of R_0 are integrable. This, once verified with further studies, may be a very important step towards the understanding of stellar systems with geometries highly departing from standard ones,

as already stated.

Moreover, from the work done by Ciotti & Giampieri (2007) about the complex version of the Plummer Sphere, all the results obtained for general shifted spherical potential has been applied to the Plummer model, in particular the equations of motion for a particle subject to the force field generated by the real part of the shifted Plummer potential have been derived and then the epicyclic approximation has been applied to the equations themselves to study the possible existence of stable quasi-circular orbits and eventual resonances for these orbits; in particular, it has been verified that the epicyclic frequencies are real quantities (with the range of interest for the shift parameter $a < 1$) for the full complex Plummer model, independently from previously selecting its real part to calculate them.

Furthermore, another important property (that we have just mentioned above) that can be mutated from the generic property for shifted spherical potential, when applied to the Plummer case, is the fact that the equation defining the condition for the potential to keep memory of the parent potential of the resonance equality $\Omega_0^2 = k_z^2$ turns to a 3rd-graded algebraic equation from a^2 as function of R_0^2 and viceversa, whose solution is unique. Moreover, it has been clarified that, in the limit for the shift parameter a going to zero, first, the leading order of the corrections for the epicyclic frequencies of the unshifted Plummer model is of order squared. Second, at least at this level of approximation, the resonance condition for planar, closed, orbits (i.e. $k_z^2 = \Omega_0^2$), it has been proved to be not verified for no values of a or R_0 . Let us stress once more that this, in principle, does not impose any restriction on other values of the shift parameter and the circular radius (for the shifted Plummer model as well as for other families of complexified spherical potentials) to guarantee that the resonant condition may be indeed verified.

As final results, some more practical applications of what discovered about the shifted Plummer model have been exposed, analyzing the energy of the circular orbit of reference as function of R_0 , for increasing values of the parameter a up to the last value allowed, named a_M (in order to preserve the positiveness of the real density distribution corresponding to the shifted Plummer potential). Next, the real zero-velocity curves and those obtained applying the epicyclic approximation have been shown and analyzed, as well as a parallel that has been brought on between our models and some other models presented in Binney & Tremaine's *Galactic Dynamics*, such as the logarithmic potential for the mean gravity field generated by spiral or elliptical galaxies, or the isochrone potential used for Theory of density waves for the galactic Spiral Arms; from what has been found it can be stated that the

developed models for the axially symmetric Plummer "Sphere" can be used to further investigate the properties of density waves in Spiral arms as well as the dynamics of galaxies themselves.

Appendix A

The Epicyclic Theory

The epicyclic approximation is a theory of dynamics originally developed as a geometrical model by the Ancient Greeks in order to describe complicated planetary motions in terms of superposition of simple(circular) orbits with different origins. This model, considered obsolete and forgotten for centuries, has been recovered, together with its mathematical implementation due to the development of Newtonian dynamics, with the necessity to introduce elliptic epicycles, and it has proved to be a really useful tool to study stellar motions not too far from circular orbits, and also imposing eventually constraints on more general orbits.

In some more rigorous mathematical terms, the epicyclic theory here illustrated is a 2^{nd} order series expansion in terms of action-angles variables for the Hamilton-Jacobi equation, whose main features will now be quickly presented. It is important to remark that an epicyclic theory, investigated to higher orders than the second, brought to resonances problem and leads at the end to problems addressed KAM Theorem, which will not be treated in this context.

A.1 The Mathematical epicyclic model

The initial assumption to attack the epicyclic theory is to consider an axisymmetric potential in cylindrical coordinates (R, z, α) , even with respect to the equatorial plane, i.e. $\Phi(R, z) = \Phi(R, -z)$, so that $z = 0$ is a reflection plane.

Next, considering a test particle of unit mass, the equations of motion for the particle subdue to the above mentioned potential are obtained from Newton's law $\ddot{\mathbf{x}} = -\nabla\Phi(\mathbf{x})$:

$$\begin{cases} \ddot{R} - R\dot{\alpha}^2 = -\frac{\partial\Phi}{\partial R}, \\ \ddot{z} = -\frac{\partial\Phi}{\partial z}, \\ 2\dot{R}\dot{\alpha} + R\ddot{\alpha} = 0. \end{cases} \quad (6.2)$$

Where use has been made of the orthogonal cylindrical frame of reference described by the unitary vectors: $\hat{\mathbf{e}}_R = (\cos \alpha, \sin \alpha, 0)$; $\hat{\mathbf{e}}_z = (0, 0, 1)$; $\hat{\mathbf{e}}_\alpha = (-\sin \alpha, \cos \alpha, 0)$; so that the position vector, its second time derivative, i.e. the acceleration, and the gradient operator can be written as:

$$\mathbf{x} = R\hat{\mathbf{e}}_R + z\hat{\mathbf{e}}_z, \quad (6.3)$$

$$\ddot{\mathbf{x}} = [\ddot{R} - R\dot{\alpha}^2]\hat{\mathbf{e}}_R + [2\dot{R}\dot{\alpha} + R\ddot{\alpha}]\hat{\mathbf{e}}_\alpha + \ddot{z}\hat{\mathbf{e}}_z, \quad (6.4)$$

and

$$\nabla = \hat{\mathbf{e}}_R \frac{\partial}{\partial R} + \hat{\mathbf{e}}_z \frac{\partial}{\partial z} + \hat{\mathbf{e}}_\alpha \frac{\partial}{R\partial\alpha}, \quad (6.5)$$

thanks to the useful relations:

$$\frac{d\hat{\mathbf{e}}_R}{dt} = \dot{\alpha}\hat{\mathbf{e}}_\alpha; \quad \frac{d\hat{\mathbf{e}}_\alpha}{dt} = -\dot{\alpha}\hat{\mathbf{e}}_R. \quad (6.6)$$

Due to the independence of Φ from the azimuthal angle, there is no force acting on the α -direction, which entails the second member of third equation in (6.2) to be equal to zero. This latter equation, multiplied by R , gives rise to a conserved quantity:

$$2R\dot{R}\dot{\alpha} + R^2\ddot{\alpha} = \frac{d}{dt}[R^2\dot{\alpha}] = 0, \quad (6.7)$$

which is exactly the vertical component of the angular momentum per unit mass, $J_z \equiv (\mathbf{x} \wedge \dot{\mathbf{x}})_z$. It is important to remark that, for a stellar system,

$J_z = R^2(t)\dot{\alpha}(t)$ is conserved for each star, but it is not necessarily the same for all the stars because it depends on the mass of each star and, more importantly, the conservation on J_z does prevent $\dot{\alpha}(t)$ to change sign all over the motion.

Finally, for completeness, we remember that the exact same result can be obtained by means of Lagrangian approach, with the aid of the lagrangian functional:

$$\mathcal{L} = \frac{1}{2}[\dot{R}^2 + R^2\dot{\alpha}^2 + \dot{z}^2] - \Phi(R, z), \quad (6.8)$$

from where, due to the cyclicity of the variable α and, applying the Euler-Lagrange Equation, for each coordinate generally indicated with q_i :

$$\frac{d}{dt} \left[\frac{\partial \mathcal{L}}{\partial \dot{q}_i} \right] - \frac{\partial \mathcal{L}}{\partial q_i} = 0 \quad (6.9)$$

we can immediately recall system (6.2) and the conservation of J_z .

At this point, thanks to the the conserved axial angular momentum, it is possible to eliminate the angular variable from the equations of motion $\dot{\alpha}(t) = J_z/R^2(t)$ to reduce the degrees of freedom for the problem, obtaining:

$$\begin{cases} \ddot{R} - \frac{J_z^2}{R^3} = -\frac{\partial \Phi}{\partial R}, \\ \ddot{z} = -\frac{\partial \Phi}{\partial z}, \end{cases} \quad (6.10)$$

and, defining the "effective potential":

$$\Phi_e \equiv \Phi + \frac{J_z^2}{2R^2}, \quad (6.11)$$

it is possible to write the equations of motion in a symmetric way for the radial and vertical variables, specifically for each test mass because Φ_e is different for each mass, differently from Φ :

$$\begin{cases} \ddot{R} = -\frac{\partial \Phi_e}{\partial R}, \\ \ddot{z} = -\frac{\partial \Phi_e}{\partial z}. \end{cases} \quad (6.12)$$

The latter form of equations of motion is particularly useful to simplify the study of the orbits, introducing the concept of *meridional plane*, \mathbb{R}_m^2 : for each test mass, the meridional plane is defined by the non-inertial two dimensional frame of reference (R, z) , rotating around the axis of symmetry

with angular velocity $\dot{\alpha}(t)$, so that the orbits $z(R)$, although they are not the real tridimensional orbits for the stars, contains information also on the angular velocity. This model allows to completely determine the motion, studying a simpler problem and it is indeed in this contest that the epicyclic theory can be implemented.

For this purpose, it is convenient to introduce 3 concepts and quantities:

- **Orbital family:** the ensemble of all the stars with the same effective potential, i.e. the same angular momentum J_z .
- **Energy in \mathbb{R}_m^2 :** E_m

$$E_m \equiv \frac{1}{2}[\dot{R}^2 + \dot{z}^2] + \Phi_e, \quad (6.13)$$

it is the physical energy of each test particle in its meridional plane and, by its very definition, it is easy to see that $E_m = E$, so that also E_m is a conserved quantity.

- **Deferent:** it is the *circular orbit* associated to a particular orbital family, so to a particular value of J_z .

In \mathbb{R}_m^2 , deferent orbit is a fixed point ($R = R_0, \dot{\alpha} = \Omega_0 = J_z/R_0^2$) and the equations of motion for a circular orbit, so evaluated for the point $(R, z) = (R_0, 0)$, reads:

$$\begin{cases} \frac{\partial \Phi_e}{\partial R} = 0, \\ \frac{\partial \Phi_e}{\partial z} = 0, \end{cases} \quad (6.14)$$

where, from the first equation we recall the centrifugal balance, that may be satisfied by different values of R_0 , so may exist different deferents, while the second equation is due to the evenness of Φ with respect to z . In particular, for the deferent, $E_m = \Phi_e(R_0, 0)$

So, given a certain value of J_z , corresponding to a specific orbital family, if the deferent orbit is then perturbed, being J_z invariant, the positivity of the kinetic energy (also in \mathbb{R}_m^2), defines an energy condition:

$$\Phi_e(R, z) \leq E_m, \quad (6.15)$$

so that just the orbits satisfying that spatial condition are allowed, and no motion is allowed any further; in particular the condition $\Phi_e(R, z) = E_m$, for the deferent, define a boundary for the region where the motion is allowed, the so-called zero-velocity curve(because an orbit satisfying that condition,

has no kinetic energy).

So being said, if a particle has an energy just above the deferent energy, its zero velocity curves are elliptic sections, centered very closely to R_0 , and for energy even greater than that, the curves are deformed and open up to the complete disappearing of any spatial limitation for the motion.

From what just exposed, the purpose now is to obtain the motion law in the epicyclic frame of work and the explicit expressions for the elliptic epicycles. The starting point to this aim is to consider a specific orbital family, i.e a specific J_z , and the corresponding deferent with energy $E_{def} \equiv E_0 = \Phi_e(R_0, 0)$ and then finding the zero velocity curves for a test mass with energy very close to E_0 , i.e. $\Phi_e(R, z) = E_0 + \delta E$, with $\delta E \ll E_0$, so that it is possible a Taylor's expansion, truncated to the second order, of $\Phi_e(R, z)$ around the deferent coordinates $(R_0, 0)$:

$$\begin{aligned} \Phi_e(R, z) \approx & \Phi_e(R_0, 0) + \left. \frac{\partial \Phi_e}{\partial R} \right|_{(R_0, 0)} [R - R_0] + \left. \frac{\partial \Phi_e}{\partial z} \right|_{(R_0, 0)} z \\ & + \frac{1}{2} \left. \frac{\partial^2 \Phi_e}{\partial R^2} \right|_{(R_0, 0)} [R - R_0]^2 + \frac{1}{2} \left. \frac{\partial^2 \Phi_e}{\partial z^2} \right|_{(R_0, 0)} z^2 \\ & + \left. \frac{\partial^2 \Phi_e}{\partial R \partial z} \right|_{(R_0, 0)} z [R - R_0] = E_0 + \delta E, \end{aligned} \quad (6.16)$$

for eq. (6.16), due to the definition of deferent, which is by construction an equilibrium point for the potential Φ_e and whose energy equals exactly the effective potential calculated at its coordinates, we get:

$$\begin{cases} \Phi_e(R_0, 0) = E_0, \\ \left. \frac{\partial \Phi_e}{\partial R} \right|_{(R_0, 0)} [R - R_0] = \left. \frac{\partial \Phi_e}{\partial z} \right|_{(R_0, 0)} = 0, \\ \left. \frac{\partial^2 \Phi_e}{\partial R \partial z} \right|_{(R_0, 0)} = 0. \end{cases} \quad (6.17)$$

And now, defining the vertical and radial epicyclic frequencies, k_R^2 and k_z^2 , respectively as:

$$k_R^2 \equiv \left. \frac{\partial^2 \Phi_e}{\partial R^2} \right|_{(R_0, 0)}, \quad \text{and} \quad k_z^2 \equiv \left. \frac{\partial^2 \Phi_e}{\partial z^2} \right|_{(R_0, 0)}, \quad (6.18)$$

the perturbed energy in the epicyclic approximation δE can be written as:

$$\delta E = \frac{1}{2} k_R^2 [R - R_0]^2 + \frac{1}{2} k_z^2 z^2. \quad (6.19)$$

So if both $k_R^2 \geq 0$ and $k_z^2 \geq 0$, the orbits for the considered mass have a minimum equals to E_0 and the zero velocity curves are elliptic section in \mathbb{R}_m^2 (*Laplace stability*).

A.1.1 Rayleigh's Formula

In some astrophysical situations it is quite difficult to compute for the gravitational effective potential of an object, so it may be tricky to calculate the epicyclic frequencies and evaluate therefore their sign. To avoid this kind of trouble, a more practical way to compute the radial epicyclic frequency, k_R^2 , is been developed, leading to the so-called Rayleigh's Formula.

To begin with, we consider the equatorial plane $z = 0$ and, by the very definition of the radial frequency k_R^2 , it can be written:

$$\left. \frac{\partial^2 \Phi_e(R, 0)}{\partial R^2} \right|_{R_0} = \frac{\partial}{\partial R} \left[\frac{\partial \Phi(R, 0)}{\partial R} + \frac{J_z^2}{R^3} \right] \Big|_{R_0}. \quad (6.20)$$

So remembering that, for circular orbits, the centrifugal balance gives:

$$\frac{V_c^2(R)}{R} = \frac{\partial \Phi(R)}{\partial R} \Rightarrow J_c^2(R) = R^3 \frac{\partial \Phi(R)}{\partial R}, \quad (6.21)$$

with $J_c^2(R) \equiv R^2 V_c^2(R)$ and, by definition, $J_c^2(R_0) = J_z^2$. Now, developing the radial derivative in eq.(6.20) and by means of eq. (6.21), it is possible to write:

$$k_R^2 = -3 \frac{J_c^2(R_0)}{R_0^4} + \frac{1}{R^3} \frac{dJ_c^2(R)}{dR} \Big|_{(R_0)} + 3 \frac{J_z^2}{R_0^4}, \quad (6.22)$$

and from the above expression it is possible to derive the *Rayleigh's Formula* or the well-known *Rayleigh's Stability Criterion*:

$$k_R^2(R) = \frac{1}{R^3} \frac{dJ_c^2(R)}{dR}, \quad (6.23)$$

which means that of $J_c^2(R)$ is a monotonically crescent function of the cylindrical radius R , then the orbits are stable, unstable otherwise. The above equation happens to be valid also for rotating fluid systems.

A clear example of the validity of the eq. (6.23) is its application to the Coulomb potential, with a spherical radius r :

$$\Phi_{Coul.} \propto r^{-1} \Rightarrow V_c \propto r^{-\frac{1}{2}} \Rightarrow J_c^2 \propto \sqrt{r}, \quad (6.24)$$

so stable orbits may exist. Finally it is important to remark that there exist potential which allows stable orbits within a certain radius R_0 and not beyond or viceversa, like the Yukawa potential or the ones generated by General Relativity corrections.

A.1.2 Epicyclic Orbits

Taking back the system in eq. (6.12), evaluated in \mathbb{R}_m^2 , and considering now a little displacement of the cylindrical radius from the value of the circular orbit, i.e. $\epsilon \equiv R - R_0, z = z$ and applying the epicyclic approximation developed in previous section, it is possible to write:

$$\begin{cases} \ddot{\epsilon} = -k_R^2 \epsilon, \\ \ddot{z} = -k_z^2 z. \end{cases} \quad (6.25)$$

These are the equations for two decoupled harmonic oscillators (if, as has been said, the epicyclic frequencies are positive). If the two frequencies are rationally proportional, with the region of space allowed for the motion bounded by the zero velocity curves, the orbits described periodic function known as Lissajous curves, otherwise, in particular if k_R^2 is negative, the epicyclic approach it is not a good way to describe the dynamics of the system anymore and some phenomena of linear instability may occur.

Anyway, within the range for the epicyclic theory to be a good approximation of real behaviour of a stellar system, focusing now just on the radial motion (now decoupled from the vertical one), the solution of eq.(6.25) for the little radial displacement is $\epsilon(t) = \epsilon_0 \cos(k_R t)$ and it is possible to express the angular velocity of rotation of the meridional plane as a function of time:

$$\dot{\alpha}(t) = \frac{J_z}{R^2(t)} = \frac{J_z}{R_0^2 \left(1 + \frac{\epsilon(t)}{R_0}\right)^2}, \quad (6.26)$$

and, as $\epsilon/R_0 \ll 1$, expanding in series and keeping just the leading terms up to the first order:

$$\dot{\alpha}(t) \approx \frac{J_z}{R_0^2} \left[1 - 2 \frac{\epsilon(t)}{R_0}\right]. \quad (6.27)$$

As first features from above equation, it can be noticed that when $\epsilon(t)$ is positive, the angular velocity of the test particle is less than the angular velocity of the associated deferent, which is by definition $\dot{\alpha}_{def} = J_z/R_0^2 \equiv \Omega_0$, i.e. $\dot{\alpha} < \Omega_0$, and viceversa, so that in the outer regions, the orbits are slower, because the epicycle is rotating counterclockwise with respect to the deferent

motion.

We are now ready to find the explicit expression for the elliptic epicycle; first, it is important to change frame of reference, moving from \mathbb{R}_m^2 to the rotating frame of reference of the deferent, in R_0 , where the velocity of the test mass is :

$$\dot{\alpha}(t) - \Omega_0 = -\frac{2\Omega_0}{R_0}\epsilon(t), \quad (6.28)$$

which evidently may change sign over the motion. With this new setting, it can be defined the angular distance between deferent and the considered particle:

$$\gamma(t) \equiv \int_0^t (\dot{\alpha}(t') - \Omega_0) dt', \quad (6.29)$$

and, from eq. (6.28) and the explicit expression for the $\epsilon(t)$, we obtain:

$$\gamma(t) = -\frac{2\Omega_0\epsilon_0}{R_0k_R} \sin(k_R t). \quad (6.30)$$

At this point, considering the general initial, cylindrical frame in reference, where the meridional plane (R, z) has been taken from, the focus now goes onto the equatorial plane, i.e resting in the z -axis and analyzing the motion in the plane (R, α). In this plane the circularity of the deferent is evident, as well as the epicycle rotating on it while the mass test run along the epicycle itself: this is the essence of the epicycle model. In order to determine finally the shape of the epicycle, a new change of coordinate frame is needed: it is possible now to define a new set of coordinate (u, v) in the (R, α)-plane, co-rotating with the epicycle, whose expressions as functions of the original cylindrical coordinates are:

$$\begin{cases} u = (R_0 + \epsilon(t)) \cos \gamma(t) - R_0. \\ v = (R_0 + \epsilon(t)) \sin \gamma(t), \end{cases} \quad (6.31)$$

and, applying the expansions series for little ϵ , retaining just the leading terms yields:

$$\begin{cases} u \approx -\frac{2\Omega_0\epsilon_0}{k_R} \sin(k_R t), \\ v \approx \epsilon_0 \cos(k_R t). \end{cases} \quad (6.32)$$

From the above expressions, summing up the squares of u and v , we obtain the explicit form for the elliptic epicycle:

$$\frac{1}{\epsilon_0^2} u^2 + \frac{k_R^2}{4\Omega_0^2 \epsilon_0^2} v^2 = 1. \quad (6.33)$$

So, from the dynamics, it appear evident that the epicycle is an ellipse with an axis ratio equal to:

$$\frac{b}{a} = \frac{2\Omega_0}{k_R}. \quad (6.34)$$

In order to conclude this presentation concerning the main features behind the epicyclic theory, lastly some properties of the epicyclic approximation for spherical Systems will be presented.

A.2 Epicyclic theory for Spherical systems

A particular class of axisymmetric potentials are spherical systems, described by a general potential $\Phi(r) = \Phi(\sqrt{R^2 + z^2})$ where r is the spherical radius.

Firstly, a more deep investigation of the epicyclic approximation for the Coulomb-like potential will be presented; for a Coulomb potential:

$$\Phi(r) = -\frac{GM}{r}, \quad (6.35)$$

where M is the total mass generating the potential field and, as it has been poited out previously, for the velocity of the circular orbit:

$$V_c^2(r) = \frac{GM}{r} = \Omega_0^2 r^2 \Rightarrow \Omega_0^2(r) = \frac{GM}{r^3}. \quad (6.36)$$

From there, applying now Rayleigh criterion ((6.23)), we find the analytic expression for the radial epicyclic frequency:

$$k_R^2 = \frac{1}{R^3} \frac{dJ_c^2(R)}{dR} = \frac{1}{R^3} \frac{d(V_c^2(r)r^2)}{dR} = \frac{GM}{r^3}. \quad (6.37)$$

So it becomes immediately evident that, for every r , $\Omega_0^2 = k_R^2$ and so, from eq. (6.34), the axis-ratio is indipendent from r and, in particular:

$$\frac{b}{a} = 2, \quad (6.38)$$

which means that epicyclic orbit closes where the deferent orbits starts again its motion.

More generally, for spherically symmetric potential, there is always a 1 : 1 resonance between k_z^2 and Ω_0 , so that, if we consider a pertubation of a circular orbit, along the radial or vertical cylindrical direction, thanks to the conservation of the total angular momentum \mathbf{J}_{TOT} , the result is an inclined

orbit compared to the equatorial plane, whose inclination stores information about the intensity of the oscillations along the z-direction, i.e. information about k_z^2 .

So, in order to prove, for spherical systems in epicyclic approximation, the above mentioned important property, i.e. the equality between the vertical epicyclic frequency k_z and deferent's orbital velocity Ω_0 , by means of the definition of k_z^2 , it can be easily shown that:

$$k_z^2 = \frac{1}{R_0} \frac{\partial \Phi(r)}{\partial r} \Big|_{r=R_0}, \quad (6.39)$$

where use has been made of the relation between the spherical radius and the cylindrical coordinates, defining the following chain rule for the derivation operator for a generic function of r :

$$\frac{\partial f(r)}{\partial q_i} = \frac{q_i}{r} \frac{\partial f(r)}{\partial r} \quad \text{with} \quad q_i = R, z, \quad (6.40)$$

while the angular velocity of circular orbit can be derived from the definition of the vertical component of the angular momentum J_z :

$$J_z^2 = \Omega_0^2 R_0^4 \quad \Rightarrow \quad \Omega_0^2 = \frac{1}{R_0} \frac{\partial \Phi(r)}{\partial r} \Big|_{r=R_0}, \quad (6.41)$$

thanks to eq. (4.54) and to the above properties. It is then evident that, for every spherical system:

$$\Omega_0^2 = k_z^2. \quad (6.42)$$

This completes this brief overview about the Epicyclic Theory.

References

- Abramowitz M., Stegun I.A., 1972, Handbook of Mathematical Functions: with Formulas, Graphs, and Mathematical Tables. Dover, New York
- Appell P., 1887, Ann. Math. Lpz., 30, 155
- Arfken G.B., Weber H.J., 1995, Mathematical Methods for Physicists, 4th Ed. Academic Press, San Diego
- Athanassoula E., 2005, MNRAS, 358, 1477
- Barnabé M., Ciotti, L., Fraternali, F., & Sancisi, R. 2005, in "Extra-planar Gas"Conference, ASP Conf. Series, ed.R. Braun, vol. 331, p. 231
- Barnabé, M., Fraternali, F., Ciotti, L., & Sancisi, R. 2006,A&A, 446, 61
- Binney J., 1981, MNRAS, 196, 455
- Binney J., Petrou M., 1985, MNRAS, 214, 449
- Binney J., Tremaine S., 2008, Galactic Dynamics, 2nd Ed.Princeton University Press, Princeton
- Bureau M., Freeman K.C., 1999, AJ, 118, 126
- Carter B., 1968, Commun. Math. Phys., 10, 280
- Chandrasekhar S., 1969, Ellipsoidal figures of equilibrium.Yale University Press, New Haven
- Chandrasekhar S., 1976, Proc. R. Soc. London A, 349, 571
- Ciotti L.,Bertin G., 2005, A& A, 437, 419
- Ciotti, L. 2000, Lectures Notes on Stellar Dynamics, Scuola Normale Superiore (Pisa) editor
- Ciotti L., Giampieri G., 2007, MNRAS, 376, 1162 (CG07)

Ciotti L., Marinacci F., 2008, MNRAS, Rev. Apr.2008

Ciotti L.,Pellegrini S., 1996, MNRAS, 279, 240

Ciotti L., Bertin, G., & Londrillo, P. 2004, in Plasmas in the laboratory and in the universe: new insights and new challenges, ed. G. Bertin, D. Farina, & R. Pozzoli, AIP Conf. Proc. 703, 322

Ciotti L., Nipoti C., Londrillo P., 2006, ApJ, 640, 741

Combes F., Debbash F., Friendli D., Pfenninger D., 1990,A& A, 233, 82

Courant R., Hilbert D., 1953, Methods of Mathematical Physics. Wiley, New York

D'Afonseca L.A., Letelier P.S., Oliveira S.R., 2005, Class.Quantum Grav., 22, 3803

Dehnen, W. 1993, MNRAS, 265, 250 De Battista V.P., Carollo C.M., Mayer L., Moore B., 2005,ApJ, 628, 678

de Zeeuw, P.T., & Pfenniger, D. 1988, MNRAS, 235, 949

de Zeeuw, P.T., & Carollo, C.M. 1996, MNRAS, 281, 1333

Emsellem E., Arsenault R., 1997, A&A, 318, L19

Erdélyi A., Magnus W., Oberhettinger F., Tricomi G.,1955, Higher Transcendental Functions. McGraw-Hill, New York

Evans, N.W. 1994, MNRAS, 267, 333

Evans, N.W., & de Zeeuw, P.T. 1992, MNRAS, 257, 152

Evans N.W., 1993, MNRAS, 260, 191

Ferrers, N.M. 1877, Quart. J. Pure and Appl. Math., 14, 1

Fricke W., 1952, Astron. Nachr., 280, 193

Gleiser R., Pullin J., 1989, Class. Quantum Grav., 6, 977

Gradshteyn I.S., Ryzhik I.M., 1980, Tables of Integrals, Series and Products, 4th Ed.Academic Press, San Diego

Hénon M., 1959, Ann. d'Astrophys., 22, 126

Hunter C., Qian E., 1993, MNRAS, 262, 401

- Jackson J.D, 1999, Classical Electrodynamics, 3rd Ed. Wiley, New York
- Jeffreys, Sir H. 1970, The Earth (fifth edition) (Cambridge University Press, Cambridge)
- Kaiser G., 2004, J. Phys. A: Math. Gen., 37, 8735
- Kellogg O.D., 1953, Foundations of potential theory. Dover, New York
- King, I. 1972, ApJL, 174, L123
- Kuijken K., Merryfield M.R., 1995, ApJ, 443, L13
- Kutuzov, S.A. 1998, Astronomy Letters, 24, n.5, 645
- Kutuzov, S.A., & Osipkov, L.P. 1980, Astron. Zh., 57, 28
- Lanzoni, B., & Ciotti, L. 2003, A&A, 404, 819
- Lebovitz, N. R. 1967, ARAA, 5, 465
- Lee, J., & Suto, Y. 2003, ApJ, 585, 151
- Lee, J., & Suto, Y. 2004, ApJ, 601, 599
- Letelier P.S., 2007, MNRAS, 381, 1031
- Letelier P.S., Oliveira S.R., 1987, J. Math. Phys., 28, 165
- Letelier P.S., Oliveira S.R., 1998, Class. Quantum. Grav., 15, 421
- Lütticke R., Dettmar R.J., Pohlen M., 2000, A&A, 362,435
- Lynden-Bell D., 1962, MNRAS, 123, 447
- Lynden-Bell D., 2000, MNRAS, 312, 301
- Lynden-Bell D., 2002, preprint (astro-ph/0207064)
- Lynden-Bell D., 2004a, Phys. Rev. D, 70, 104021
- Lynden-Bell D., 2004b, Phys. Rev. D, 70, 105017
- Miyamoto M., Nagai R., 1975, PASJ, 27, 533
- Morse P.M., Feshbach H., 1953, Methods of Theoretical Physics. McGraw-Hill, New York
- Muccione, V., & Ciotti, L. 2003, in Galaxies and Chaos, Lecture Notes on Physics, ed. G.Contopoulos & N. Voglis,626,387 (Springer-Verlag, New York)

Muccione, V., & Ciotti, L. 2004, A&A, 421, 583
 Newman E.T., 1973, J. Math. Phys., 14, 102
 Newman E.T., Janis A.I., 1965, J. Math. Phys., 6, 915
 Newman E.T., Couch E.C., Chinnapared K., Exton A.,
 Prakash A., Torrence R., 1965, J. Math. Phys., 6, 918
 Page D.N., 1976, Phys. Rev. D, 14, 1509
 Patsis P.A., Skokos Ch., Athanassoula E., 2002, MNRAS, 337, 578
 Pfenniger, D. 1984, A&A, 134, 373
 Plummer H.C., 1911, MNRAS, 71, 460
 Quillen A.C., 2002, AJ, 124, 722
 Rosseland, S. 1926, ApJ, 63, 342
 Satoh C., 1980, PASJ, 32, 41
 Shaw M., Wilkinson A., Carter D., 1993, A&A, 268, 511
 Tassoul, J.L. 1978, Theory of rotating stars (Princeton University Press,
 Princeton)
 Teukolsky S., 1973, ApJ, 185, 635
 Toomre A., 1982, ApJ, 259, 535
 Tremaine, S., et al. 1994, AJ, 107, 634
 Vogt D., Letelier P.S., 2005, PASJ, 57, 871
 Vogt D., Letelier P.S., 2007, PASJ, 59, 319
 Waxman, A. M. 1978, ApJ, 222, 61
 Whittaker E.T., Watson G.N., 1950, A course of modern analysis. Cam-
 bridge University Press, Cambridge